TOPICAL REVIEW

Nucleation of superconductivity and vortex matter in superconductor–ferromagnet hybrids

Supercond. Sci. Technol. **22** (2009) 053001 (48pp) doi:10.1088/0953-2048/22/5/053001

TOPICAL REVIEW

Nucleation of superconductivity and vortex matter in superconductor–ferromagnet hybrids

A Yu Aladyshkin[1,2], A V Silhanek[1], W Gillijns[1] and V V Moshchalkov[1]

[1] INPAC—Institute for Nanoscale Physics and Chemistry, Nanoscale Superconductivity and Magnetism and Pulsed Fields Group, K U Leuven, Celestijnenlaan 200D, B-3001 Leuven, Belgium
[2] Institute for Physics of Microstructures, Russian Academy of Sciences, 603950, Nizhny Novgorod, GSP-105, Russia

E-mail: aladyshkin@ipm.sci-nnov.ru, alejandro.silhanek@fys.kuleuven.be, werner.gillijns@fys.kuleuven.be and victor.moshchalkov@fys.kuleuven.be

Received 7 November 2008, in final form 9 February 2009
Published 30 March 2009
Online at stacks.iop.org/SUST/22/053001

Abstract

The theoretical and experimental results concerning the thermodynamical and low-frequency transport properties of hybrid structures, consisting of spatially separated conventional low-temperature superconductors (S) and ferromagnets (F), are reviewed. Since the superconducting and ferromagnetic parts are assumed to be electrically insulated, no proximity effect is present and thus the interaction between both subsystems is through their respective magnetic stray fields. Depending on the temperature range and the value of the external field H_{ext}, different behavior of such S/F hybrids is anticipated. Rather close to the superconducting phase transition line, when the superconducting state is only weakly developed, the magnetization of the ferromagnet is solely determined by the magnetic history of the system and it is not influenced by the field generated by the supercurrents. In contrast to that, the nonuniform magnetic field pattern, induced by the ferromagnet, strongly affects the nucleation of superconductivity, leading to an exotic dependence of the critical temperature T_c on H_{ext}. Deeper in the superconducting state the effect of the screening currents cannot be neglected anymore. In this region of the phase diagram T–H_{ext} various aspects of the interaction between vortices and magnetic inhomogeneities are discussed. In the last section we briefly summarize the physics of S/F hybrids when the magnetization of the ferromagnet is no longer fixed but can change under the influence of the superconducting currents. As a consequence, the superconductor and ferromagnet become truly coupled and the equilibrium configuration of this 'soft' S/F hybrid requires rearrangements of both superconducting and ferromagnetic characteristics, as compared with 'hard' S/F structures.

(Some figures in this article are in colour only in the electronic version)

Contents

List of main notation

Acronyms

GL	Ginzburg–Landau
DWS	Domain-wall superconductivity
F	Ferromagnet or ferromagnetic
OP	Order parameter
RDS	Reverse-domain superconductivity
S	Superconductor or superconducting
1D	One-dimensional
2D	Two-dimensional

Latin letters

$\mathbf{A}$	Vector potential, corresponding to the total magnetic field: $\mathbf{B} = \mathrm{rot}\,\mathbf{A}$
$\mathbf{a}$	Vector potential, describing the nonuniform component of the magnetic field, $\mathbf{b} = \mathrm{rot}\,\mathbf{a}$
$\mathbf{B}$	Total magnetic field: $\mathbf{B} = \mathbf{H}_{\mathrm{ext}} + \mathbf{b}$
$\mathbf{b}$	Nonuniform component of the magnetic field induced by ferromagnet
c	Speed of light
D_{s}	Thickness of the superconducting film
D_{f}	Thickness of the ferromagnetic film (or single crystal)
f	Absolute value of the normalized OP wavefunction: $f = \sqrt{(\mathrm{Re}\,\psi)^2 + (\mathrm{Im}\,\psi)^2}$
$\mathbf{j}_{\mathrm{ext}}$	The density of the external current: $\mathrm{rot}\,\mathbf{H}_{\mathrm{ext}} = (4\pi/c)\,\mathbf{j}_{\mathrm{ext}}$
$\mathbf{j}_{\mathrm{s}}$	The density of superconducting currents
G_{sf}	Free (Gibbs) energy of the S/F hybrid
G_{m}	Term in the free energy functional accounting for the spatial variation of the magnetization
$\mathbf{H}_{\mathrm{ext}}$	External magnetic field
$\mathbf{H}_{\mathrm{ex}}$	Exchange field
H_{c1}	Lower critical field: $H_{\mathrm{c1}} = \Phi_0 \ln(\lambda/\xi)/(4\pi\lambda^2)$
H_{c2}	Upper critical field: $H_{\mathrm{c2}} = \Phi_0/(2\pi\xi^2) = H_{\mathrm{c2}}^{(0)}(1 - T/T_{\mathrm{c0}})$
$H_{\mathrm{c2}}^{(0)}$	Upper critical field at $T = 0$: $H_{\mathrm{c2}}^{(0)} = \Phi_0/(2\pi\xi_0^2)$
h	Separation between superconducting and ferromagnetic films
L	Angular momentum of Cooper pairs (vorticity): $\psi = f(r)\,\mathrm{e}^{\mathrm{i}L\varphi}$
ℓ_H	Magnetic length: $\ell_H = \sqrt{\Phi_0/(2\pi\lvert H_{\mathrm{ext}}\rvert)}$
ℓ_b^*	Effective magnetic length determined by a local magnetic field b_z^*: $\ell_b^* = \sqrt{\Phi_0/(2\pi\lvert b_z^*\rvert)}$
ℓ_ψ	Typical width of the localized OP wavefunction
$\mathbf{M}$	Magnetization of the ferromagnet
M_{s}	Magnetization of the ferromagnet in saturation
$\mathbf{m}_0$	Dipolar moment of a point-like magnetic particle
R_{s}	Radius of the superconducting disc
R_{f}	Radius of the ferromagnetic disc-shaped dots
$\mathbf{R}_{\mathrm{d}}$	Position of a point magnetic dipole: $\mathbf{R}_{\mathrm{d}} = \{X_{\mathrm{d}}, Y_{\mathrm{d}}, Z_{\mathrm{d}}\}$
T_{c0}	Superconducting critical temperature at $B = 0$
w	Period of the one-dimensional domain structures in ferromagnet

Greek letters

α, β	Constants of the standard expansion of the density of the free energy with respect to $\lvert\Psi\rvert^2$
$\epsilon_{\mathrm{v}}^{(0)}$	Self-energy of the vortex line in thin superconducting film: $\epsilon_{\mathrm{v}}^{(0)} = (\Phi_0/4\pi\lambda)^2\, D_{\mathrm{s}} \ln\lambda/\xi$
Θ	The OP phase: $\Theta = \arctan(\mathrm{Im}\,\psi/\mathrm{Re}\,\psi)$
λ	Temperature-dependent magnetic field (London) penetration length: $\lambda = \lambda_0/\sqrt{1 - T/T_{\mathrm{c0}}}$
λ_0	Magnetic field penetration length at $T = 0$
ξ	Temperature-dependent superconducting coherence length: $\xi = \xi_0/\sqrt{1 - T/T_{\mathrm{c0}}}$
ξ_0	Ginzburg–Landau coherence length at $T = 0$
π	3.141 592 653 . . .
ρ	Electrical resistivity
Φ_0	Magnetic flux quantum: $\Phi_0 = \pi\hbar c/e \simeq 2.07$ Oe cm^2
Ψ	Superconducting order parameter (OP) wavefunction
Ψ_0	OP saturated value, $\Psi_0 = \sqrt{-\alpha/\beta}$
ψ	Normalized OP wavefunction, $\psi = \Psi/\Psi_0$

Coordinate systems

Throughout this paper we use both the Cartesian reference system (x, y, z) and cylindrical reference system (r, φ, z), where the z axis is always taken perpendicular to the superconducting film/disc.

1. Introduction

According to the classical Bardeen–Cooper–Schrieffer theory of superconductivity, the ground state of the superconducting condensate consists of electron pairs with opposite spins (the so-called spin-singlet state) bound via phonon interactions [1, 2]. As early as 1956, Ginzburg [3] pointed out that this fragile state of matter could be destroyed by the formation of a homogeneous ferromagnetic ordering of spins if its corresponding magnetic field exceeds the thermodynamical critical field of the superconductor. Later on, Matthias *et al* [4–6] demonstrated that, besides the orbital effect (i.e. a pure electromagnetic interaction between the ferromagnetic and superconducting subsystems), there is also a strong suppression of superconductivity arising from the exchange interaction which tends to align the spins of the electrons in detriment to Cooper pair formation. Anderson and Suhl [7] predicted that a compromise between these antagonistic states can be achieved if the ferromagnetic phase is allowed to break into domains of sizes much smaller than the superconducting coherence length ξ in such a way that, from the superconductivity point of view, the net magnetic moment averages to zero. Alternatively, Larkin and Ovchinnikov [8] and Fulde and Ferrel [9] theoretically predicted that superconductivity can survive in a uniform ferromagnetic state if the superconducting order parameter is spatially modulated.

In general terms, the effective polarization of the conduction electrons, either due to the external field $H_{\rm ext}$ (orbital effect) or the exchange field $H_{\rm ex}$ (paramagnetic effect), leads to a modification (suppression and modulation) of the superconducting order parameter. Typically, in ferromagnetic metals the exchange field is considerably higher than the internal magnetic field and it dominates the properties of the system. However, in some cases, where both fields can have opposite directions, an effective compensation of the conduction electrons' polarization can occur and consequently superconductivity can be recovered at high fields $H_{\rm ext} \simeq -H_{\rm ex}$ (Jaccarino and Peter [10]). Bulaevskii *et al* [11] gave an excellent overview of both experimental and theoretical aspects of the coexistence of superconductivity and ferromagnetism where both orbital and exchange effects are taken into account.

The progressive development of material deposition techniques and the advent of refined lithographic methods have made it possible to fabricate superconductor–ferromagnet structures (S/F) at nanometer scales. Unlike the investigations dealing with the coexistence of superconductivity and ferromagnetism in ferromagnetic superconductors (for a review see Flouquet and Buzdin [12]), the ferromagnetic and superconducting subsystems in artificial heterostructures can be physically separated. As a consequence, the strong exchange interaction is limited to a certain distance around the S/F interface whereas the weaker electromagnetic interaction can persist to longer distances into each subsystem. In recent reviews, Izyumov *et al* [13], Buzdin [14] and Bergeret *et al* [15] discussed in detail the role of proximity effects in S/F heterostructures dominated by exchange interactions[3]. In order to unveil the effect of electromagnetic coupling it is imperative to suppress proximity effects by introducing an insulating buffer material between the S and F films. In an earlier report, Lyuksyutov and Pokrovsky [33] addressed the physical implications of both electromagnetic coupling and exchange interaction in the S/F systems deep into the superconducting state.

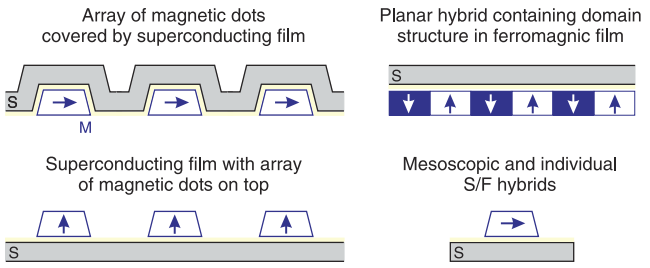

Figure 1. Typical examples of considered S/F hybrid systems with dominant orbital interaction.

In the present review we are aiming to discuss the thermodynamic and low-frequency transport phenomena in S/F hybrid structures dominated by electromagnetic interactions. We focus only on S/F hybrids consisting of conventional low-T_c superconductors without weak links[4]. The S/F heterostructures with pure electromagnetic coupling can be described phenomenologically using Ginzburg–Landau and London formalisms rather than sophisticated microscopical models. Some typical examples of such structures found in the literature are shown schematically in figure 1. As an illustration of the continuous growth of interest in S/F heterostructures with suppressed proximity effect we refer to figure 2, which shows the number of publications during the last two decades.

This review is organized as follows. Section 2 is devoted to the nucleation of the superconducting order parameter under inhomogeneous magnetic fields, induced by single domain walls and periodic domain structures in plain ferromagnetic films or by magnetic dots. A similar problem for individual symmetric microstructures was reviewed by Chibotaru *et al* [40]. Section 3 is devoted to the static and dynamic properties of S/F systems at low temperatures when the superconducting OP becomes fully developed and the screening effects cannot be disregarded any longer. The vortex pinning properties of S/F

[3] In particular, trilayered S/F/S structures with transparent S/F interfaces allow us to realize Josephson junctions with an arbitrary phase difference between the superconducting electrodes, which depend on the thickness of the ferromagnetic layer (see, e.g., the papers of Prokić *et al* [16], Ryazanov *et al* [17], Kontos *et al* [18], Buzdin and Baladie [19], Oboznov *et al* [20] and references therein). The antipode F/S/F heterostructures attract considerable attention in connection with the investigation of unusual properties of such layered hybrid structures governed by the mutual orientation of the vectors of the magnetization in the 'top' and 'bottom' ferromagnetic layers (see, e.g., the papers of Deutscher and Meunier [21], Ledvij *et al* [22], Buzdin *et al* [23], Tagirov [24], Baladié *et al* [25], Gu *et al* [26, 27], Peña *et al* [28], Moraru *et al* [29], Rusanov *et al* [30], Steiner and Ziemann [31], Singh *et al* [32]).

[4] Ferromagnetic dots are shown to induce an additional phase difference in Josephson junctions, leading to a significant modification of the dependence of the Josephson critical current I_c on the external magnetic field $H_{\rm ext}$ (so-called Fraunhofer diffraction pattern, see, e.g., the textbook of Barone and Paterno [34]), which becomes sensitive to the magnetization of ferromagnetic particles (Aladyshkin *et al* [35], Vdovichev *et al* [36], Fraerman *et al* [37], Held *et al* [38], Samokhvalov [39]).

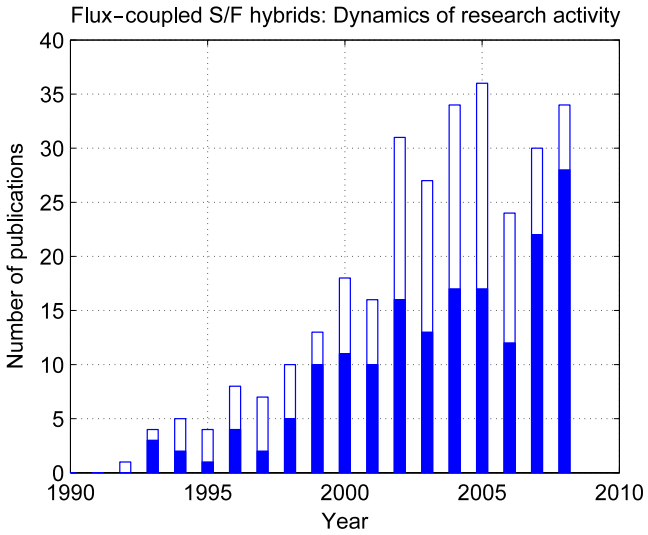

Figure 2. The histogram shows an increase of the number of publications dealing with investigations of the S/F hybrids where the conventional low-T_c superconductors interact with magnetic textures mainly via stray magnetic fields: blue bars correspond to experimental papers, while white bars refer to purely theoretical contributions.

hybrids have been recently analyzed by Vélez *et al* [41] and the fabrication of ordered magnetic nanostructures has been earlier considered by Martín *et al* [42]. In the last section 4 we briefly introduce the problem of 'soft' magnets in combination with superconducting materials, where now the superconducting currents and the magnetic stray field emanating from the ferromagnetic material mutually influence each other. In the conclusion, we formulate a number of relevant issues that, to our understanding, remain unsettled and deserve further investigations. The appendix summarizes the experimental and theoretical research activities on the considered S/F heterostructures, where we present a classification based on the choice of materials for experimental research and on the model used for theoretical treatment.

Importantly, we would like to note already in the introduction that the literature and references used by the authors in this review by no means can be considered as a complete set. Due to the dynamic and rather complex character of the subject and also to the limited space in this review, inevitably quite a lot of important and interesting contributions could have been missed and, therefore, in a way, the references used reflect the 'working list' of publications the authors of this review are dealing with.

2. Nucleation of superconductivity in S/F hybrids (high-temperature limit)

2.1. Ginzburg–Landau description of a magnetically coupled S/F hybrid system

2.1.1. Derivation of the Ginzburg–Landau equations. In order to describe hybrid structures, consisting of a type-II superconductor and a ferromagnet, for the case that no diffusion of Cooper pairs from superconductor to ferromagnet takes place, the phenomenological Ginzburg–Landau (GL) theory can be used. As a starting point we consider the properties of S/F hybrids for external magnetic fields $\mathbf{H}_{\rm ext}$ below the coercive field of the ferromagnet which is assumed to be relatively large. In this case the magnetization of the ferromagnet $\mathbf{M}$ is determined by the magnetic history only and it does neither depend on $\mathbf{H}_{\rm ext}$ nor on the distribution of the screening currents inside the superconductor. Such a 'hard-magnet approximation' is frequently used for a theoretical treatment and it appears to be approximately valid for most of the experimental studies presented in this section. The review of the properties of hybrid S/F systems consisting of superconductors and soft magnets will be presented later on in section 4.

Following Landau's idea of phase transitions of the second kind, the equilibrium properties of a system close to the phase transition line can be obtained by minimization of the free energy functional (see, e.g., the textbooks of Abrikosov [43], Schmidt [44], Tinkham [45]):

$$G_{\rm sf} = G_{\rm s0} + G_m + \int_V \left\{ \alpha\,|\Psi|^2 + \frac{\beta}{2}\,|\Psi|^4 + \frac{1}{4m}\left|-{\rm i}\hbar\nabla\Psi - \frac{2e}{c}\mathbf{A}\Psi\right|^2 + \frac{\mathbf{B}^2}{8\pi} - \mathbf{B}\cdot\mathbf{M} - \frac{\mathbf{B}\cdot\mathbf{H}_{\rm ext}}{4\pi}\right\} {\rm d}V, \tag{1}$$

where the integration should be performed over the entire space[5]. Here $G_{\rm s0}$ is a field- and temperature-independent part of the free energy, $\alpha = \alpha_0\,(T - T_{\rm c0})$, α_0 and β are positive temperature-independent constants, Ψ is an effective wavefunction of the Cooper pairs, $\mathbf{B}(\mathbf{r}) = {\rm rot}\,\mathbf{A}(\mathbf{r})$ is the magnetic field and the corresponding vector potential, $T_{\rm c0}$ is the critical temperature at $B = 0$, e and m are charge and mass of carriers (e.g. electrons) and c is the speed of light. The term $G_{\rm m}$, which will be explicitly introduced in the last section 4, accounts for the self-energy of the ferromagnet which depends on the particular distribution of magnetization. This term seems to be constant for hard ferromagnets with a fixed distribution of magnetization. Therefore it does not influence the order parameter (OP) pattern and the superconducting current distribution in hard S/F hybrids. Introducing a dimensionless wavefunction $\psi = \Psi/\Psi_0$, normalized by the OP value $\Psi_0 = \sqrt{\alpha_0(T_{\rm c0} - T)/\beta}$, in saturation, one can rewrite equation (1) in the following form:

$$G_{\rm sf} = G_{\rm s0} + G_m + \int_V \left\{ \frac{\Phi_0^2}{32\pi^3\lambda^2}\left(-\frac{1}{\xi^2}|\psi|^2 + \frac{1}{2\xi^2}|\psi|^4 + \left|\nabla\psi - {\rm i}\frac{2\pi}{\Phi_0}\mathbf{A}\psi\right|^2\right) + \frac{\mathbf{B}^2}{8\pi} - \mathbf{B}\cdot\mathbf{M} - \frac{\mathbf{B}\cdot\mathbf{H}_{\rm ext}}{4\pi}\right\} {\rm d}V, \tag{2}$$

[5] Hereafter we used the Gauss (centimeter-gram-second) system of units, therefore all vectors $\mathbf{B}$, $\mathbf{M}$ and $\mathbf{H}_{\rm ext}$ have the same dimensionality: $[B]$ = Gauss (G), $[M]$ = Oersted (Oe), $[H_{\rm ext}]$ = Oersted (Oe).

expressed via the temperature-dependent coherence length $\xi^2 = \hbar^2/[4m\,\alpha_0(T_{c0} - T)]$, the London penetration depth $\lambda^2 = mc^2\beta/[8\pi e^2\,\alpha_0(T_{c0}-T)]$ and the magnetic flux quantum $\Phi_0 = \pi\hbar c/e$.

Although the Ginzburg–Landau model was proven to be consistent only at temperatures close to the superconducting critical temperature (Gorkov [46]), the applicability of this model seems to be much broader, at least from a qualitative point of view. After minimization of the free energy functional equation (2) with respect to the OP wave function ψ and $\mathbf{A}$, respectively, one can derive the two coupled Ginzburg–Landau equations [43–45]:

$$-\xi^2\left(\nabla - \mathrm{i}\frac{2\pi}{\Phi_0}\mathbf{A}\right)^2\psi - \psi + |\psi|^2\psi = 0, \tag{3}$$

$$\mathrm{rot\ rot}\,\mathbf{A} = \frac{4\pi}{c}\mathbf{j}_s + 4\pi\ \mathrm{rot}\,\mathbf{M} + \frac{4\pi}{c}\mathbf{j}_{ext}, \tag{4}$$

where

$$\mathbf{j}_s = \frac{c}{4\pi}\frac{|\psi|^2}{\lambda^2}\left(\frac{\Phi_0}{2\pi}\nabla\Theta - \mathbf{A}\right)$$

represents the density of superconducting currents, while $\mathbf{j}_{ext} = (c/4\pi)\,\mathrm{rot}\,\mathbf{H}_{ext}$ is the density of the currents corresponding to external sources and Θ is the OP phase, $\psi(\mathbf{r}) = f(\mathbf{r})\,\mathrm{e}^{\mathrm{i}\Theta(\mathbf{r})}$.

2.1.2. Linearized GL equation. It is quite natural to expect that at the initial stage of the formation of superconductivity (i.e. close to the phase transition line $T_c(H_{ext})$, which separates the normal and superconducting state in the T–H_{ext} plane), the density of the superconducting condensate will be much smaller than the fully developed OP value: $|\psi|^2 \ll 1$. This allows one to neglect: (i) the nonlinear term $|\psi|^2\psi$ in equation (3) and (ii) the corrections to the vector potential $\mathbf{A}$ caused by the screening currents in equation (4), since the supercurrents $\mathbf{j}_s$ are also proportional to $|\psi|^2$. Thus, the nucleation of superconductivity can be analyzed in the framework of the linearized GL equation [43–45]:

$$-\left(\nabla - \mathrm{i}\frac{2\pi}{\Phi_0}\mathbf{A}\right)^2\psi = \frac{1}{\xi^2}\psi, \tag{5}$$

in a given magnetic field described by the vector potential distribution

$$\mathbf{A} = \frac{1}{c}\int\frac{\mathbf{j}_{ext}(\mathbf{r}')}{|\mathbf{r}-\mathbf{r}'|}\,\mathrm{d}^3\mathbf{r}' + \int\frac{\mathrm{rot}\,\mathbf{M}(\mathbf{r}')}{|\mathbf{r}-\mathbf{r}'|}\,\mathrm{d}^3\mathbf{r}'. \tag{6}$$

The solution of equation (5) consists of a set of eigenvalues $(1/\xi^2)_n$, corresponding to the appearance of a certain OP pattern ψ_n, for every value of the applied magnetic field H_{ext}. The critical temperature of the superconducting transition T_c is determined by the lowest eigenvalue of the problem: $T_c = T_{c0}\{1 - \xi_0^2\,(1/\xi^2)_{min}\}$.

2.1.3. The phase boundary for plain superconducting films. First, we would like to present the well-known solution of the linearized GL equation (5) corresponding to the OP nucleation in a plain superconducting film, infinite in the lateral direction and placed in a transverse *uniform* magnetic field $\mathbf{H}_{ext} = H_{ext}\,\mathbf{z}_0$ [43–45]. Taking the gauge $A_y = xH_{ext}$, one can see that equation (5) depends explicitly on the x coordinate only; therefore its general solution can be written in the form $\psi = f(x)\,\mathrm{e}^{\mathrm{i}ky+\mathrm{i}qz}$, where the wavevectors k and q should adjust themselves to provide the maximization of the T_c value. Using this representation in equation (5), it is easy to see that the spectrum of eigenvalues $(1/\xi^2)_n$ is similar to the energy spectrum of the harmonic oscillator but shifted: $(1/\xi^2)_n = 2\pi(2n+1)H_{ext}/\Phi_0 + q^2$ and the $(1/\xi^2)$ minimum (the maximum of T_c) corresponds to $n = 0$ and $q = 0$ for any H_{ext} value, $(1/\xi^2)_{min} = 2\pi H_{ext}/\Phi_0$. The critical temperature of the superconducting transition[6] as a function of a uniform transverse magnetic field is given by $T_c = T_{c0}[1 - 2\pi\xi_0^2\,H_{ext}/\Phi_0]$ or

$$1 - \frac{T_c}{T_{c0}} = \frac{|H_{ext}|}{H_{c2}^{(0)}}, \tag{7}$$

where $H_{c2}^{(0)} = \Phi_0/(2\pi\xi_0^2)$ is the upper critical field at $T = 0$. The inversely proportional dependence of the shift of the critical temperature $1 - T_c/T_{c0}$ on the square of the OP width $\ell_H^2 = \Phi_0/(2\pi|H_{ext}|)$ can be interpreted in terms of the quantum-size effect for Cooper pairs in a uniform magnetic field. It should be mentioned that the effect of the sample's topology on the eigenenergy spectrum $(1/\xi^2)_n$ becomes extremely important for mesoscopic superconducting systems, whose lateral dimensions are comparable with the coherence length ξ. Indeed, this additional confinement of the OP wavefunction significantly modifies the OP nucleation in mesoscopic superconductors and the corresponding phase boundaries $T_c(H_{ext})$ differ considerably from that typical for bulk samples and films infinite in the lateral directions (see Chibotaru *et al* [40], Moshchalkov *et al* [47, 48], Berger and Rubinstein [49]).

2.2. Magnetic confinement of the OP wavefunction in an inhomogeneous magnetic field: general considerations

The main focus in this section is to describe the nucleation of the superconducting order parameter in a static *nonuniform* magnetic field $\mathbf{H}_{ext} + \mathbf{b}(\mathbf{r})$ based on a simple approach[7]. This method makes it possible to see directly a correspondence between the position of the maximum of the localized wavefunction ψ and the critical temperature T_c in the presence of a spatially modulated magnetic field $\mathbf{b}(\mathbf{r})$, generated

[6] It is well known that superconductivity nucleates in the form of a Gaussian-like OP wavefunction $\psi(x, y) = \mathrm{e}^{-(x-x_0)^2/2\ell_H^2}\,\mathrm{e}^{\mathrm{i}ky}$, localized in the lateral direction at distances of the order of the so-called magnetic length $\ell_H^2 = \Phi_0/(2\pi|H_{ext}|)$ and uniform over the film thickness. The oscillatory factor $\mathrm{e}^{\mathrm{i}ky}$ describes the displacement of the OP maximum positioned at $x_0 = k\Phi_0/(2\pi H_{ext})$ without a change of the $(1/\xi^2)_{min}$ value. It is interesting to note that the confinement of the OP wavefunction is determined by the magnetic length ℓ_H, i.e. the OP width is a function of the external field H_{ext}. On the other hand, the temperature-dependent coherence length ξ is a natural length scale describing the spatial OP variations. The equality $\ell_H^2 = \xi^2$ defines the same phase boundary in the T–H_{ext} plane as that given by equation (7).

[7] We introduce the following notation: $\mathbf{b} = \mathrm{rot}\,\mathbf{a}$ characterizes the nonuniform component of the magnetic field only, while $\mathbf{B} = \mathbf{H}_{ext} + \mathbf{b} = \mathrm{rot}\,\mathbf{A}$ is the total magnetic field distribution; the external field $\mathbf{H}_{ext}$ is assumed to be uniform.

by a ferromagnet. For simplicity, we assume that the thin superconducting film is infinite in the (x, y) plane, i.e. perpendicular to the direction of the external field $\mathbf{H}_{\rm ext} = H_{\rm ext}\,\mathbf{z}_0$. This allows us to neglect the possible appearance of superconductivity in the sample perimeter (surface superconductivity [43–45]) and focus only on the effect arising from the nonuniform magnetic field.

2.2.1. Importance of out-of-plane component of the field. It should be emphasized that the formation (or destruction) of superconductivity in thin superconducting films is sensitive to the spatial variation of the out-of-plane component of the total magnetic field. Indeed, the upper critical fields $H_{c2}^{\perp}$ and $H_{c2}^{\parallel}$ for the out-of-plane and in-plane orientation for a uniform applied magnetic field can be estimated as follows [43–45]:

$$H_{c2}^{\perp} \sim \frac{\Phi_0}{\xi^2}, \qquad H_{c2}^{\parallel} \sim \frac{\Phi_0}{\xi D_s}, \tag{8}$$

where D_s is the thickness of the superconducting sample. For rather thin superconducting films and/or close to the superconducting critical temperature $D_s \ll \xi = \xi_0(1 - T/T_{c0})^{-1/2}$, therefore $H_{c2}^{\perp} \ll H_{c2}^{\parallel}$. In other words, superconductivity will generally be destroyed by the out-of-plane component of the magnetic field rather than by the in-plane component, and thus, to a large extent, the spatial distribution of the out-of-plane component determines the OP nucleation in thin-film structures. Since a uniform magnetic field is known to suppress the critical temperature, one can expect that the highest T_c value should correspond to the OP wavefunction localized near regions with the lowest values of the perpendicular magnetic field $|B_z(\mathbf{r})|$, provided that $B_z = H_{\rm ext} + b_z(\mathbf{r})$ varies slowly in space.

If the field $H_{\rm ext}$ exceeds the amplitude of the internal field modulation (i.e. $H_{\rm ext} < -\max b_z$ and $H_{\rm ext} > -\min b_z$), the total magnetic field is nonzero in the whole sample volume, and the favorable positions for the OP nucleation are at the locations of minima of $|B_z(\mathbf{r})| = |H_{\rm ext} + b_z(\mathbf{r})|$. If the characteristic width ℓ_ψ of the OP wavefunction, which will be defined later, is much less than the typical length scale ℓ_b of the magnetic field variation, then locally the magnetic field can be considered as uniform at distances of the order of ℓ_ψ and it approximately equals $\min|H_{\rm ext} + b_z(\mathbf{r})|$. Then, using the standard expression for the upper critical field equation (7) and substituting the effective magnetic field instead of the applied field, one can obtain the following estimate for the phase boundary:

$$1 - \frac{T_c}{T_{c0}} \simeq \min \frac{|H_{\rm ext} + b_z(\mathbf{r})|}{H_{c2}^{(0)}}, \qquad |H_{\rm ext}| \gg \max|b_z|. \tag{9}$$

According to this expression, the dependence $T_c(H_{\rm ext})$ is still linear asymptotically even in the presence of a nonuniform magnetic field. However, the critical field will be shifted upwards (for $H_{\rm ext} > 0$) and downward (for $H_{\rm ext} < 0$) by an amount close to the amplitude of the field modulation. Generally speaking, such a 'magnetic bias' can be asymmetric with respect to the $H_{\rm ext} = 0$ provided that $\max b_z(x) \neq |\min b_z(x)|$.

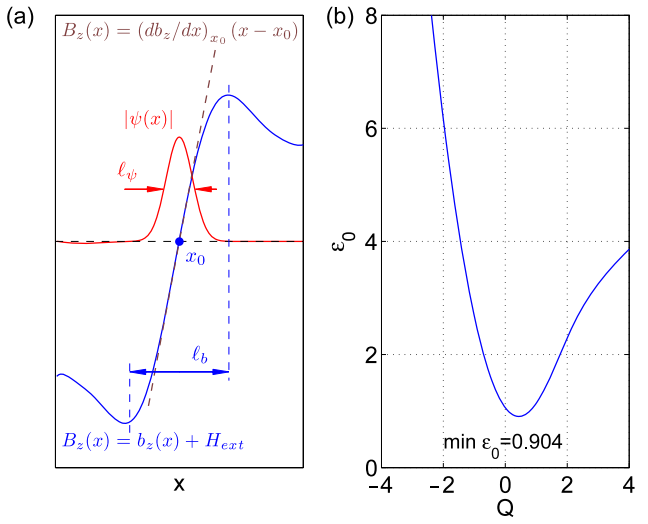

Figure 3. (a) Schematic representation of the OP wavefunction $\psi(x)$ localized near the point x_0, where the z component of the total magnetic field $B_z = H_{\rm ext} + b_z$ vanishes. Provided that the OP width is much smaller than the typical length scales of the magnetic field ($\ell_\psi \ll \ell_b$), the actual field distribution $B_z(x)$ can be approximated by a linear dependence $B_z(x) \simeq (\mathrm{d}b_z/\mathrm{d}x)_{x_0}(x - x_0)$. (b) Energy spectrum ε_0 versus Q of the model problem equation (11).

For relatively low $H_{\rm ext}$ values, when the absolute value of the external field is less than the amplitude of the field modulation ($-\max b_z < H_{\rm ext} < -\min b_z$), the z component of the total magnetic field $H_{\rm ext} + b_z(x)$ becomes zero locally somewhere inside the superconducting film. As a result, superconductivity is expected to appear first near the positions where $H_{\rm ext} + b_z(\mathbf{r}_0) = 0$ (see panel (a) in figure 3). It is natural to expect that the details of the OP nucleation depend strongly on the exact topology of the stray field as well as the field gradient near the lines of zero field. As an example we will analyze the formation of superconductivity in a thin superconducting film placed in an inhomogeneous magnetic field modulated along a certain direction.

2.2.2. OP nucleation in a magnetic field modulated in one direction. Following Aladyshkin *et al* [50], we estimated the dependence of $T_c(H_{\rm ext})$ for a thin superconducting film in the presence of a nonuniform magnetic field modulated along the x direction, where (x, y, z) is the Cartesian reference system. Let the external field be oriented perpendicular to the plane of the superconducting film, $\mathbf{H}_{\rm ext} = H_{\rm ext}\,\mathbf{z}_0$, while the z component of the total magnetic field vanishes at the point x_0, i.e. $H_{\rm ext} + b_z(x_0) = 0$. The vector potential, corresponding to the field distribution $B_z(x) = H_{\rm ext} + b_z(x)$, can be chosen in the form $A_y(x) = xH_{\rm ext} + a_y(x)$, where $b_z = \mathrm{d}a_y/\mathrm{d}x$. Since there is no explicit dependence on the y coordinate in the linearized GL equation (5), the solution uniform over the sample thickness can be generally found as $\psi(x, y) = f_k(x)\,\mathrm{e}^{\mathrm{i}ky}$ and the absolute value of the OP satisfies the following equation:

$$-\frac{\mathrm{d}^2 f_k}{\mathrm{d}x^2} + \left(\frac{2\pi}{\Phi_0}xH_{\rm ext} + \frac{2\pi}{\Phi_0}a_y(x) - k\right)^2 f_k = \frac{1}{\xi^2} f_k. \tag{10}$$

Now the parameter k cannot be excluded by a shift of the origin of the reference system; therefore one should determine the particular k value in order to minimize $(1/\xi_0^2)(1 - T_c/T_{c0})$ and thus to maximize the T_c value.

For an unidirectional modulation of the field, the curves of zero field, where we expect the preferable OP nucleation, are straight lines parallel to the y axis and their positions depend on the external field, $x_0 = x_0(H_{ext})$. Expanding the vector potential inside the superconducting film in a power series around the point x_0, one can get

$$A_y(x) \simeq x_0 H_{ext} + a_y(x_0) + \tfrac{1}{2} b_z'(x_0)(x - x_0)^2 + \cdots.$$

This local approximation is valid as long as

$$|b_z''(x_0)\ell_\psi / b_z'(x_0)| \ll 1.$$

Introducing a new coordinate $\tau = (x - x_0)/\ell_\psi$ and the following auxiliary parameters ℓ_ψ and Q_k:

$$\ell_\psi = \sqrt[3]{\frac{\Phi_0}{\pi |b_z'(x_0)|}},$$

$$Q_k = -\sqrt[3]{\frac{\Phi_0}{\pi b_z'(x_0)}} \left(\frac{2\pi}{\Phi_0} x_0 H_{ext} + \frac{2\pi}{\Phi_0} a_y(x_0) - k \right),$$

we can reduce equation (10) to the bi-quadratic dimensionless equation:

$$-\frac{d^2 f}{d\tau^2} + (\tau^2 - Q_k)^2 f = \varepsilon f$$
$$\text{where } \varepsilon = \frac{\ell_\psi^2}{\xi_0^2}\left(1 - \frac{T}{T_{c0}}\right). \tag{11}$$

Thus, the problem of the calculation of the highest T_c value in the presence of an arbitrary slowly varying magnetic field as a function of both the external field and the parameters of the 'internal' fields is reduced to the determination of the lowest eigenvalue $\varepsilon_0 = \varepsilon_0(Q)$ of the model equation (11). As was shown in [51], the function $\epsilon_0(Q)$ is characterized by the following asymptotical behavior: $\varepsilon_0(Q) \simeq Q^2 + \sqrt{-Q}$ for $Q \ll -1$ and $\epsilon_0(Q) \simeq 2\sqrt{Q}$ for $Q \gg 1$ and it has the minimum value $\varepsilon_{min} = 0.904$ (panel (b) in figure 3).

Extracting T_c from $\varepsilon_0 = (1 - T_c/T_{c0}) \cdot \ell_\psi^2/\xi_0^2$, the approximate expression of the phase boundary takes the following form:

$$1 - \frac{T_c}{T_{c0}} \simeq \frac{\xi_0^2}{\ell_\psi^2} \min_k \varepsilon_0(Q_k) \simeq \xi_0^2 \left(\pi \frac{|b_z'(x_0)|}{\Phi_0} \right)^{2/3},$$
$$-\max b_z < H_{ext} < -\min b_z. \tag{12}$$

If there are several points $x_{0,i}$ where the external field compensates the field generated by the ferromagnetic structure, then the right-hand part of equation (12) should be minimized with respect to $x_{0,i}$. The application of equation (12) for the model cases $b_z = 4M_s \arctan(D_f/x)$ (single domain wall) and $b_z = B_0 \cos(2\pi x/w)$ (periodic domain structure) were given in [50].

2.2.3. OP nucleation in axially symmetrical magnetic field. Similar to the discussion above, one can expect that in the presence of an axially symmetrical magnetic field superconductivity will nucleate in the form of ring-shaped channels of radius $r = r_0$, where $H_{ext} + b_z(r_0) = 0$. The independence of the linearized GL equation (5) on the angular φ coordinate results in a conservation of the angular momentum (vorticity) L of the superconducting wavefunction. Thus, a nonuniform magnetic field makes it possible to have an appearance of giant (multiquanta) vortex states, which are energetically unfavorable in plain (non-perforated) large-area superconducting films, but have been observed in mesoscopic superconductors (Moshchalkov *et al* [47, 48], Berger and Rubinstein [49]) and nanostructured films with antidot lattices (Baert *et al* [52], Moshchalkov *et al* [53]). Expanding the vector potential in the vicinity of r_0 and repeating similar transformations as above, one can get the following approximate expression[8] for the phase transition line (Aladyshkin *et al* [51, 54]):

$$1 - \frac{T_c}{T_{c0}} \simeq \frac{\xi_0^2}{\ell_\psi^2}\left(\min_L \varepsilon_0(Q_L) - \frac{\ell_\psi^2}{4r_0^2} \right),$$
$$-\max b_z < H_{ext} < -\min b_z,$$

where the parameters $\ell_\psi = \sqrt[3]{\Phi_0/(\pi |db_z/dr|_{r_0})}$ and $Q_L = -[2\pi r_0 A_\varphi(r_0)/\Phi_0 - L]\,\ell_\psi/r_0$ depend on the external field. Thus, this model predicts field-induced transitions between giant vortex states with different vorticities. Since the vorticity L is a discrete parameter, the changes of the favorable L value while sweeping the external field leads to abrupt changes in dT_c/dH_{ext}. Similar periodic oscillations of T_c were originally observed by Little and Parks [55, 56] for a superconducting cylinder in a parallel magnetic field and later for any mesoscopic superconductor in a perpendicular magnetic field (for a review see Chibotaru *et al* [40]).

2.2.4. Effect of nonuniform magnetic field on two-dimensional electron gas. It is interesting to note that there is a formal similarity between the linearized GL equation (5) and the stationary Schrödinger equation (see, e.g., [57]) for a charged free spinless particle in a magnetic field:

$$-\frac{\hbar^2}{2m}\left(\nabla - \frac{ie}{\hbar c}\mathbf{A}\right)^2 \psi = E\psi, \tag{13}$$

where ψ is the single-particle wavefunction, e is the charge and m is the mass of this particle. Based on this analogy, one can map the results, obtained for a normal electronic gas in the ground state, on the properties of the superconducting condensate near the 'superconductor–normal metal' transition on the T–H_{ext} diagram.

In particular, the effect of a unidirectional magnetic field modulation on the energy spectrum of a two-dimensional electronic gas (2DEG) was analyzed by Müller [58], Xue

[8] Note that the case of a point magnetic dipole approximation fails for $L = 0$ since the maximum of the OP wavefunction is located at $r = 0$ and this theory cannot correctly describe neither the OP nucleation nor the phase boundary $T_c(H_{ext})$ at negative H_{ext} values close to the compensation field $B_0 = -\max b_z(r)$.

and Xiao [59], Peeters and Vasilopoulos [60], Peeters and Matulis [61], Wu and Ulloa [62], Matulis *et al* [63], Ibrahim and Peeters [64], Peeters *et al* [65], Gumbs and Zhang [66], Reijniers and Peeters [67, 68] and Nogaret *et al* [69, 70]. Remarkably, in a magnetic field varying linearly along a certain direction, quasi-classical electronic trajectories propagating perpendicularly to the field gradient ∇B_z are confined to a narrow one-dimensional channel localized around the region where $B_z = 0$ [58]. A more detailed numerical treatment revealed a lifting of the well-known degeneracy of the Landau states on the centers of the Larmor orbit, inherent to electrons in a uniform magnetic field. Periodic magnetic field patterns with zero and nonzero average values was shown to transform the standard Landau spectrum $E = \hbar\omega_c(n + 1/2)$ into a periodic $E(k_y)$ dependence, describing the broadening of the discrete Landau levels into minibands as in the case of one-dimensional potential (here $\omega_c = |e|H_{ext}/(mc)$ is the cyclotron frequency). An oscillatory change of the width of the energy bands as H is swept was shown to give rise to oscillations in the magnetoresistance of 2DEG at low H_{ext} values, which reflect the commensurability between the diameter of the cyclotron orbit at the Fermi level and the period of the magnetic field modulation [59]. The mentioned oscillatory magnetoresistance due to commensurability effects was later on corroborated experimentally by Carmona *et al* [71]. The influence of two-dimensional magnetic modulations on the single-particle energy spectrum was theoretically considered by Hofstadter [72]. A modification of the scattering of two-dimensional electrons due to the presence of either ferromagnetic dots or superconducting vortices was shown to lead to a non-trivial change of the conductivity in various hybrid systems: 2DEG/superconductor (Geim *et al* [73], Brey and Fertig [74], Nielsen and Hedegård [75], Reijniers *et al* [76]) and 2DEG/ferromagnet (Khveshchenko and Meshkov [77], Ye *et al* [78], Solimany and Kramer [79], Ibrahim *et al* [80], Sim *et al* [81], Dubonos *et al* [82], Reijniers *et al* [83, 84]). The effect of an inhomogeneous magnetic field on the weak-localization corrections to the classical conductivity of disordered 2DEG was considered by Rammer and Shelankov [85], Bending [86], Bending *et al* [87–89], Mancoff *et al* [90], Shelankov [91] and Wang [92].

2.3. Planar S/F hybrids with ferromagnetic bubble domains: theory

The aforementioned Ginzburg–Landau formalism can be applied in the case of a nonuniform magnetic field generated by the domain structure of a plain magnetic film. The problem of the OP nucleation in planar S/F hybrid structures was theoretically analyzed for hard ferromagnets characterized by an out-of-plane magnetization $\mathbf{M} = M_z(x)\,\mathbf{z}_0$ by Aladyshkin *et al* [50], Buzdin and Mel'nikov [93], Samokhin and Shirokoff [94], Aladyshkin *et al* [95] and Gillijns *et al* [96]. It is also worth mentioning the pioneering paper of Pannetier *et al* [97], where the OP nucleation in a periodic sinusoidal magnetic field generated by a meander-like lithographically prepared metallic coil was considered.

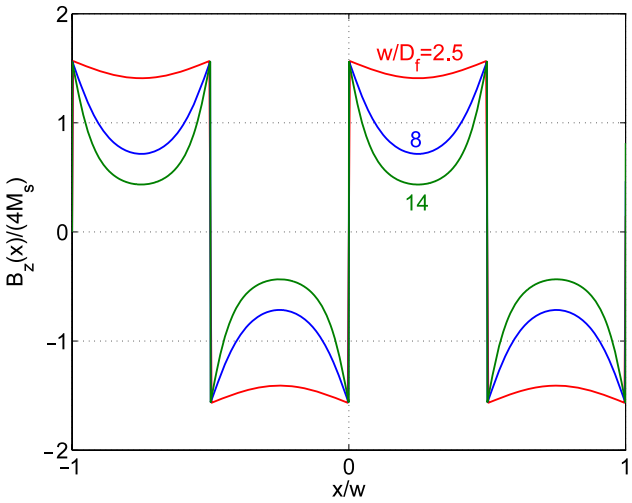

Figure 4. Transverse z component of the magnetic field, induced by one-dimensional periodic distribution of magnetization with the amplitude M_s and the period w, calculated at the distance $h \ll D_f$ above the ferromagnetic film of a thickness D_f.

The distribution of the vector potential $\mathbf{a}(\mathbf{r})$ can be obtained, either by integration of the last term in the rhs of equation (6) or by a direct consideration of the magnetostatic problem. Provided that the width of the domain walls δ is much smaller than other relevant length scales, the field distributions can be calculated analytically for some simple configurations (Aladyshkin *et al* [95], Sonin [98, 99]). Choosing the gauge $A_y = x\,H_{ext} + a_y(x, z)$, one can easily see that the linearized GL equation (5) does not depend on the y coordinate: hence we can generally find the solution in the form $\psi(x, y, z) = f_k(x, z)\exp(iky)$, where the function $f_k(x, z)$ should be determined from the following 2D equation:

$$-\frac{\partial^2 f_k}{\partial x^2} - \frac{\partial^2 f_k}{\partial z^2} + \left[\frac{2\pi}{\Phi_0}a_y(x, z) + \frac{2\pi}{\Phi_0}x H_{ext} - k\right]^2 f_k = \frac{1}{\xi^2}f_k. \tag{14}$$

If the superconducting film has insulating interfaces at the top and bottom surfaces and $\mathbf{A}\cdot\mathbf{n} = 0$ at the surface ∂V_s of the superconductor, one should apply the standard boundary conditions: $\partial f_k/\partial n|_{\partial V_s} = 0$ (here $\mathbf{n}$ is the normal vector).

The spatial distribution of the magnetic field, induced by the periodic 1D domain structure, strongly depends on the relationship between the width of the magnetic domains w and the thickness of the ferromagnetic film D_f as well as on the distance h between superconductor and ferromagnet (figure 4). If the superconducting film thickness D_s is much smaller than the typical length scales of the nonuniform magnetic field (w and D_f), in a first approximation one can neglect the OP variations in the z direction and omit the term $\partial^2 f_k/\partial z^2$ in equation (14). As a result, the OP nucleation in a thin superconducting film is determined by the spatial profile of the perpendicular magnetic field only, while the effect of the parallel field can be ignored.

2.3.1. Criterion for the development of domain-wall superconductivity. In this section we will discuss the

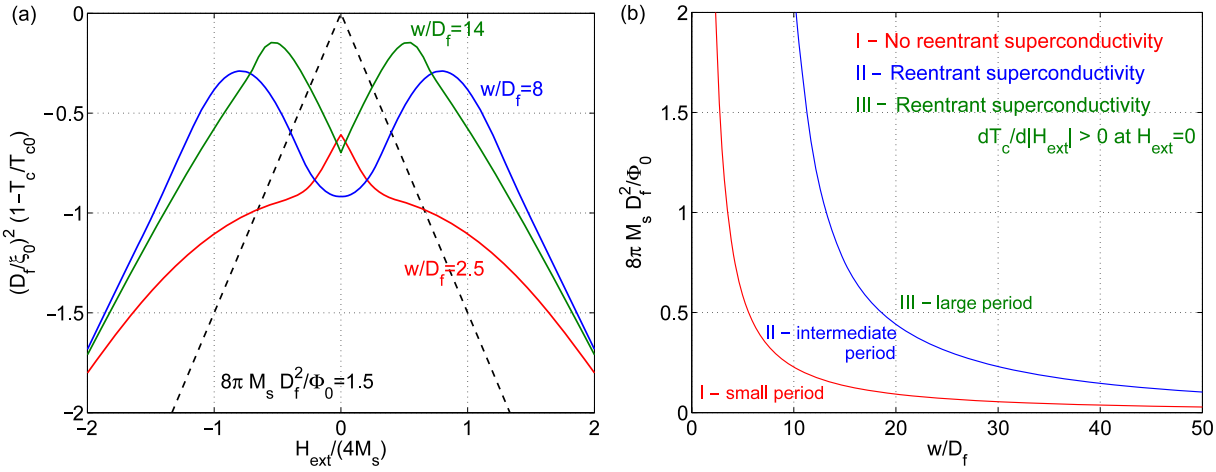

Figure 5. (a) Examples of the phase transition lines $T_c(H_{ext})$ for a planar S/F structure containing a periodic 1D domain structure (M_s is the saturated magnetization, D_f is the ferromagnetic film thickness, w is the period of the domain structure, the thickness of the superconducting film $D_s \ll (D_f, w)$ and the separation between superconducting and ferromagnetic films $h/D_f \ll 1$). The black dashed line corresponds to the $T_c(H_{ext})$ dependence in the absence of the nonuniform field. (b) Different regimes of localized superconductivity in the presence of a 1D domain structure in the M_s–w plane, obtained numerically for $D_s \ll (D_f, w)$ and $h/D_f \ll 1$. In regions II and III the phase boundary $T_c(H_{ext})$ exhibits reentrant superconductivity. The slope $dT_c/d|H_{ext}|$ at $H_{ext} = 0$ can be positive (III), zero (II) or negative (II, near the separating line I–II). Region I corresponds to the monotonic $T_c(H_{ext})$ dependence. Both figures were adapted with permission from Aladyshkin A Yu and Moshchalkov V V 2006 *Phys. Rev.* B **74** 064503 [95]. Copyright (2006) by the American Physical Society.

possibility of localizing the OP wavefunction near a domain wall at zero external field. Obviously, the regime of domain-wall superconductivity (DWS) can be achieved only if the typical b_z^* value inside the magnetic domains is rather large in order to provide an exponential decay of the OP, described by the effective magnetic length $\ell_b^* = \sqrt{\Phi_0/2\pi|b_z^*|}$, within a half-width of the domain: $\ell_b^* < w/2$. For thick ferromagnetic films ($w/D_f \ll 1$) the magnetic field inside domains is almost uniform and it can be estimated as $b_z^* \simeq 2\pi M_s$, giving us the rough criterion of the realization of the DWS regime and the critical temperature $T_c^{(0)}$ at $H_{ext} = 0$: $\pi^2 M_s w^2/\Phi_0 > 1$ and $(T_{c0} - T_c^{(0)})/T_{c0} \simeq 2\pi M_s/H_{c2}^{(0)}$. Of course, $2\pi M_s/H_{c2}^{(0)}$ should be less than unity, otherwise superconductivity will be totally suppressed.

By applying an external field of the order of the compensation field, $H_{ext} \simeq 2\pi M_s$, one can get local compensation of the field above the domains with opposite polarity and a doubling of the field above the domains of the same polarity. Since superconductivity is expected to form at regions with zero field (which are $w/2$ wide), the maximal critical temperature can be estimated as follows: $(T_{c0} - T_c^{max})/T_{c0} \simeq 4\xi_0^2/w^2$ (a consequence of the quantum-size effect for Cooper pairs in a nonuniform magnetic field). Therefore, T_c^{max} will exceed $T_c^{(0)}$, pointing out the non-monotonic $T_c(H_{ext})$ dependence for the same M_s and w parameters, which are necessary to have the DWS regime at $H_{ext} = 0$. The typical phase boundary $T_c(H_{ext})$, corresponding to the DWS regime at $H_{ext} = 0$ and shown in panel (a) in figure 5, is characterized by the presence of a pronounced reentrant behavior and the parabolic dependence of T_c on H_{ext} at low fields (curve labeled $w/D_f = 8$). This type of phase boundary was predicted by Pannetier *et al* [97] for a superconducting film in a field of parallel metallic wires carrying a dc current, and by Buzdin and Mel'nikov [93] and Aladyshkin *et al* [50, 95] for planar S/F hybrids.

2.3.2. Localized superconductivity in S/F hybrids for $w/D_f \ll 1$ and $w/D_f \gg 1$. For S/F hybrids with smaller periods of the field modulation ($\pi^2 M_s w^2/\Phi_0 \ll 1$) the OP distribution cannot follow the rapid field variations and, as a consequence, at $H_{ext} \simeq 0$ there is a broad OP wavefunction, spreading over several domains and resulting in an effective averaging of the nonuniform magnetic field. In this case the critical temperature was shown to decrease monotonically with increasing $|H_{ext}|$ (curve labeled $w/D_f = 2.5$ in figure 5(a)), similar to the case of superconducting films in a uniform magnetic field. By applying an external field, one can shrink the width of the OP wavefunction and localize it within one half-period above the domains with opposite magnetization. The interplay between both the external field and the periodic magnetic field, which determines the resulting OP width, leads to a sign change of the second derivative d^2T_c/dH_{ext}^2. At high H_{ext} values the width of the OP wavefunction, positioned at the center of the magnetic domain, is determined by the local field $B_{loc} \simeq |H_{ext}| - 2\pi M_s$; therefore we come to a biased linear dependence $1 - T_c/T_{c0} \simeq ||H_{ext}| - 2\pi M_s|/H_{c2}^{(0)}$. These qualitative arguments were supported by numerical solutions of the linearized GL equation [95].

The case $w/D_f \gg 1$ should be treated separately since the z component of the field inside the magnetic domains is very inhomogeneous: the absolute value $|b_z(x)|$ reaches a minimum $b_z^* = 8\pi M_s D_f/w$ at the domain center, while the maximal value is still equal to $2\pi M_s$ at the domain walls. It was shown that the $|b_z(x)|$ minima are favorable for the OP nucleation at $H_{ext} = 0$. In this regime, the OP localization in the center of the domains at $H_{ext} = 0$ is possible as

long as $4\pi^2 M_s w D_f/\Phi_0 > 1$. At the same time the nucleation near domain walls is suppressed by the mentioned field enhancement near the domain walls. The sudden displacement of the localized OP wavefunction between the centers of the domains of positive and negative magnetization, when inverting the H_{ext} polarity, results in a new type of phase boundary $T_c(H_{ext})$ with a singularity at $H_{ext} = 0$ [95]. It is important to note that, for $w/D_f \gg 1$ and $H_{ext} = 0$ the critical temperature *increases* linearly with almost the same slope $dT_c/d|H_{ext}| = T_{c0}/H_{c2}^{(0)}$ as the T_c value decreases in an applied uniform magnetic field (curve labeled $w/D_f = 14$ in figure 5(a)).

2.4. Planar S/F hybrids with ferromagnetic bubble domains: experiments

2.4.1. OP nucleation in perpendicular magnetic field. To the best of our knowledge, the first observation of reentrant superconductivity[9] in planar S/F hybrids was reported by Yang *et al* [101] who measured the electrical resistance of a superconducting Nb film grown on top of a ferromagnetic $BaFe_{12}O_{19}$ substrate characterized by an out-of-plane magnetization. Later on, the same system Nb/$BaFe_{12}O_{19}$ was examined by Yang *et al* in [102]. From the parameters typical for the domain structure in $BaFe_{12}O_{19}$ single crystals and Nb films ($M_s \simeq 10^2$ Oe, $w \simeq 2\ \mu$m, $D_f \simeq 90\ \mu$m, $H_{c2}^{(0)} \simeq 30$ kOe), the following estimates can be obtained: $w/D_f \simeq 0.02$, $\pi^2 M_s w^2/\Phi_0 > 10^2$ and $2\pi M_s/H_{c2}^{(0)} \simeq 0.02$. Therefore, such a ferromagnet is suitable for the realization of the DWS regime at $H_{ext} = 0$. The appearance of these localized superconducting paths guided by domain walls was shown to result in a broadening of the superconducting resistive transition at low magnetic fields. As the field H_{ext} is ramped up, the superconducting areas shift away from the domain walls towards the wider regions above the domains with an opposite polarity (so-called reversed-domain superconductivity, RDS) where the absolute value of the total magnetic field is minimal because of the compensation effect. As a consequence, the superconducting critical temperature T_c increased with increasing $|H_{ext}|$ up to 5 kOe. Once the external field exceeds the saturation field H_s of the ferromagnet ($H_s \simeq 5.5$ kOe at low temperatures), the domain structure in the ferromagnet disappears and the phase boundary abruptly returns back to the standard linear dependence $(1 - T_c/T_{c0}) \simeq |H_{ext}|/H_{c2}^{(0)}$. Since the width and the shape of the magnetic domains continuously depend on the external field, the theory developed in section 2.2 is not directly applicable for the description of the experiment, although it qualitatively explains the main features of the OP nucleation in such S/F systems.

Substituting Nb by a superconductor with a smaller $H_{c2}^{(0)}$ value (e.g. Pb with $H_{c2}^{(0)} \simeq 1.7$ kOe, Yang *et al* [103]) allows one to study the effect of the superconducting coherence length $\xi_0 = \sqrt{\Phi_0/2\pi H_{c2}^{(0)}}$ on the localization of the OP. It was shown by Yang *et al* [103] that the increase of the $M_s/H_{c2}^{(0)}$ ratio suppresses the critical temperature of the formation of domain-wall superconductivity at zero external field[10]; therefore superconductivity in Pb/$BaFe_{12}O_{19}$ hybrids appeared only near the compensation fields above the reversed domains.

Direct visualization of localized superconductivity in Nb/$PbFe_{12}O_{19}$ structures was performed by Fritzsche *et al* [104]. The basic idea of this technique is the following: if the sample temperature becomes close to a local critical temperature at a certain position (x, y), then a laser pulse, focused on that point, can induce the local destruction of superconductivity due to heating. The observed increase of the global resistance R of the superconducting bridge can be associated with the derivative $dR(x, y)/dT$. By varying the temperature and scanning the laser beam over the Nb bridge under investigation, it is possible to image the areas with different critical temperatures. For example, it allows one to attribute the formation of well-defined regions with rather high local critical temperatures above magnetic domains at the compensation field with the appearance of reversed-domain superconductivity.

The effect of the amplitude of the field modulation on the OP nucleation was considered by Gillijns *et al* [105, 106] on thin-film trilayered hybrid F/S/F structures. In contrast to the $BaFe_{12}O_{19}$ single crystal discussed above, the multilayered Co/Pd films are characterized by a high residual out-of-plane magnetization, $M_s \sim 10^2$ Oe, almost independent of the external field at $|H_{ext}| < H_{coer}$, where $H_{coer} \simeq 10^3$ Oe is the typical coercive field at low temperatures. The use of two ferromagnetic films with slightly different coercive fields allowed them to prepare different magnetic configurations and thus to control the amplitude of the nonuniform field inside the superconductor due to the superposition of the partial stray fields via an appropriate demagnetizing procedure. The effective doubling of the amplitude of the internal field for a configuration with two demagnetized ferromagnetic films (containing bubble domains) leads to a broadening of the temperature interval, where the $T_c(H_{ext})$ line demonstrates the non-monotonic behavior. In other words, the critical temperature of domain-wall superconductivity at $H_{ext} = 0$ expectedly decreases as the effective magnetization increases. In addition, the enhancement of the internal field results in a shift of the T_c maxima to higher H_{ext} values, which corresponds to reversed-domain superconductivity.

The spatial extension where the field compensation takes place is a crucial parameter defining the nucleation of superconductivity: an OP trapped in a broader region results in a higher T_c value and vice versa (Gillijns *et al* [96], Aladyshkin *et al* [107]). The magnetic state of the ferromagnet can be reversibly changed after the following procedure of an incomplete demagnetization: $H_{ext} = 0 \Rightarrow H_{ext} = H_s \Rightarrow H_{ext} = H_{ret} \Rightarrow H_{ext} = 0$, where H_s is the saturation field

[9] The experimental observation of the influence of a periodic magnetic field, generated by an array of parallel wires with current I flowing alternatively in opposite directions, on the properties of an Al superconducting bridge was reported by Pannetier *et al* [97]. Since the $\max|b_z| \propto I$, reentrant superconductivity can be realized for rather high I values, as was shown experimentally. It should be noted that already in the 1960s Artley *et al* [100] experimentally studied the effect of the domain walls in a thin permalloy film on the superconducting transition of a thin indium film.

[10] In section 2.3 we argued that the critical temperature, $T_c^{(0)}$, at zero external field is proportional to $1 - 2\pi M_s/H_{c2}^{(0)}$.

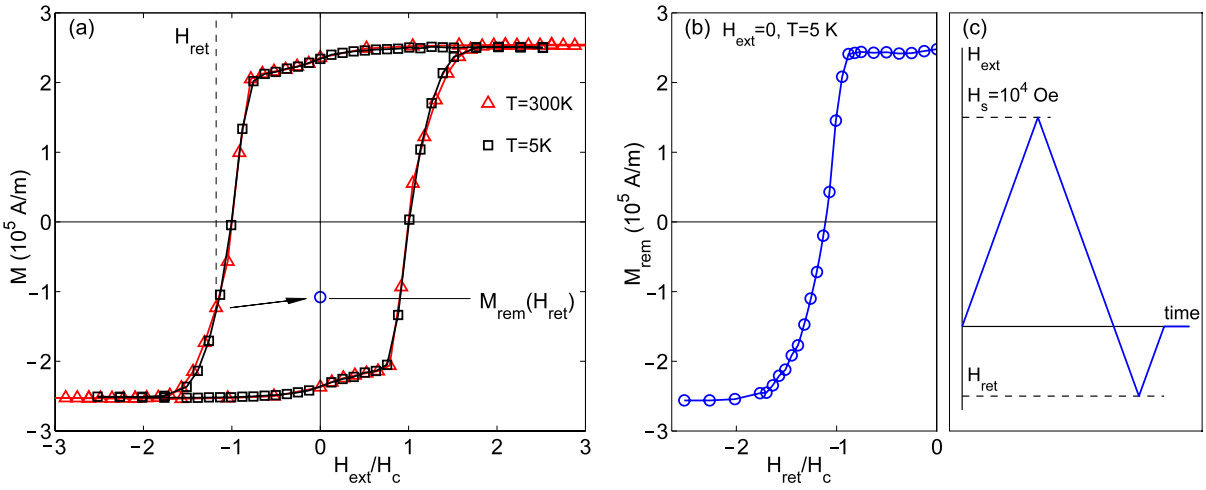

Figure 6. Preparation of the magnetic state in a ferromagnetic Co/Pt film with a desirable remanent magnetization $M_{\rm rem}$. (a) Magnetization loops $M(H_{\rm ext})$ at 300 K (triangles) and 5 K (squares): the magnetic field axis is normalized by the corresponding coercive fields $H_{\rm c}$; (b) remanent magnetization $M_{\rm rem}$, measured at 5 K and $H_{\rm ext} = 0$ after saturation in positive fields (up to 10^4 Oe) and subsequent application of a returning field $H_{\rm ret}$ (this procedure is shown schematically in panel (c)). Both figures were adapted with permission from Gillijns *et al* 2007 *Phys. Rev.* B **76** 060503 [96]. Copyright (2007) by the American Physical Society.

(see figure 6). As a result, one can obtain any desirable remanent magnetization $-M_{\rm s} < M_{\rm rem} < M_{\rm s}$ (as well as any average width of the magnetic domains) by varying the $H_{\rm ret}$ value. At $H_{\rm ret} < 0$ the formation of the negative domains decreases the average width of the positive domains and it causes a drastic lowering of the height of the $T_{\rm c}$ peak, positioned at negative fields and attributed to the appearance of superconductivity above large positive domains (curves $H_{\rm ret} = -3.93$ and -4.15 kOe in figure 7). This observation is a direct consequence of the increase of the ground energy of the 'particle-in-a-box' with decreasing width of the box. When $M_{\rm rem}$ is close to zero, thus indicating the presence of an equal distribution of positive and negative domains, a nearly symmetric phase boundary with two maxima of the same amplitude is recovered (curve $H_{\rm ret} = -4.55$ kOe in figure 7). For higher $H_{\rm ret}$ values, the first peak, located at negative fields, disappears, whereas the peak at positive fields shifts up in temperature and is displaced to lower magnetic field values (curves $H_{\rm ret} = -4.61$ and -5.00 kOe in figure 7). This second peak eventually evolves into a linear phase boundary when the ferromagnetic film is fully magnetized in the negative direction.

2.4.2. OP nucleation in parallel magnetic field. We would like to mention a few related papers devoted to the nucleation of superconductivity in various planar S/F structures, where superconducting and ferromagnetic layers were not electrically insulated and thus an effect of exchange interaction cannot be excluded.

An appearance of domain walls in permalloy film leading to dips in a field dependence of the resistivity of a superconducting Nb film was observed by Rusanov *et al* [108]. The position of these resistivity minima were found to be dependent on the sweep direction of the in-plane-oriented external field. An opposite effect (maxima of resistivity at temperatures below $T_{\rm c0}$) was observed by Bell *et al* [109] for thin-film amorphous S/F structures consisting of superconducting MoGe films and ferromagnetic GdNi layers. It was interpreted as a flow of weakly pinned vortices induced by the stray field of magnetic domains in the ferromagnetic layers. Zhu *et al* [110] demonstrated that the domain structure in multilayered CoPt films can be modified by applying an in-plane external field during the deposition process. This deposition field does not change the overall perpendicular magnetic anisotropy of the Co/Pt films but it induces a weak in-plane magnetic anisotropy and eventually alters the domain patterns. Indeed, after demagnetizing with an in-plane ac magnetic field oriented along the deposition field direction, one can prepare the domain structure in the form of largely parallel stripe domains. In contrast to that, the same multilayered structure fabricated at zero field or demagnetized with an out-of-plane ac field exhibits a nearly random labyrinth-type domain pattern. Sweeping the external field $H_{\rm ext}^{\parallel}$, one can control the arrangement of domain walls and drive the S/F hybrid from normal to superconducting state for the same temperature and magnetic field.

2.5. S/F hybrids with 2D periodic magnetic field: theory and experiments

In this section we continue the discussion concerning the properties of large-area S/F hybrids in which the nonuniform magnetic field is created by regular arrays of ferromagnetic dots. The fabrication of such magnetic structures makes it possible to achieve full control of the spatial characteristics of the nonuniform magnetic field (both the topology and the period), which can eventually be designed practically at will. One can expect that, due to the field-compensation effect the inhomogeneous magnetic field modulated in both directions will affect the OP nucleation in the same way as for the planar S/F structures. However, the 2D periodicity of

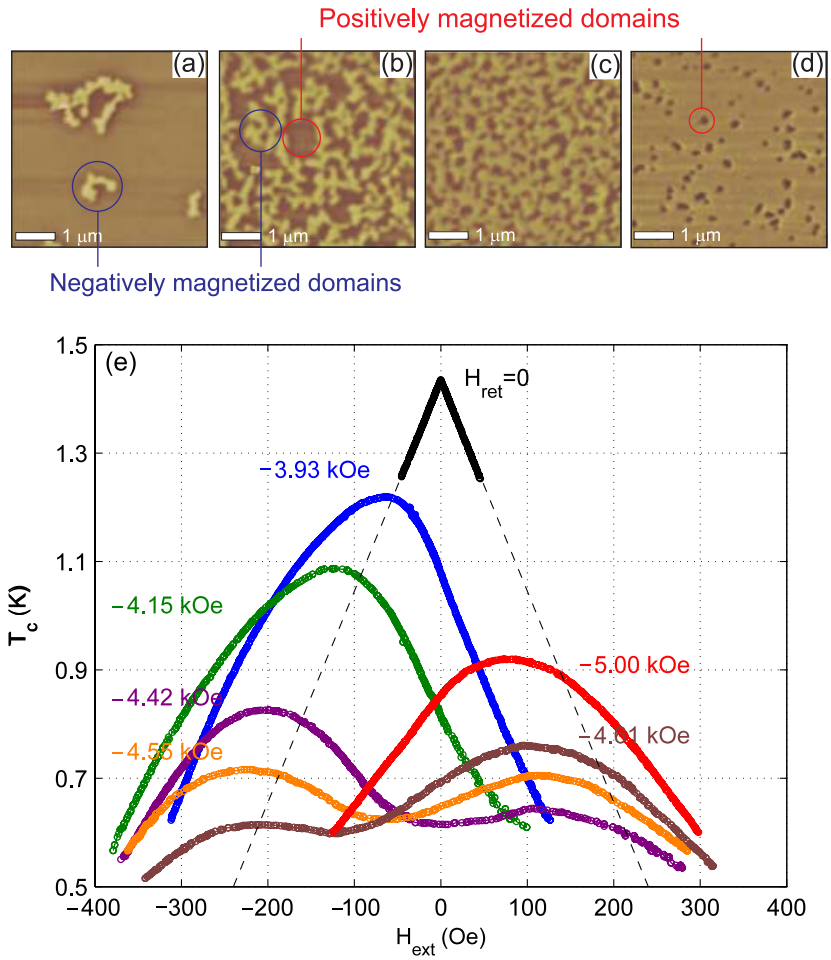

Figure 7. (a)–(d) MFM images obtained at $T = 300$ K for $H_{\rm ret}$ values equal to -1.75 kOe (a), -2.00 kOe (b), -2.50 kOe (c), -3.00 kOe (d), the coercive field $H_{\rm c}^{300\ \rm K} = 1.91$ kOe. The dark (bright) color represents domains with positive (negative) magnetization. (e) A set of experimental phase boundaries $T_{\rm c}(H_{\rm ext})$ obtained for the same bilayered S/F sample (a superconducting Al film on top of a Co/Pt multilayer) in various magnetic states measured after the procedure of an incomplete demagnetization: $H_{\rm ext} = 0 \Rightarrow H_{\rm ext} = 10$ kOe $\Rightarrow H_{\rm ext} = H_{\rm ret} \Rightarrow H_{\rm ext} = 0$ for various returning fields $H_{\rm ret}$ indicated on the diagram, the coercive field $H_{\rm c}^{5\ \rm K} = 3.97$ kOe. All these plots were adapted with permission from Gillijns *et al* 2007 *Phys. Rev.* B **76** 060503 [96]. Copyright (2007) by the American Physical Society.

the magnetic field naturally leads to the appearance of well-defined commensurability effects for such hybrid systems. In other words, a resonant change in the thermodynamical and transport properties of the superconducting films appears as a function of the external magnetic field $H_{\rm ext}$, similar to that observed for superconductors with periodic spatial modulation of their properties (e.g. perforated superconducting films [52, 53]). These matching phenomena take place at particular $H_{{\rm ext},n}$ values that can be used as indicators, allowing us to find a relationship between the most probable microscopic arrangement of the vortices in the periodic potential and the global characteristics of the considered S/F hybrids measured in the experiments.

2.5.1. Commensurate solutions of the GL equations. The periodic solutions of the GL equations in the presence of a nonuniform 2D periodic magnetic field can be constructed by considering one or more magnetic unit cells (of total area S) and applying the following boundary conditions:

$$\begin{aligned} \mathbf{A}(\mathbf{r}+\mathbf{b}_k) &= \mathbf{A}(\mathbf{r}) + \nabla\eta_k(\mathbf{r}), \\ \Psi(\mathbf{r}+\mathbf{b}_k) &= \Psi(\mathbf{r})\ \exp\left(2\pi i\eta_k(\mathbf{r})/\Phi_0\right), \end{aligned} \tag{15}$$

where $\mathbf{b}_k$, $k = \{x, y\}$ are the lattice vectors and η_k is the gauge potential (Doria *et al* [111]). The gauge transformation equation (15) is possible provided that the flux induced by the external magnetic field $H_{\rm ext}S$ through the chosen area S is equal to an integer number of flux quanta, $n\Phi_0$, which gives us the matching fields $H_{\rm n}^{\rm ext} = \pm n\Phi_0/S$.

The formation of different vortex patterns in S/F hybrids, containing square arrays of the magnetic dots with perpendicular magnetization, at $H_{\rm ext} = 0$ were studied by Priour and Fertig [112, 113] and Milošević and Peeters [114, 115]. Since the total flux through an underlying superconducting film, infinite in the lateral direction, equals zero, vortices cannot nucleate without corresponding antivortices, keeping the total vorticity zero. It was shown that the number of vortex–antivortex pairs depends

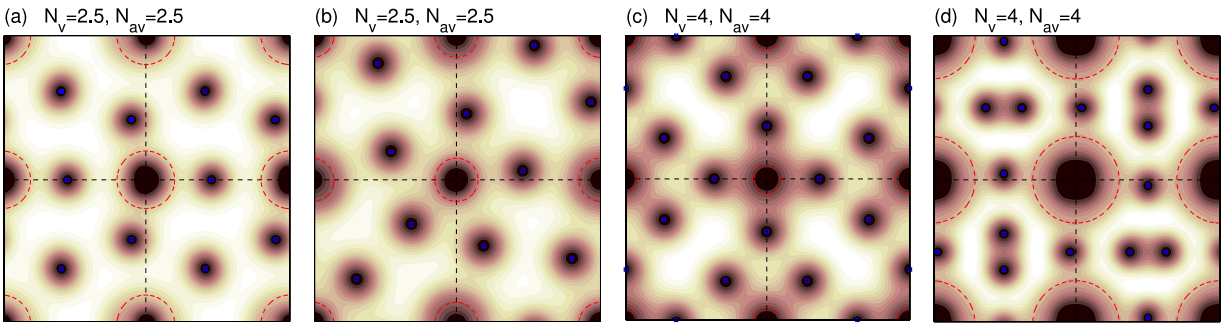

Figure 8. Contour-plots of the Cooper pair density $|\psi|^2$ of stable vortex phases in superconducting thin films in the presence of a square array of circular magnetic dots with dipolar moments oriented perpendicular to the film plane, by the courtesy of M V Milošević (unpublished): (a) radius of ferromagnetic dot $R_f = 400$ nm, saturated magnetization $M_s = 600$ Oe, temperature $T/T_{c0} = 0.80$; (b) $R_f = 300$ nm, $M_s = 980$ Oe, $T/T_{c0} = 0.75$; (c) $R_f = 200$ nm, $M_s = 2830$ Oe, $T/T_{c0} = 0.75$, (c) $R_f = 600$ nm, $M_s = 620$ Oe, $T/T_{c0} = 0.75$. The highest $|\psi|$ values are shown in lighter shades and the lowest densities in darker shades. The red dashed line schematically depicts the edges of the magnetic dot, blue squares mark the position of antivortices. The number of vortices N_v and antivortices N_{av} per unit cell are indicated on the plots. The calculations were performed for a large 2×2 supercell with periodic boundary conditions and for the following parameters: $\kappa = \lambda/\xi = 1.11$, the period of the magnetic dot array is 2000 nm, $\xi_0 = 90$ nm, thickness of the oxide below the magnets is 20 nm, thickness of the ferromagnetic dots is 400 nm.

on the dipolar moment of the magnetic dot. The equilibrium vortex phase, corresponding to the minimum of the free energy functional, can exhibit a lower symmetry than the symmetry of the nonuniform magnetic field. In order to get such vortex states of reduced symmetry, the GL equations with periodic boundary conditions should be considered in a large supercell (2×2, 4×4, etc). In most cases vortices are confined to the dot regions, while the antivortices, depending on the dot's magnetization, can form a rich variety of regular lattice states with broken orientational and mirror symmetries (figure 8). The creation of vortex–antivortex pairs in the case of ferromagnetic dots with in-plane magnetization was considered by Milošević and Peeters [116]. As expected, vortex–antivortex pairs appear under the poles of each magnet according to their specific inhomogeneous magnetic field, keeping the total flux through the superconducting film equal to zero.

The influence of the external field on the formation of symmetrical and asymmetrical commensurate vortex configurations in thin superconducting films in the presence of a square array of out-of-plane magnetized dots was investigated by Milošević and Peeters [114, 115, 117, 118, 122]. The simulations were carried out only for some discrete values $H_{ext,n}$ of the external field, corresponding to the magnetic flux quantization per magnetic supercell of area S. Vortices were shown to be attracted by the magnetic dots in the parallel case (at $H_{ext,n} > 0$ for $M_z > 0$) and repelled in the antiparallel case (at $H_{ext,n} < 0$ for $M_z > 0$). In the parallel case the vortex configurations for the integer matching fields are similar to that for the vortex pinning by regular arrays of antidots, with the difference that the vortex structures under the dots are visible and obey the symmetry of the dots (Milošević and Peeters [129]).

The temperature dependence of the magnetization threshold for the creation of vortex–antivortex pairs was considered in [118]. It was noted that the system will not necessarily relax to the ground state, if there are metastable states, corresponding to local minima in the free energy. As

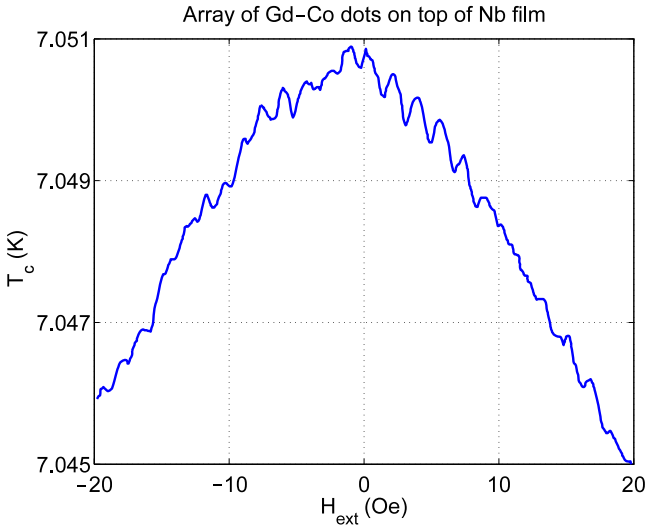

Figure 9. Phase transition line of a superconducting Nb film with a ferromagnetic $Gd_{33}Co_{67}$ particle array (the period 4 μm). Reprinted from Otani *et al* 1993 Magnetostatic interactions between magnetic arrays and superconducting thin films *J. Magn. Magn. Mater.* **126** 622–5 [119]. Copyright (1993) with permission from Elsevier.

long as the given vortex state is still stable and it is separated from other stable vortex configurations by a finite energy barrier (analogous to the Bean–Livingston barrier for the vortex entry into superconducting samples), then the vorticity remains the same even when changing temperature. However, an increase in temperature, resulting in a decrease of the height of the energy barriers and strengthening of the thermal fluctuations, can eventually cause a phase transition between the vortex states with different numbers of vortices. The modification of the ground state (at $H_{ext} = 0$) by the creation of extra vortex–antivortex pairs, when changing temperature and/or increasing the M_s value, manifests itself as cusps in the phase boundary separating superconductor from the normal

metal phase in the M_s–T diagram, similar to the Little–Parks oscillations in the $T_c(H_{ext})$ dependence [55, 56].

2.5.2. Oscillatory nature of the phase transition line (in-plane dot's magnetization). The influence of two-dimensional square arrays of micron-sized, in-plane magnetized particles (SmCo, GdCo, FeNi) on the electrical resistance of a superconducting Nb film, usually interpreted as field-induced variations of the critical temperature, were experimentally studied by Pannetier *et al* [97], Otani *et al* [119] and Geoffroy *et al* [120]. The oscillatory dependence of the resistivity ρ on the perpendicularly oriented external field H_{ext} with a period ΔH_{ext} close to Φ_0/a^2 was observed at $T < T_{c0}$ only when the dots had been magnetized before cooling (here a is the period of the magnetic dot array). The appearance of minima in the $\rho(H_{ext})$ dependence, which are reminiscent of the Little–Parks oscillations for multiply connected superconductors and superconducting networks (see the monograph of Berger and Rubinstein [49] and references therein), were attributed to the variation of the critical temperature, $T_c = T_c(H_{ext})$ due to the fluxoid quantization in each magnetic unit cell (figure 9).

2.5.3. Tunable field-induced superconductivity for arrays of out-of-plane magnetized dots. The fabrication of periodic arrays of multilayered Co/Pd and Co/Pt magnetic dots with out-of-plane magnetic moments allows one to observe both the matching phenomena and the modified OP nucleation due to the field-compensation effect. The stray field induced by positively magnetized dots has a positive z component of the magnetic field under the dots and a negative one in the area in between the dots. Thus, the magnetic field in the region in between the dots will be effectively compensated at $H_{ext} > 0$, stimulating the appearance of superconductivity at nonzero H_{ext} values (magnetic-field-induced superconductivity). Lange *et al* [121] demonstrated that the T_c maximum is located at $H_{ext} = 0$ for the demagnetized magnetic dots and it is shifted towards a certain $H_{ext,n}$ which depends on the dot's magnetization (see the panel (a) in figure 10). This quantized shift of the T_c was attributed to the field compensation in the interdot areas accompanied by an annihilation of the interstitial antivortices under the action of the external field, since (i) the number of antivortices is determined by the magnetic moment of the dots and (ii) the interstitial antivortices can be fully canceled only at the matching fields $H_{ext,n} = n\Phi_0/a^2$ (Milošević and Peeters [122]). Thus, the appearance of periodic kinks in the $T_c(H_{ext})$ phase boundary with a period coinciding with the first matching field H_1 can be associated with the fluxoid quantization, confirming that superconductivity indeed nucleates in multiply connected regions of the film.

The results of further investigations on similar hybrid systems (an array of micron-sized Co/Pt dots on top of an Al film) was presented by Gillijns *et al* [123–125]. As a consequence of the rather large diameter of the dots, the demagnetized dot's state microscopically corresponds to a magnetic multi-domain state with very weak stray field. As was demonstrated in [123], the remanent magnetization of the dots, which were initially demagnetized, depends monotonically on the maximal applied field (excursion field) H_{ret}. Thus the total remanent magnetic moment of the dot becomes variable and tunable, thereby changing the influence of the ferromagnet on the superconductor in a continuous way. It was found that a gradual increase of the dot's magnetization from zero to a certain saturated value results (i) in a quantized displacement of the main T_c maximum towards nH_1 (n is integer) due to the quantized character of the field-induced superconductivity (panel (b) in figure 10) and (ii) in an enhancement of the local T_c maxima, attributed to the formation of a commensurate vortex phase at discrete matching fields, which becomes more pronounced as compared to [121].

The effect of changing the average remanent magnetization M_{rem} and the radius R_f of the magnetic dots on the superconducting properties of an Al film deposited on top of a periodic array of such dots was studied by Gillijns *et al* [124, 125]. Indeed, once the dot's magnetization becomes saturated, the only way to further increase the magnetic flux from each magnet can be achieved by increasing the lateral size of the dots. It was experimentally found that the larger the R_f value, the smaller the necessary ΔM needed to shift the main $T_c(H_{ext})$ maximum by one matching field.

Both the field compensation and matching effects in plain Al films with a square array of ferromagnetic Co/Pt discs were investigated by Gillijns *et al* [96] and Aladyshkin *et al* [107]. Due to the presence of the out-of-plane magnetized dots, there are *three* different areas where the OP can potentially nucleate: above the positive or negative domains, inside the magnetic dot, and in between the dots. In the demagnetized state the interdot field is close to zero, therefore superconductivity starts to nucleate at this position at relatively low magnetic fields, resulting in an almost linear phase boundary centered at $H_{ext} = 0$. By magnetizing the dots positively (i) the amplitude of the field between the dots increases negatively and (ii) the typical width of the positive domains becomes larger than that for negative domains. Therefore the peak, associated with the OP localization between the dots, shifts towards positive fields. In addition, a second local T_c maximum, corresponding to the appearance of superconductivity above the broader positive domains, appears, while the OP nucleation above narrower negative domains is still suppressed. For negatively magnetized dots the reverse effect occurs. It is important to note that the amplitude of the main T_c peak, corresponding to the OP nucleation between the dots, remains almost constant, since the mentioned area of the OP localization is almost independent of the dot's magnetic state (figure 11).

2.5.4. Individual ferromagnetic dots above/inside superconducting films. Marmorkos *et al* [126] studied a possibility to create giant vortices by a ferromagnetic disc with out-of-plane magnetization embedded in a thin superconducting film within full nonlinear self-consistent Ginzburg–Landau equations. Later, using the same model Milošević and Peeters [127–129] considered the formation of vortex–antivortex structures in plain superconducting films, infinite in the lateral direction, in the field of an isolated ferromagnetic disc with out-of-plane magnetization within the full nonlinear

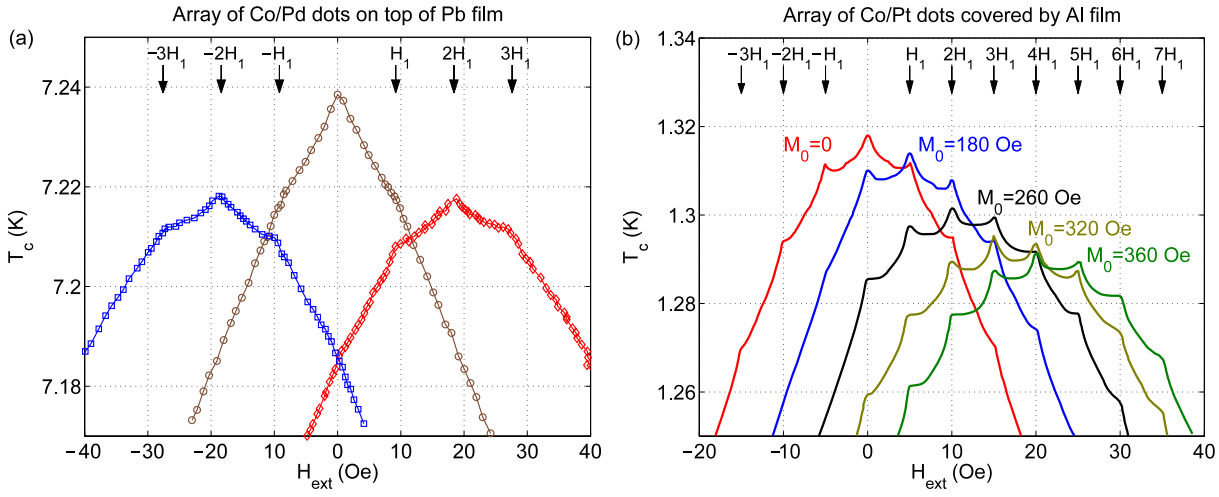

Figure 10. Field-induced superconductivity in a superconducting film with an array of magnetic dots: (a) the $T_c(H_{ext})$ dependences obtained for a Pb film after demagnetization of the ferromagnetic dot array (the brown central curve marked by circles), saturation of the dots in a large positive H_{ext} (the red right curve marked by diamonds) and saturation in a large negative H_{ext} (the blue left curve marked by squares), adapted figure with permission from Lange *et al* 2003 *Phys. Rev. Lett.* **90** 197006 [121], copyright (2003) by the American Physical Society. The period of the lattice was 1.5 μm. The arrows depict the corresponding matching fields. (b) Superconducting transition $T_c(H)$ of an Al film for different magnetic states of the square array of the ferromagnetic dots of period 2 μm, adapted figure with permission from Gillijns *et al* 2006 *Phys. Rev.* B **74** 220509 [123], copyright (2006) by the American Physical Society. By increasing the magnetization a clear shift of $T_c(H_{ext})$ and a decrease of T_c^{max} is observed.

Ginzburg–Landau theory. Antivortices were shown to be stabilized in shells around a central core of vortices (or a giant vortex) with magnetization-controlled 'magic numbers' (figure 12). The transition between the different vortex phases while varying the parameters of the ferromagnetic dot (namely, the radius and the magnetization) occurs through the creation of a vortex–antivortex pair under the magnetic disc edge.

2.6. Mesoscopic S/F hybrids: theory and experiments

In all the description of nucleation of superconductivity so far, we have ignored the effects of the sample's borders. It is well known that the OP patterns in mesoscopic superconducting samples with lateral dimensions comparable to the superconducting coherence length and magnetic penetration depth is substantially influenced by the geometry of the superconductor (see the review of Chibotaru *et al* [40] and references therein). As a result, the presence of the sample's boundaries allows the appearance of exotic states (giant vortex states, vortex clusters, shell configurations, etc), otherwise forbidden for bulk superconductors and non-patterned plain superconducting films (Schweigert and Peeters [440], Kanda *et al* [441], Grigorieva *et al* [442, 443]). Since, as we have pointed out above, a nonuniform magnetic field is an alternative way to confine the superconducting OP in a certain H_{ext} and T range, mesoscopic S/F hybrids seem to be of interest for studying the interplay between different mechanisms of confinement of the superconducting condensate.

It is important to note that the screening effects can still be omitted provided that the lateral size of the thin superconducting sample is smaller than the effective penetration depth $\lambda_{2D} = \lambda^2/D_s$. In this case the self-interaction of the superconducting condensate can be taken into account solving the nonlinear decoupled GL equation:

$$-\xi^2\left[\nabla - i\frac{2\pi}{\Phi_0}\mathbf{A}\right]^2\psi - \psi + |\psi|^2\psi = 0, \qquad (16)$$

where the vector potential distribution is given by the external sources and the ferromagnet only (see equation (6)).

2.6.1. Interplay between different regimes of the OP nucleation. As we anticipated above, a very interesting phenomenon in mesoscopic S/F hybrids is the interplay between competing regimes of the OP nucleation, which can be clearly seen in the case of a small-sized magnetic dot of radius R_f placed above a mesoscopic superconducting disc, $R_f \ll R_s$. Indeed, the $|\psi|$ maximum can be generally located either at the central part of the superconducting disc, close to the magnetic dot (magnetic-dot-assisted superconductivity), or at the outer perimeter of the superconducting disc (surface superconductivity). For a positively magnetized dot the regime of the magnetic-dot-assisted superconductivity, associated with the appearance of superconductivity in the region with compensated magnetic field, can be realized only for $H_{ext} < 0$. At the compensation field ($|H_{ext}| \simeq B_0$) and provided that $\sqrt{\Phi_0/(2\pi B_0)} \ll R_s$ the enhancement of the z component of the field near the disc edge acts as a magnetic barrier for the superconducting condensate and it prevents the edge nucleation of superconductivity even in small-sized superconductors (B_0 being the maximum of the self-field of the magnetized dot). The OP nucleation near the magnetic dot becomes possible, if the critical temperature $T_c^{(0)}$ of the formation of localized superconductivity with the OP

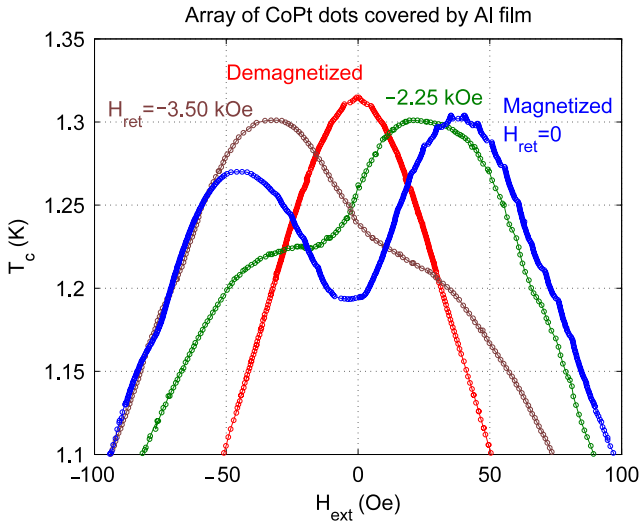

Figure 11. The phase boundaries $T_c(H_{ext})$ for an S/F hybrid, consisting of an Al film and an array of magnetic dots, in the demagnetized state, in the completely magnetized state in positive direction as well as in several intermediate magnetic states, adapted figure with permission from Gillijns *et al* 2007 *Phys. Rev.* B **76** 060503 [96]. Copyright (2007) by the American Physical Society. The period ΔH_{ext} of the T_c oscillations, which are distinctly seen in the curve corresponding to the magnetized states, is equal to 5.1 Oe and it exactly coincides with the matching field, i.e. $\Delta H_{ext} = \Phi_0/S$, where $\Phi_0 = 2 \times 10^{-7}$ Oe cm^2 is the flux quantum and $S = 4\ \mu$m^2 is the area of the unit cell. Note that field and temperature intervals shown here are much broader than those presented in figure 10 (b).

maximum at the superconducting disc center

$$1 - \frac{T_c^{(0)}}{T_{c0}} \simeq \frac{2\pi\xi_0^2}{\Phi_0}\left|H_{ext} + B_0\right|.$$

exceeds the critical temperature for the edge nucleation regime

$$1 - \frac{T_{c3}}{T_{c0}} \simeq 0.59\frac{2\pi\xi_0^2}{\Phi_0}\left|H_{ext}\right|,$$

corresponding to the critical field of surface superconductivity $H_{c3} = 1.69\,H_{c2}$ [43–45]. Due to the different slopes $dT_c^{(0)}/dH_{ext}$ and dT_{c3}/dH_{ext} and the offsets, one can conclude that the edge OP nucleation regime apparently dominates both for positive and large negative H_{ext} values. Only in the intermediate field range does the highest critical temperature correspond to the formation of superconductivity near the magnetic particle.

2.6.2. Little–Parks oscillations in mesoscopic samples. The nucleation of superconductivity in axially symmetrical mesoscopic S/F structures (e.g. superconducting discs or rings in the field of a perpendicularly magnetized ferromagnetic circular dot) were studied theoretically by Aladyshkin *et al* [54], Cheng and Fertig [130] and Milošević *et al* [131, 132] and experimentally by Golubović *et al* [133–136, 140] and Schildermans *et al* [137]. Due to the cylindrical symmetry of the problem, superconductivity was found to appear only in the form of giant vortices $\psi(r,\theta) = f_L(r)\exp(iL\theta)$, where L is the angular momentum L of the Cooper pairs (vorticity). The appearance of vortex–antivortex configurations in superconducting discs of finite radius at temperatures close to T_c is possible, although these states were predicted to be metastable states.

The observed periodic cusp-like behavior of the $T_c(H_{ext})$ dependence was attributed to the field-induced transition between states with different vorticity similar to that of mesoscopic superconductors in a uniform magnetic field. However, the stray field, induced by the magnetized dot, was shown to be responsible for a peculiar asymmetry of the oscillatory $T_c(H_{ext})$ phase boundary and a shift of the main T_c maximum towards nonzero H_{ext} values [54, 133–135]. The mentioned abrupt modification of the preferable nucleation regime when sweeping H_{ext} can lead to a double change in the slope of the $T_c(H_{ext})$ envelope from $T_{c0}/H_{c3}^{(0)}$ to $T_{c0}/H_{c2}^{(0)}$ [54, 137] (see curve $H_m = 3.4$ kOe in figure 13). The restoration of the slope close to $T_{c0}/H_{c2}^{(0)}$ can be interpreted as an effective elimination of the boundary effects in mesoscopic S/F samples at the compensation field (near the main T_c maximum). Interestingly, the nonuniform magnetic field can be used to control the shift in the field dependence of the

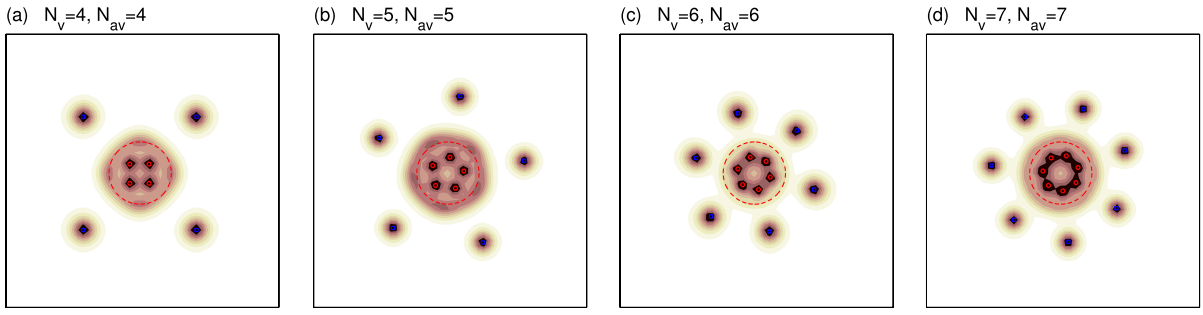

Figure 12. Contour plots of the Cooper pair density $|\psi|^2$, illustrating the appearance of vortex–antivortex shell structures in large-area superconducting films in the field of a perpendicularly magnetized disc for different magnetic moments m of the ferromagnetic particle: $m/m_0 = 25$ (a), 29 (b), 35 (c) and 38 (d), where $m_0 = H_{c2}\,\xi^3$, courtesy of M V Milošević (unpublished). The highest $|\psi|$ values are shown in lighter shades and the lowest densities in darker shades. It is important to note that only the central part of the superconducting film ($45\,\xi \times 45\,\xi$) is shown here: the red dashed line schematically depicts the edge of the magnetic dot. Red circles correspond to the vortex cores, while blue squares mark the position of antivortices. The number of vortices N_v and antivortices N_{av} are indicated on the plots. The simulations were performed for the following parameters: $\kappa = \lambda/\xi = 1.2$, the lateral size of superconducting sample is $256\,\xi \times 256\,\xi$, the radius of ferromagnetic disc is 4.53 ξ and the thicknesses of superconductor and ferromagnet are equal to 0.1 ξ.

maximal critical current $I_c(H_{ext})$ for a bias current flowing through the superconducting loop, which allows one to tune the internal phase shift in superconducting networks (Golubovic *et al* [136]).

It is important to note that the periodicity ΔH_{ext} of the Little–Parks oscillations in the $T_c(H_{ext})$ dependence is explicitly given by the area where the superconducting OP is confined. For edge nucleation only the area enclosed by the superconductor determines the period of the oscillations, which can be roughly estimated as $\Delta H_{ext} \simeq \Phi_0/R_s^2$. However, in the case of the magnetic-dot-assisted nucleation (in the vicinity of the compensation field) the area of the OP localization is determined by the spatial characteristics of the nonuniform magnetic field (either the dot's radius R_f or the vertical separation between the dot and the superconductor Z_d). Therefore $\Delta H_{ext} \simeq \Phi_0/\max\{R_f^2, Z_d^2\}$. As a consequence, the change of the nucleation regimes manifests itself as an abrupt modification of the oscillatory $T_c(H_{ext})$ dependence. In particular, both the amplitude and the period of the Little–Parks oscillations become much larger, provided that $(Z_d, R_f) \ll R_s$ and the OP wavefunction localizes far from the sample's edges (Aladyshkin *et al* [54], Carballeira *et al* [138]).

2.6.3. Symmetry-induced vortex–antivortex patterns. Mesoscopic S/F hybrids of a reduced symmetry (e.g. structures consisting of a superconductor/ferromagnet discs and/or regular polygons) represent nice model systems for studying symmetry-induced phenomena. The formation of different vortex–antivortex configurations was studied theoretically by Carballeira *et al* [138] and Chen *et al* [139] for mesoscopic superconducting squares with a circular ferromagnetic dot magnetized perpendicularly. It was shown that the symmetry-consistent solutions of the Ginzburg–Landau equations[11], earlier predicted for mesoscopic superconducting polygons by Chibotaru *et al* [40], are preserved for regular superconducting polygons in the stray field of a ferromagnetic disc. However, since spontaneously formed vortices and antivortices interact with the magnetic dot in a different way, it leads to a modification of the symmetry-induced vortex patterns (see figure 14). In particular, the dot can be used to enlarge these vortex–antivortex patterns, thus facilitating their experimental observation with local vortex-imaging techniques ('magnetic lensing').

2.6.4. Embedded magnetic particles. Doria [142, 143] and Doria *et al* [144, 145] studied theoretically the formation of vortex patterns induced by magnetic inclusions embedded in a superconducting material but electrically insulated from the multiply connected superconductor. Since, in the absence of an external field, flux lines should be closed, vortex lines are expected to start and end at the magnetic inclusions. The

[11] By symmetry-consistent solutions we mean those vortex configurations reflecting the symmetry of the problem. For instance, in a mesoscopic superconducting square with vorticity $L = 3$, the state consisting of four vortices and a central antivortex may have lower energy than the configuration of three equidistant vortices, which breaks the square symmetry (Chibotaru *et al* [141]).

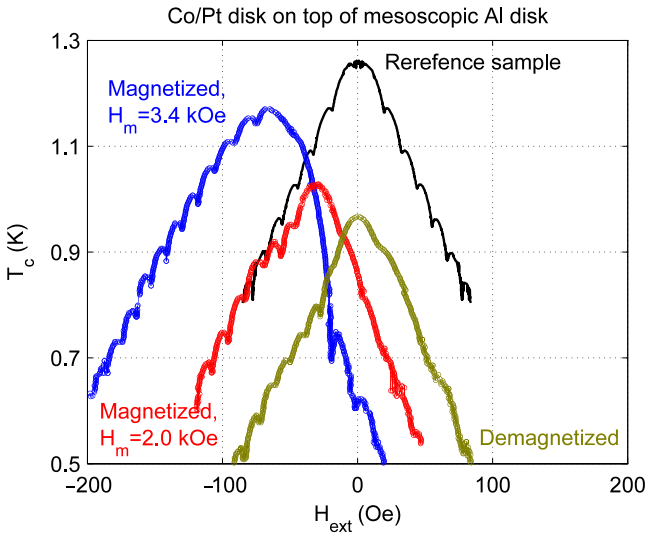

Figure 13. The phase transition lines $T_c(H_{ext})$, obtained experimentally for the mesoscopic S/F hybrid system with a 0.1 R_n criterion for three different magnetic states (completely magnetized, partly magnetized and demagnetized states), R_n and H_m being the normal-state resistance and the magnetizing field, adapted from figure with permission from Schildermans *et al* 2008 *Phys. Rev.* B **77** 214519 [137]. Copyright (2008) by the American Physical Society. The considered S/F system consists of a superconducting Al disc covered by a ferromagnetic Co/Pt multilayered film of the same radius $R_s = R_f = 0.825\mu$m. The black solid line represents the $T_c(H_{ext})$ dependence for the reference Al disc of the same lateral size.

calculations, performed in the framework of GL theory for a mesoscopic superconducting sphere with a single magnetic point-like particle in its center, reveal that the confined vortex loops arise in triplets from the normal core when the magnetic moment reaches the scale defined by $m_0 = \Phi_0\xi/2\pi$ (figure 15). Therefore a vortex pattern is made of confined vortices, loops and also broken loops that spring to the surface in the form of pairs. This vortex state provides a spontaneous vortex phase scenario for bulk superconductors with magnetic inclusions, where the growth of the vortex loops interconnects neighboring magnetic inclusions.

2.6.5. Effect of the finite thickness of the superconducting film. The effect of the finite thickness of the superconducting film on the $T_c(H_{ext})$ dependence was studied theoretically by Aladyshkin *et al* [54], Aladyshkin and Moshchalkov [95] and Schildermans *et al* [137]. It follows from Maxwell's equations that the faster the spatial variation of the magnetic field in the lateral (x, y) directions, the faster the decay of the field in the transverse z direction. However, the OP variation along the sample's thickness can be effectively suppressed by a requirement of vanishing the normal derivative $\partial\psi/\partial n$ of the superconducting OP at the top and bottom surfaces of the superconductor. Indeed, the external field applied along the z direction makes the OP variations over the superconducting film thickness more energetically unfavorable than in the lateral direction, especially for H_{ext} values of

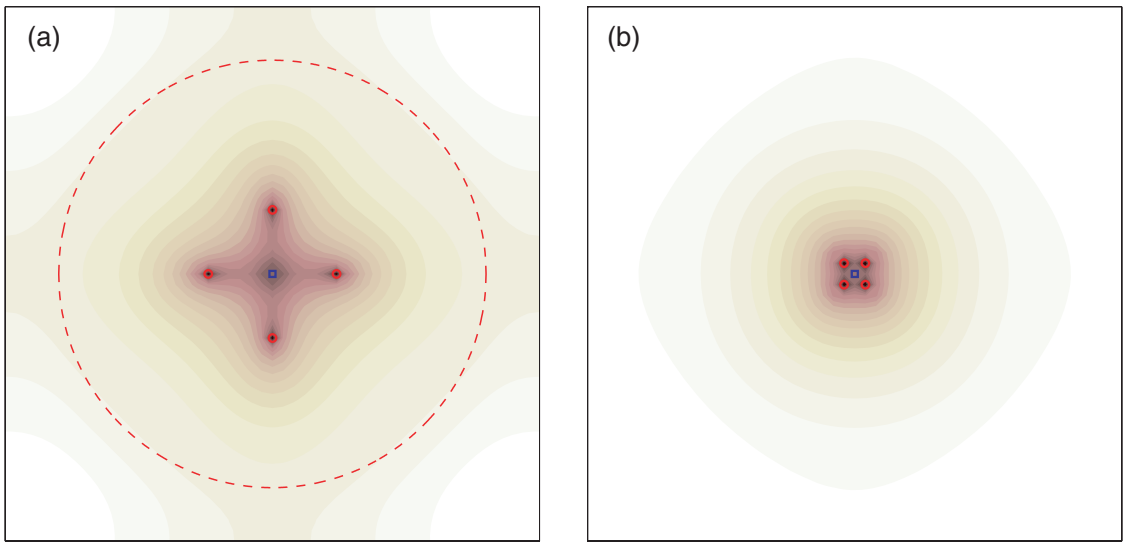

Figure 14. A comparison between the vortex–antivortex patterns that can be observed for vorticity $L = 3$ (a) with and (b) without the magnetic dot on top of the superconducting square, by the courtesy of C Carballeira and Q H Chen (unpublished). The red dashed line depicts the edge of the magnetic dot of the radius $R_s = 0.4a$, a is the lateral size of the sample, $H_{ext}/a^2 = -4.25$ (a) and $H_{ext}/a^2 = 5.50$ (b). Red circles correspond to the vortex cores, while blue square marks the position of antivortex. As can be seen, the vortex–antivortex pattern rotates 45° and expands dramatically in the presence of the magnetic dot.

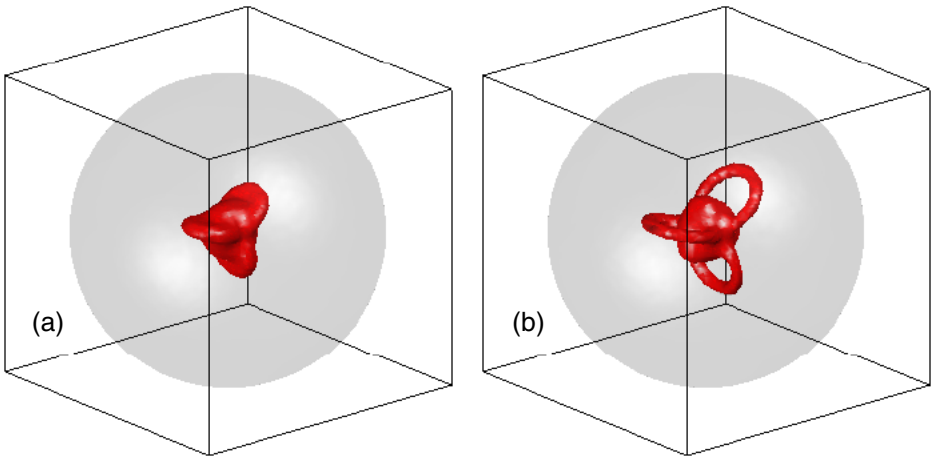

Figure 15. Confined vortex loops arise in sets of threes inside a mesoscopic superconducting sphere (radius 15 ξ), as shown here for two consecutive values of the point-like magnetic moment that occupies its center: (a) $m/m_0 = 16$; (b) $m/m_0 = 21$, by courtesy of M M Doria (unpublished).

the order of the compensation field or higher. The field dependence $T_c(H_{ext})$ for rather thick superconducting films in the high-field limit is similar to the phase transition line described by equation (7). This behavior results from the effective averaging of the inhomogeneous magnetic field by the quasi-uniform OP wavefunction over the sample thickness, which substantially weakens the effect arising from the field modulation in the lateral direction. In other words, only the lateral inhomogeneity leads to the anomalous $T_c(H_{ext})$ dependence and reentrant superconductivity in particular, while the transverse field nonuniformity masks this effect. Interestingly, the location where superconductivity starts to nucleate shifts towards the point with zero total magnetic field (not only the z component of the magnetic field) as the thickness of the superconductor increases (Aladyshkin *et al* [54]).

3. Vortex matter in nonuniform magnetic fields at low temperatures

3.1. London description of a magnetically coupled S/F hybrid system

In section 2 we have reviewed the theoretical modeling within the GL formalism and the experimental data concerning the superconducting properties of S/F hybrids rather close to the

phase transition line $T_c(H_{ext})$. In this section we consider the properties of S/F hybrids for a fully developed superconducting OP wavefunction, i.e. for $T \ll T_{c0}$. In this limit, the superconducting properties of the S/F hybrids can be correctly described by the London theory, omitting any spatial variations of the OP. As before, we assume that the coercive field of the ferromagnet is much higher than the upper critical field of the superconductor. This guarantees that, during the investigation of the superconducting properties, no changes in the ferromagnetic element(s) will occur.

At rather low temperatures one should take into account that the magnetic field, induced by screening (Meissner) currents or by vortices, can no longer be neglected and will strongly interact with the ferromagnet. The free energy functional of the S/F hybrid can be written in the following form [44, 45]:

$$G_{sf} = G_{s0} + G_m + \int_V \left\{ \frac{\lambda^2}{8\pi} \left(\mathrm{rot}\,\mathbf{B}\right)^2 + \frac{\mathbf{B}^2}{8\pi} - \mathbf{B}\cdot\mathbf{M} - \frac{\mathbf{B}\cdot\mathbf{H}_{ext}}{4\pi} \right\} \mathrm{d}V. \tag{17}$$

As before, G_{s0} is the self-energy of the superconductor, while the term G_m depends on the magnetization of the ferromagnet only. Assuming that G_m is constant for a given distribution of magnetization and minimizing this functional G_{sf} with respect to the vector potential $\mathbf{A}$, one can obtain the London–Maxwell equation:

$$\mathbf{B} + \lambda^2\,\mathrm{rot}\,\mathrm{rot}\,\mathbf{B} = \Phi_0 \sum_i \delta(\mathbf{r} - \mathbf{R}_{v,i})\,\mathbf{z}_0 + 4\pi\lambda^2\,\mathrm{rot}\,\mathrm{rot}\,\mathbf{M}, \tag{18}$$

where summation should be done over all vortices, positioned at points $\{\mathbf{R}_{v,i}\}$ and $\delta(r)$ is the Dirac delta function[12]. In equation (18) we assumed that each vortex line, parallel to the z axis and carrying one flux quantum, generates a phase distribution $\Theta = \varphi$ with $\mathrm{rot}(\nabla\Theta) = \mathrm{rot}\,([\mathbf{z}_0 \times \mathbf{r}_0]/r) = \delta(r)\,\mathbf{z}_0$ (here (r, φ, z) are cylindrical coordinates with the origin chosen at the vortex). It should be noticed that the solution of equation (18) gives the magnetic field distribution for a given vortex configuration, and in order to find the field pattern one should find the minimum of the total free energy G_{sf} with respect to the vortex positions $\{\mathbf{R}_{v,i}\}$.

3.2. Interaction of a point magnetic dipole with a superconductor

Next we consider the generic problem of the interaction of a superconductor with a point magnetic dipole positioned at a height Z_d above the superconducting sample. Introducing the OP phase, which determines the density of supercurrents $\mathbf{j}_s = c/(4\pi\lambda^2)\,[\Phi_0/(2\pi)\nabla\Theta - \mathbf{A}]$, the free energy functional equation (17) at $H_{ext} = 0$ can be rewritten as $G_{sf} = G_{s0} + G_m + G_s$, where

$$G_s = \int \left\{ \frac{\Phi_0^2}{32\pi^3\lambda^2}(\nabla\Theta\cdot\nabla\Theta) - \frac{\Phi_0}{16\pi^2\lambda^2}(\nabla\Theta\cdot\mathbf{A}) - \frac{1}{2}\,\mathbf{B}\cdot\mathbf{M} \right\} \mathrm{d}V \tag{19}$$

[12] We follow the standard definition of the δ function: $\delta(x, y) = 0$ for any $x \neq 0$, $y \neq 0$ and $\int_{-\infty}^{-\infty}\int_{-\infty}^{-\infty} \delta(x, y)\,\mathrm{d}x\,\mathrm{d}y = 1$.

similar to that obtained by Erdin *et al* [146]. Due to the linearity of equation (18), we can introduce the field $\mathbf{B}_v = \mathrm{rot}\,\mathbf{A}_v$, generated by a single vortex line positioned at $\mathbf{r} = \mathbf{R}_v$ and the field $\mathbf{B}_m = \mathrm{rot}\,\mathbf{A}_m$, corresponding to the screening (Meissner) current distribution induced by the magnetic dipole[13] As a result, for the particular case of a point magnetic dipole, $\mathbf{M} = \mathbf{m}_0\,\delta(\mathbf{r} - \mathbf{R}_d)$, the energy of the system G_s depending on the supercurrents can be represented as a sum of the self-energy of the vortex $\epsilon_v^{(0)}$, which is independent of the dipolar moment, and a term G_{int}, responsible for the interaction between the dipole and superconductor (e.g. Wei *et al* [147], Carneiro [148]):

$$G_{int} = -\tfrac{1}{2}\,\mathbf{m}_0\cdot\mathbf{B}_m(\mathbf{R}_d) - \mathbf{m}_0\cdot\mathbf{B}_v(\mathbf{R}_d). \tag{20}$$

The first term in equation (20) corresponds to the interaction between the magnetic dipole and the local field at the dipole's position $\mathbf{B}_m(\mathbf{R}_d)$ due to the screening currents. The second term in equation (20) gives the energy of the interaction between the vortex and the magnetic dipole, which consists of two parts: (i) the 'hydrodynamical' interaction between circulating supercurrents due to the vortex on the one hand and the dipole on the other hand and (ii) the interaction between the stray field of the vortex with the magnetic moment. Interestingly both contributions turn out to be equal to $(-1/2)\,\mathbf{m}_0\cdot\mathbf{B}_v(\mathbf{R}_d)$.

3.2.1. *Interaction between a point magnetic dipole and the Meissner currents.*

In the case of a superconductor without vortices (the so-called Meissner state, $\mathrm{rot}(\nabla\Theta) = 0$), the interaction between the dipole and the superconductor is given by $U_m = (-1/2)\,\mathbf{m}_0\cdot\mathbf{B}_m(\mathbf{R}_d)$. It can easily be seen that this energy contribution is always positive, since the screening currents induced by a dipole generate a magnetic field which is opposite to the orientation of the dipole. This is, in principle, just a reformulation of the fact that a magnetic dipole will be repelled by a superconducting film with a force $\mathbf{f} = -\partial U_m/\partial\mathbf{R}_d$. The related problem of levitating a ferromagnetic particle over various superconducting structures was considered theoretically by Wei *et al* [147], Xu *et al* [149], Coffey [150, 151] and Haley [152, 153]. In particular, in the limiting case $Z_d/\lambda \gg 1$ the magnetic levitation force was found to vary linearly with λ, regardless of the shape of the magnet. The fact that λ (as well as the vertical component of the force) shows an exponential temperature dependence for s-wave superconductors, linear-T for d-wave superconductors and quadratic-T^2 dependence in a wide low-temperature range for materials with $s + id$ symmetry of the gap can assist in distinguishing the type of pairing in real samples based on magnetic force microscopy (MFM) measurements [149].

[13] These fields $\mathbf{B}_v$ and $\mathbf{B}_m$ are the solutions of the following differential equations:

$$\mathbf{B}_v + \lambda^2\,\mathrm{rot}\,\mathrm{rot}\,\mathbf{B}_v = \Phi_0\,\delta(\mathbf{r} - \mathbf{R}_v)\,\mathbf{z}_0,$$
$$\mathbf{B}_m + \lambda^2\,\mathrm{rot}\,\mathrm{rot}\,\mathbf{B}_m = 4\pi\lambda^2\,\mathrm{rot}\,\mathrm{rot}\,\mathbf{M}.$$

3.2.2. Creation of vortices by the stray field of a magnetic dipole. In reality, magnetic dipoles which have a high dipolar moment or are localized rather close to the superconductor can suppress the Meissner state due to the dipole's stray field. The possible appearance of a vortex would change the total energy of the S/F hybrid system by $G_s = \epsilon_v^{(0)} + \epsilon_{mv}$, where $\epsilon_{mv} \propto -m_0$ accounts for the dipole–vortex interaction. Clearly, one can make $G_s < 0$ by increasing m_0 and therefore it will become energetically favorable to generate vortices in the system. Such a scenario for the formation of the mixed state was considered, for example, by Wei *et al* [147, 154] for a vertically magnetized dipole placed above a thin superconducting film. As a consequence of equation (20), the appearance of a vortex line in the superconductor drastically changes the resulting force acting on the magnetic dipole (Xu *et al* [149], Wei *et al* [147, 154]).

It is important to notice that, in the case of superconducting films infinite in the lateral direction and cooled in zero magnetic field, a spontaneously induced vortex should be accompanied by an antivortex in order to provide flux conservation imposed by Maxwell's equations[14]. The destruction of the Meissner state in a zero-field-cooled superconducting film was theoretically studied by Mel'nikov *et al* [155] and Aladyshkin *et al* [156]. In this case the formation of the mixed state occurs via the penetration of vortex semi-loops which split into vortex–antivortex pairs. The local suppression of the Bean–Livingston energy barrier [157], which controls the process of vortex penetration, takes place when the screening current density will be of the order of the depairing current density. The threshold distance $Z_d^* = Z_d^*(T)$, corresponding to the suppression of the energy barrier can be experimentally detected by measuring a nonzero remanent magnetization as long as pinning is relevant. Interestingly, such a non-contact technique allows one to estimate the depairing current density and its temperature dependence in thin superconducting $YBa_2Cu_3O_7$ films [155, 156, 158]. Since the surface energy barrier in superconductors with a flat surface is known to be suppressed by applying an external field of the order of the critical thermodynamical field $H_{cm} = \Phi_0/(2\sqrt{2}\pi\lambda\xi)$ [43], one can get a rough criterion for the persistence of the vortex-free state in the presence of a magnetic dipole: $m_0/Z_d^3 \lesssim H_{cm}$. A different criterion should be obtained in case the dipole is already present close to the superconductor and the whole system is cooled down below the superconducting temperature. Under this field-cooled condition a lower critical magnetization to induce a vortex–antivortex pair is expected.

The problem of the formation of vortex–antivortex pairs in superconducting films in the presence of vertically and horizontally magnetized dipoles at $H_{ext} = 0$ was considered theoretically by Milošević *et al* [159, 160] and Carneiro [148]. It was shown that an equilibrium vortex pattern could consist of spatially separated vortices and antivortices (for rather thin superconducting films) or, when the superconducting film thickness increases and becomes comparable to the London penetration depth, curved vortex lines, which start and terminate at the surface of the superconductor.

[14] In mesoscopic superconducting systems, the returning flux lines generated by an out-of-plane magnetized dipole can bypass the border of the sample and the existence of an antivortex is not required.

3.2.3. Magnetic pinning. Now we will discuss the properties of S/F hybrids where the magnetization of the ferromagnet and the distance between ferromagnet and superconductor are assumed to be fixed, resulting in a constancy of the interaction energy with the screening currents induced by the ferromagnet. In this case, any variation of the free energy of the S/F hybrid in the presence of vortices (either induced by the ferromagnetic element or by external sources) can be attributed to the rearrangements of the vortex pattern. The part of the interaction energy G_{int}, proportional to the magnetization of the ferromagnet and sensitive to the vortex positions, is usually called the magnetic pinning energy U_p.

In order to illustrate the angular dependence of the interaction between a point magnetic dipole of fixed magnetization and a vortex, we refer to the following expression (Carneiro [148], Milošević *et al* [159, 160]):

$$U_p(r_\perp) \approx \frac{\Phi_0 D_s}{2\pi\lambda}\left[-\frac{1}{2}\left(\frac{m_{0,z}}{\Phi_0\lambda}\right)\frac{1}{\sqrt{r_\perp^2 + Z_d^2}} + \frac{1}{2}\left(\frac{m_{0,x}}{\Phi_0\lambda}\right)\frac{r_\perp\cos\phi}{\sqrt{r_\perp^2 + Z_d^2}(Z_d + \sqrt{r_\perp^2 + Z_d^2})}\right], \quad (21)$$

obtained for a thin superconducting film $D_s \ll \lambda$ and for vortex–dipole separations smaller than the effective penetration depth $\lambda_{2D} = \lambda^2/D_s$. Here $m_{0,x}$ and $m_{0,z}$ are the in-plane and out-of-plane components of the dipolar moment, $r_\perp = \sqrt{x^2 + y^2}$, $\mathbf{R}_d = (0, 0, Z_d)$ is the position of the dipole and ϕ is the angle between the x axis and the vector position of the vortex in the plane of the superconductor $\mathbf{r}_\perp$. The resulting pinning potentials for an in-plane and out-of-plane magnetized dipole, derived from equation (21), are shown in figure 16. The pinning of vortices (and antivortices) in the superconducting films of a finite thickness on the magnetic dipole at $H_{ext} = 0$ was analyzed by Milošević *et al* [159, 160] and Carneiro [148, 161]. In addition, Carneiro considered the magnetic pinning for the case of a dipole able to rotate freely in the presence of the external magnetic field [162–164] or external current [162].

In [148] it was shown that this magnetic pinning potential has a depth of $m_0/(4\pi\lambda)$ and penetrates a distance λ into the film whereas its range parallel to the film surface is a few times λ. This finding points out the relevance of the penetration depth λ to characterize the purely magnetic pinning potential. Since typical λ values are similar for a broad spectrum of superconducting materials, this suggests that magnetic pinning represents a promising way of increasing the critical current not only in conventional superconductors but also in high-T_c superconductors. Notice that the fact that the magnetic pinning range is determined by λ sets a limit for the minimum distance between magnetic particles, beyond which the vortex lines cannot resolve the field modulation and therefore the pinning efficiency decreases. Having in mind that many practical applications typically involve high-T_c superconductors with $\xi \ll \lambda$, it becomes clear that this maximum density of pinning sites to trap individual vortices is much lower than that limited due to core pinning.

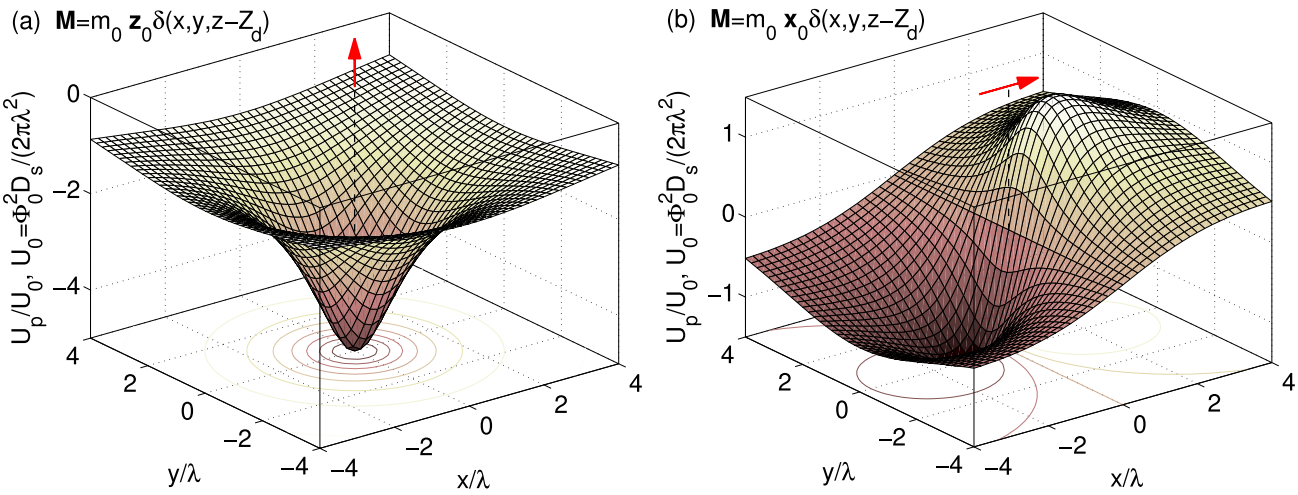

Figure 16. The spatial dependence of the energy of a single vortex in a field of point magnetic dipole, $\mathbf{M} = \mathbf{m}_0\delta(x, y, z - Z_d)$, calculated according to equation (21) for the height $Z_d/\lambda = 1$ and the dipole strength $m_0/(\Phi_0\lambda) = 10$: (a) vertically magnetized dipole, $\mathbf{m}_0 = m_0\mathbf{z}_0$, (b) horizontally magnetized dipole, $\mathbf{m}_0 = m_0\mathbf{x}_0$.

It is important to mention that real nanoengineered ferromagnetic elements are quite far from point dipoles but rather consist of extended volumes of a magnetic material, such as magnetic dots and stripes. In this case, due to the principle of superposition, the magnetic pinning energy needs to be integrated over the volume of the ferromagnet V_f to determine the interaction between a vortex line and a finite size permanent magnet:

$$U_p(\mathbf{r}) = -\int_{V_f} \mathbf{M}(\mathbf{r}') \cdot \mathbf{B}_v(\mathbf{r} - \mathbf{r}')\, d^3r'. \qquad (22)$$

The magnetic pinning in an infinite superconducting film produced by individual ferromagnetic objects of finite size was considered for the following cases: a ferromagnetic sphere magnetized out-of-plane (Tokman [165]), magnetic discs, rings, rectangles, and triangles magnetized out-of-plane (Milošević *et al* [160, 166]), magnetic bars and rectangular dots magnetized in-plane (Milošević *et al* [167]), circular dots magnetized either in-plane or out-of-plane (Erdin *et al* [146], Erdin [168]), circular and elliptic dots and rings magnetized out-of-plane (Kayali [169, 170], Helseth [171]) and columnar ferromagnetic rods (Kayali [172]). The analysis of the pinning properties of a vortex in a semi-infinite superconducting film due to magnetic dots was done by Erdin [173]. Similar to the case of a point magnetic dipole, the extended magnetic objects are able to generate vortex–antivortex pairs provided that the size and the magnetization are large enough.

We would like to note that the attraction of a superconducting vortex to a source of inhomogeneous magnetic field (e.g. coil on a superconducting quantum interference device or magnetized tip of a magnetic force microscope) makes it possible to precisely manipulate the position of an individual vortex. Such experiments were performed by Moser *et al* [174], Gardner *et al* [175] and Auslaender *et al* [176] for high-T_c superconducting thin films and single crystals at intermediate temperatures when intrinsic pinning become weaker. This technique apparently opens unprecedented opportunities, for example, for a direct measuring of the interaction of a moving vortex with the local disorder potential and for preparing exotic vortex states like entangled vortices (Reichhardt [177]).

Equation (22) shows that the pinning potential does not only depend on the size and the shape of the ferromagnetic elements but also on the particular distribution of the magnetization (i.e. on their exact magnetic state). It is expected that the average pinning energy is less efficient for magnetic dots in a multi-domain state whereas it should reach a maximum for single-domain structures. In other words, if the size of the magnetic domains is small in comparison with λ or the separation distance Z_d, then a vortex line would feel the average field emanating from the domains and the magnetic pinning should be strongly suppressed. This flexibility of magnetic pinning centers makes it possible to tune the effective pinning strength, as we shall discuss below.

The question now arises whether the pinning potential produced by a magnetic dipole will remain efficient when a vortex–antivortex pair is induced by the magnetic dipole. In order to answer this question it is necessary to minimize the mutual interaction between the induced vortex–antivortex pair, the magnetic element and the test vortex generated by the external field. The magnetic moment—test vortex interaction is a linear function of m_0 always favoring the test vortex to sit on the positive pole of the magnet, whereas the induced currents—test vortex interaction will follow the Little–Parks oscillations (due to the creation of vortices by the dipole).

For the case of an in-plane dipole, Milošević *et al* [167] demonstrated that all these terms produce a subtle balance of forces which lead to a switching of the optimum pinning site from the positive to the negative magnetic pole, as m_0 is increased. For the case of the out-of-plane magnetic dipole, once a vortex–antivortex pair is induced, the test vortex will annihilate the antivortex, leaving a single vortex on top of the magnetic dot (Gillijns *et al* [123]).

3.3. Magnetic dots in the vicinity of a plain superconducting film

The rich variety of possibilities considered theoretically in the previous section for an individual ferromagnetic element in close proximity to a superconducting film represents an experimental challenge in part due to the difficulties associated with recording small induced signals. A very successful way to overcome this limitation consists of studying the average effect of a periodic array of dots at the expense of blurring sharp transitions, such as the vortex–antivortex generation, or inducing new collective phenomena associated with the periodicity of the magnetic templates. An important experimental condition that should be satisfied in order to justify the analogies drawn between individual dipoles and arrays of dipoles is the lack of magnetostatic interactions between neighboring dipoles. In other words, it is necessary to ensure that the field generated by a dipole at the position of its nearest neighbors lies below the coercive field of the chosen ferromagnetic materials (Cowburn *et al* [178, 179], Novosad *et al* [180, 181]).

3.3.1. Commensurability effects in S/F hybrids with periodic arrays of magnetic dots. In the early 1970s, Autler [182, 183] proposed that a periodic array of ferromagnetic particles should give rise to an enhancement of the critical current of the superconducting material. Recent developments on lithographic techniques have made it possible to prepare superconducting structures containing a regular array of magnetic dots (Co, Ni, Fe) at the submicrometer scale of desirable symmetry in a controlled way (Otani *et al* [119], Geoffroy *et al* [120], Martín *et al* [184–187], Morgan and Ketterson [188, 189], Hoffmann *et al* [190], Jaccard *et al* [191], Villegas *et al* [192–194], Stoll *et al* [195], Van Bael *et al* [196–201], Van Look *et al* [202]). The S/F hybrids containing periodic arrays of magnetic elements with out-of-plane magnetization (multilayered Co/Pt and Co/Pd

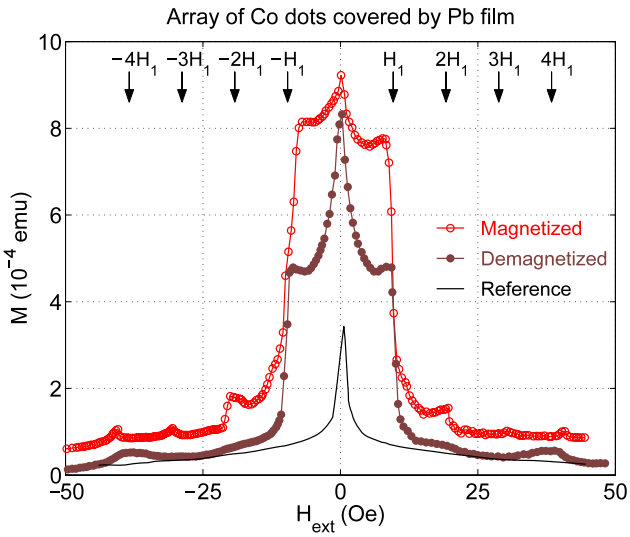

Figure 17. Upper half of the magnetization loop M versus H_{ext} at $T/T_{c0} = 0.97$ for a superconducting Pb film (50 nm thickness) on top of a triangular lattice of Au/Co/Au dots (period 1.5 μm corresponding to a first matching field of 9.6 Oe) before and after magnetizing the dots (filled and open symbols, respectively) and for a reference Pb 50 nm film (solid line), adapted figure with permission from Van Bael *et al* 1999 *Phys. Rev.* B **59** 14674 [196]. Copyright (1999) by the American Physical Society. The curve for the magnetized dots is slightly shifted upwards for clarity.

structures) were fabricated and investigated by Van Bael *et al*, [198–201, 203, 204] and Lange *et al* [205, 206]. In all these works, it was found that the presence of the lattice of magnetic dots leads either to (i) a resonant change in the magnetoresistance $\rho(H_{ext})$ and the appearance of pronounced equidistant minima of resistivity with the period $H_1 = \Phi_0/S_0$ determined by the size of the magnetic unit cell S_0 [119, 120, 184–187, 189–195] or (ii) to the presence of

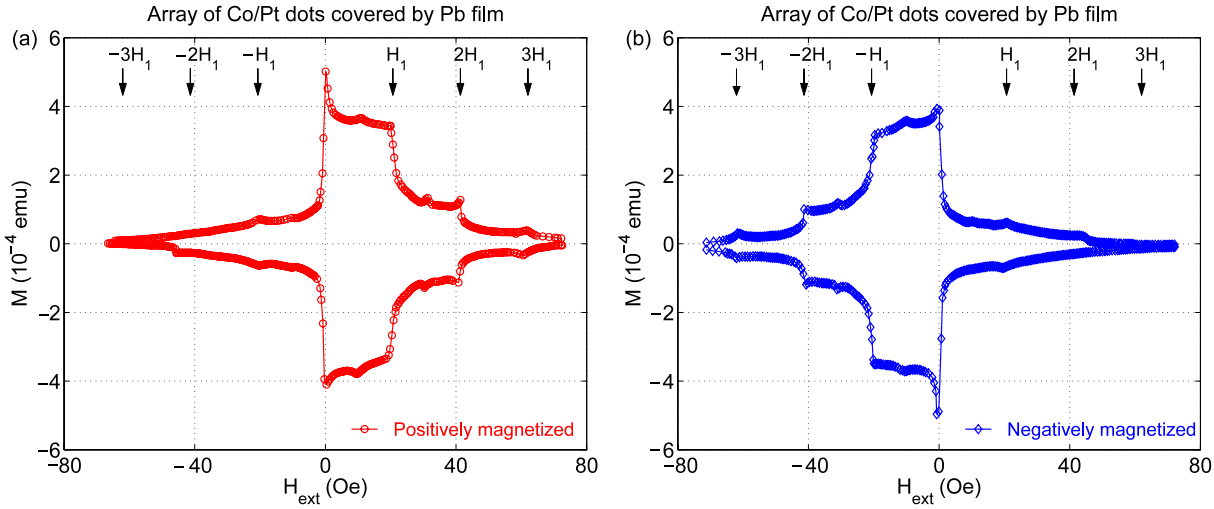

Figure 18. Magnetization curves M versus H_{ext} at $T = 7$ K ($T_{c0} = 7.17$ K, $T/T_{c0} = 0.976$) for a superconducting Pb film (50 nm thickness) on top of a Co/Pt dot array (the period is 1.0 μm, the first matching field is 20.68 Oe) with all dots aligned in the positive (a) and negative (b) direction. Both figures were adapted with permission from Van Bael *et al* 2003 *Phys. Rev.* B **68** 014509 [204]. Copyright (2003) by the American Physical Society.

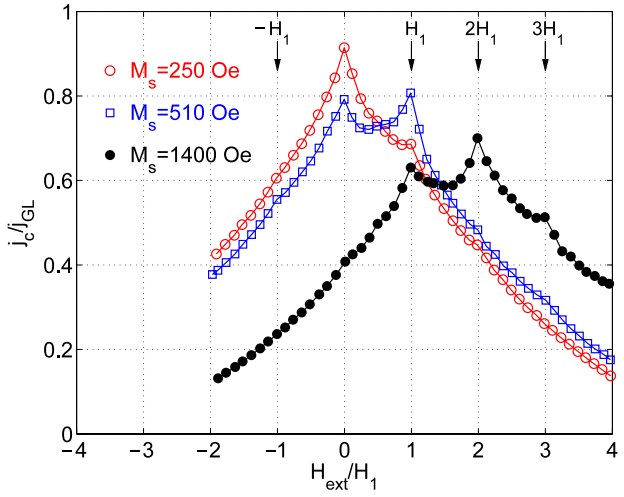

Figure 19. Field dependence of the critical depinning current j_c, calculated for a periodic array of out-of-plane magnetized dots. The values of the dot's magnetization are indicated in the plot. j_{GL} is the density of the depairing (Ginzburg–Landau) current, $T/T_{c0} = 0.9$, adapted figure with permission from Milošević and Peeters 2005 *Europhys. Lett.* **70** 670–6, copyright 2005 by IOP Publishing. It is worth noting that (i) $j_c(H_{ext})$ is asymmetric similar to that shown in figure 18 and (ii) the quantized displacement of the j_c maximum toward nonzero H_{ext} value is sensitive to the magnetization of the dots.

distinct features as peaks or plateaus in the field dependence of the critical current $I_c(H_{ext})$ or in the magnetization curve $M(H_{ext})$ [188–190, 196, 198–206].

Such matching effects are also very well known for spatially modulated superconducting systems with antidot lattices without ferromagnetic constituents (e.g. Baert *et al* [52], Moshchalkov *et al* [53], Hebard *et al* [207], Rosseel *et al* [208], Harada *et al* [209], Metlushko *et al* [210]). These periodic anomalies are commonly explained in terms of commensurability effects between the vortex lattice governed by the external field and the artificially introduced pinning potential at an integer number of vortices per unit cell at $H_{ext} = \pm nH_1$ (with n integer). Typically these lithographically defined arrays are limited to a minimal period of the unit cell of the order of a few hundred nanometers, giving rise to a maximum matching field $H_1 \simeq 10$–10^2 Oe. Alternative methods for introducing more closely packed particles and thus larger H_1 values can be achieved by Bitter decoration (Fasano *et al* [211, 212], Fasano and Menghini [213]) or a diversity of self-assembled techniques (Goyal *et al* [214], Villegas *et al* [215], Welp *et al* [216, 217], Vinckx *et al* [218], Vanacken *et al* [219]).

The field dependence of the critical current $I_c(H_{ext})$ and magnetization $M(H_{ext})$, can be symmetrical or asymmetrical with respect to $H_{ext} = 0$ depending on the dot's net magnetization (compare figures 17 and 18). The latter takes place for arrays of magnetic dots with out-of-plane magnetization [198–201, 203–206]. Indeed, vertically magnetized dots with average magnetic moment $\langle \mathbf{m} \rangle_z > 0$, similar to point magnetic dipoles, produce a stronger pinning potential for vortices (at $H_{ext} > 0$ when $\langle \mathbf{m} \rangle \parallel \mathbf{H}_{ext}$) than for antivortices ($H_{ext} < 0$). In contrast to that, in-plane magnetized dots are able to pin vortices and antivortices at the magnetic poles equally well (see equation (21) and figure 16). This explains the experimentally observed field polarity dependent (asymmetric) pinning for arrays of out-of-plane magnetized particles (figures 18 and 19).

The interaction between vortices and a periodic array of hard magnetic dots on top or underneath a plain superconducting film within the London approximation[15] was theoretically analyzed by Helseth [225], Lyuksyutov and Pokrovsky [226], Šášik and Hwa [227], Erdin [228], Wei [229, 230] and Chen *et al* [231]. These calculations show that, at $H_{ext} = 0$ for out-of-plane magnetized dots, vortex–antivortex pairs can be created in thin film superconductors with the vortices always sitting on top of the magnetic dot and the antivortices located in between the dots. For in-plane magnetized dots (or magnetic bars), the vortex and antivortex will be located at opposite sides of the magnetic dots as described above for individual magnetic dipoles. Unlike the case of an isolated dipole, the threshold magnetization value needed to create a vortex–antivortex pair is also a function of the period of the lattice (Milošević and Peeters [114]). Direct visualization of vortex lattice via scanning Hall probe microscopy was achieved for a square array of in-plane dots by Van Bael *et al* [197] and for out-of-plane dots by Van Bael *et al* [204] and Neal *et al* [232]. It is known that the preferred vortex configuration in a homogeneous defect-free superconducting film should be close to a triangular lattice because of the repulsive vortex–vortex interaction [43–45]. The artificially introduced pinning appears to be the most effective provided that each vortex is trapped by a pinning center, i.e. when the symmetry of the pinned vortex lattice coincides with that imposed by the topology of the internal magnetic field. The transition between square and distorted triangular vortex lattice, induced by variation of the strength of the periodic pinning potential and the characteristic length scale of this interaction, was considered by Pogosov *et al* [233] for superconductors with a square array of pinning centers. Experimentally the field-induced reconfiguration of the vortex lattice (from rectangular to square) for superconducting Nb films and rectangular arrays of circular magnetic Ni and Co dots was reported by Martín *et al* [185] and Stoll *et al* [195] as an abrupt increase of the period of the oscillation in the $\rho(H_{ext})$ dependence (resulting from the shrinkage of the period of the vortex lattice) and decrease of the amplitude of such oscillations (due to a weakening of the effective pinning) while increasing $|H_{ext}|$.

The dependence of the magnetic pinning in superconducting Nb films on the diameter of the Ni dots was studied by Hoffmann *et al* [190]. They found that more minima appear in the magnetoresistance (or maxima in the critical current) as the

[15] This issue seems to be part of a more general problem of the interaction of vortex matter with a periodic potential regardless the nature of the pinning in the superconducting system (see, for example, Reichhardt *et al* [220–224] and references therein). In this review we discuss only the results obtained for the S/F hybrids, keeping in mind that similar effects can be observed for non-magnetic patterned superconductors as well.

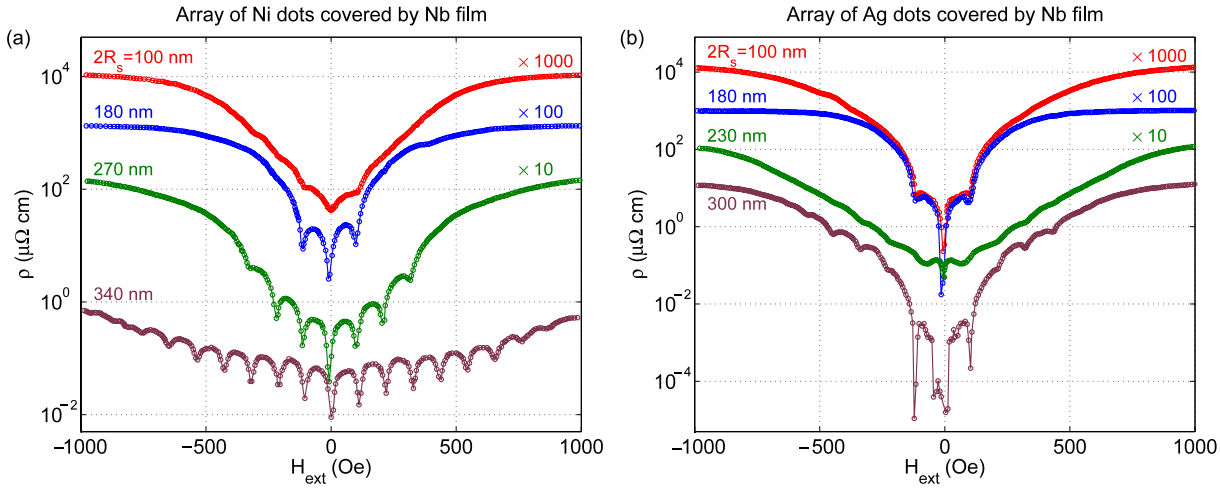

Figure 20. (a) Field dependence of the electrical resistance ρ for a superconducting Nb film covering periodic arrays of the magnetic Ni dots with different dot's diameter (indicated in the plot), but for the same lattice constant 400 nm. The curves are shifted by factors of 10 from each other for clarity. (b) Dependences $\rho(H_{\rm ext})$ for samples with different diameters of non-magnetic Ag dots. Both figures were adapted with permission from Hoffmann *et al* 2000 *Phys. Rev.* B **61** 6958 [190], copyright (2000) by the American Physical Society.

lateral dot's size increases, indicating thus an enhanced pinning (panel (a) in figure 20). This effect can be caused by the two parameters which increase with the dot size: the total magnetic moment $\langle \mathbf{m} \rangle$ (proportional to the dot's volume $V_{\rm f} = \pi R_{\rm f}^2 D_{\rm f}$) and the area of the order of $\pi R_{\rm f}^2$, where superconductivity might be locally suppressed due to the high stray field or proximity effect. In addition, larger magnetic dots can stabilize giant vortices carrying more than one flux quantum.

3.3.2. Periodic arrays of magnetic antidots. The antipode of arrays of magnetic dots is a perforated ferromagnetic film (so-called magnetic antidots), which also produces a periodic magnetic field. This system can be regarded as the limiting case of large magnetic dots with a diameter larger than the period of the periodic lattice.

Magnetic antidots in multilayered Co/Pt films, characterized by an out-of-plane remanent magnetization, and their influence on the superconducting properties of Pb films were studied by Lange *et al* [205, 234–236]. From magnetostatic considerations, such submicron holes in a ferromagnetic thin film generate a very similar field pattern as an array of magnetic dots of the same geometry, but with opposite sign. As a consequence, the enhanced magnetic pinning and the pronounced commensurability peaks in the $M(H_{\rm ext})$ dependence are observed for the opposite polarity of the external field (i.e. at $H_{\rm ext} < 0$ for positively magnetized film and vice versa), see figure 21. However the matching effects are considerably weakened in the demagnetized state of the Co/Pt multilayer with holes as compared with the demagnetized array of magnetic dots, thus indicating that an irregular domain structure effectively destroys a long-range periodicity [205].

Van Bael *et al* [237] and Raedts *et al* [238] explored perforated Co film with in-plane anisotropy. In this case the magnetic field distribution becomes non-trivial since such magnetic antidots effectively pin magnetic domain walls which generate a rather strong magnetic field. As a result, neither matching effects nor pronounced asymmetry were observed in the magnetization curves of the superconducting layer, but only an overall enhancement of the critical current after the sample was magnetized along the in-plane easy axis, in comparison with the demagnetized state.

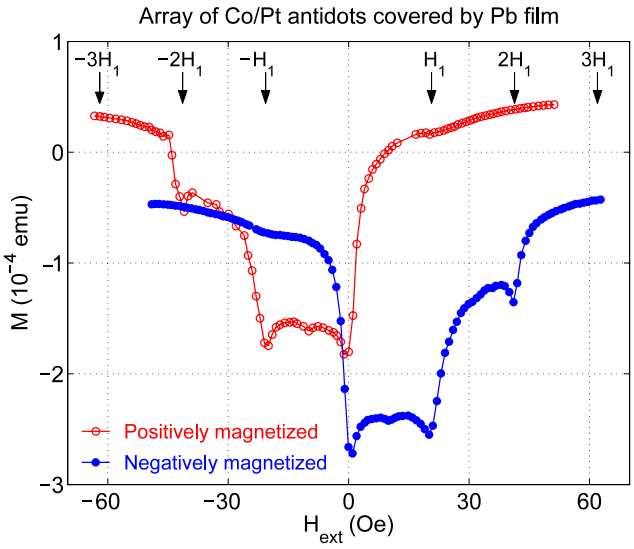

Figure 21. Magnetization curves $M(H_{\rm ext})$ at $T = 7.05$ K ($T_{\rm c0} = 7.20$ K, $T/T_{\rm c0} = 0.972$) of a superconducting Pb film on top of a magnetic Co/Pt antidot lattice (the period is 1.0 μm, the first matching field is 20.68 Oe) after saturation in a positive field ($M_z > 0$, open circles) and after saturation in a negative field ($M_z < 0$, filled circles), adapted figure with permission from Lange *et al* 2005 *Europhys. Lett.* **57** 149 [235]. Copyright (2005) by IOP Publishing.

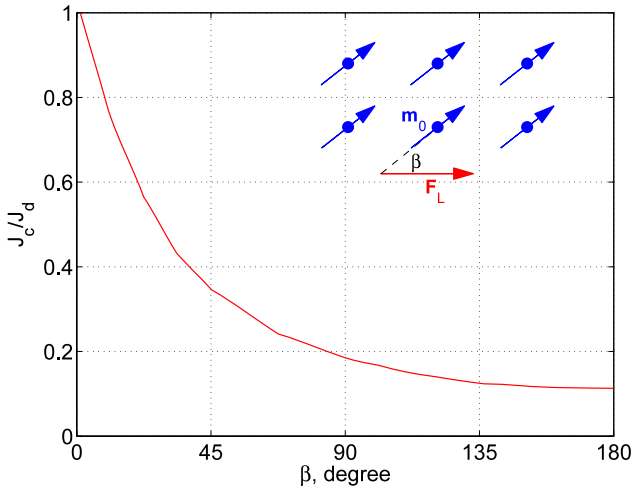

Figure 22. Critical current, J_c, for a vortex pinned by a dipole array as a function of the angle β between the magnetic moments and the driving force. Here J_d is the depairing current. Reprinted from Carneiro G 2005 *Physica* C **432** 206–14. Copyright (2005) with permission from Elsevier.

3.3.3. Anisotropy of the transport characteristics and guidance of vortices. In any periodic array of pinning centers, transport properties such as magnetoresistance $\rho(H)$ and the critical current $J_c(H)$ exhibit a dependence not only on the absolute value of H_{ext}, but also on the direction of the applied transport current with respect to the principal translation vectors of the periodic pinning array (Villegas *et al* [193, 194], Soroka and Huth [239], Vélez *et al* [240], Silhanek *et al* [241], Wördenweber *et al* [242]). Interestingly, the direction of the Lorentz force $\mathbf{f}_L = c^{-1}[\mathbf{j} \times \mathbf{B}]$ and the drift velocity of the vortex lattice do not generally coincide. It was demonstrated that, for rectangular arrays of magnetic dots, the minimum of resistivity corresponds to a motion of the vortex lattice along the long side of the array cell. Such behavior was predicted by Reichhardt *et al* [223] by numerical simulations, indicating that a rectangular array of pinning centers induces an easy direction of motion for the vortex lattice (and larger dissipation as well) along the short side of the array cell.

Similar anisotropic transport properties were studied by Carneiro [243] for the case of a periodic array of in-plane magnetic dipoles. In order to illustrate the angular dependence of the critical depinning current on the angle β between the direction of the injected current and the magnetic moment of in-plane oriented dipoles we refer to figure 22. Interestingly, Verellen *et al* [244] showed that this resulting guided vortex motion in square arrays of magnetic rings can be rerouted by 90° simply by changing the dipole orientation or can even be suppressed by inducing a flux-closure magnetic vortex state with very low stray fields in the rings. Similar anisotropic vortex motion was recently observed in Nb films with a periodic array of one-dimensional Ni lines underneath by Jaque *et al* [245]. The mentioned channeling of vortices lead to an anisotropic vortex penetration that has been directly visualized by means of magneto-optics experiments (Gheorghe *et al* [246], see figure 23(b)).

3.3.4. Mechanisms of pinning in S/F hybrids. It should be noticed that the magnetic pinning originating from the spatial modulation of the 'internal' magnetic field generally competes with so-called core pinning resulting from structural inhomogeneities in real samples (either regular or random defects). In addition to random intrinsic pinning, the fabrication of an array of magnetic particles naturally leads to an alteration of the local properties of the superconducting film (e.g. due to proximity effects, corrugation of the superconducting layer or local suppression of the critical temperature). As a consequence, both magnetic and structural modulation share the same periodicity and a clear identification of the actual pinning type becomes difficult.

A direct comparison of the pinning properties of arrays of magnetic versus non-magnetic dots has been addressed by Hoffmann *et al* [190] and Jaccard *et al* [191]. These reports show that, even though both systems display commensurability features, the pinning produced by magnetic arrays of Ni dots is substantially stronger than that produced by non-magnetic Ag particles (figure 20). In our opinion, the main issue whether the enhanced pinning for the sample with ferromagnetic Ni dots actually arises from purely magnetic interactions and not from an additional suppression of the local critical temperature, e.g. due to the enhanced magnetic field near magnetic dots, remains unclear. In principle, the most straightforward way to distinguish the two competing pinning mechanisms is the mentioned field polarity of the magnetic pinning for the S/F hybrids with dots magnetized perpendicularly, i.e. exploring the broken field polarity symmetry.

Clear evidence of the field polarity dependent pinning properties has been reported by Gheorghe *et al* [246] in Pb films on top of a square array of $[Co/Pt]_{10}$ dots with a well-defined out-of-plane magnetic moment. In this work the authors show that the critical current of the hybrid system can be increased by a factor of 2 when the magnetic dots are switched from low stray field in the demagnetized state (disordered magnetic moment) to high stray field in the magnetized state (nearly single domain state) at temperatures as low as $T \simeq 0.3\,T_{c0}$ (see figure 24). Additional evidence of an increase of the critical current at low temperatures (far from the superconducting/normal phase boundary) produced by magnetic dots was reported by Terentiev *et al* [248–250].

3.3.5. Tunable pinning centers. An apparent advantage of using magnetic pinning centers is their flexibility (tunability) in contrast to core pinning on structural inhomogeneities. Indeed, according to equation (22) the magnetic pinning should be sensitive to the particular distribution of magnetization inside the ferromagnetic elements. Depending on the geometrical details of the dot and the magnetic anisotropy of the chosen material a huge variety of magnetic states can be found. For instance, domain formation is expected to be suppressed for structures with lateral dimensions smaller than tens of nm (Raabe *et al* [251]), whereas for larger sizes the magnetic sample breaks into domains of different orientation (Seynaeve *et al* [252]). The exact transition from single domain to multi-domain structures depends on the shape, dimensions, temperature and particular material, among other parameters.

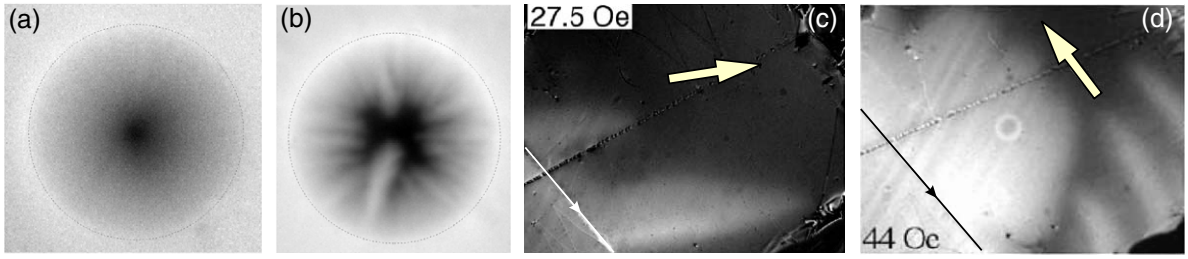

Figure 23. (a) Magneto-optical image of a non-patterned superconducting Pb disk at $T = 2$ K and $H_{ext} = 50$ Oe, demonstrating an isotropic flux penetration. White corresponds to a high local magnetic field and black to zero local field. The external field is applied parallel to the dot's magnetic moment. (b) Magneto-optical image of a circular Pb sample decorated by fully magnetized Co/Pt dots, obtained at $T = 2$ K and $H_{ext} = 72$ Oe. Both figures were adapted with permission from Gheorghe *et al* 2008 *Phys. Rev.* B **77** 054502 [246]. Copyright (2008) by the American Physical Society. (c) Magneto-optical image of flux entry in a superconducting $NbSe_2$ single crystal at $H_{ext}^{\perp} = 16.5$ Oe, $T = 4.5$ K following the preparation of stripe domain structures in a permalloy film by turning on and off an in-plane field of $H_{ext}^{\parallel} = 1$ kOe at an angle of 45° with respect to the sample edge at $T > T_{c0}$. The brightness of the magneto-optical contrast corresponds to the vortex density. The large yellow arrow shows the preferential flux entry direction coinciding with the direction of the stripe domains in the Py film. The thin solid line with arrow marks the sample edge. (d) Same as in panel (c) after application and switching off of $H_{ext}^{\parallel} = 1$ kOe along the sample edge at $T > T_{c0}$. Both figures were adapted with permission from Vlasko-Vlasov *et al* 2008 *Phys. Rev.* B **77** 134518 [247]. Copyright (2008) by the American Physical Society.

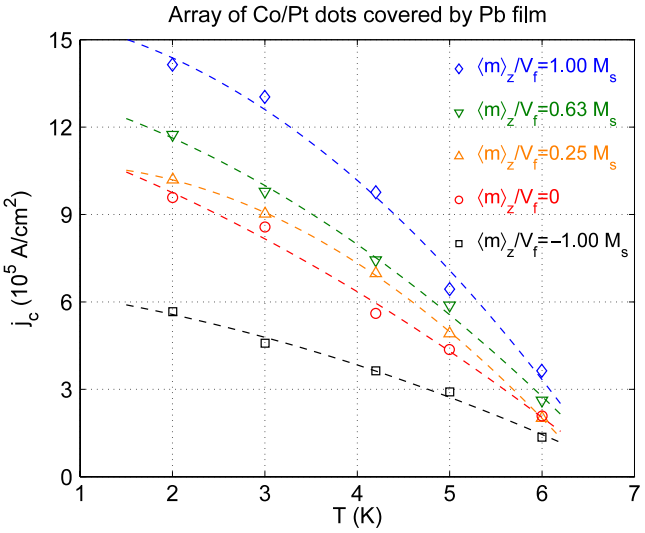

Figure 24. Temperature dependence of the critical current density j_c, estimated from magneto-optical images, for a superconducting Pb film with square array of the ferromagnetic Co/Pt dots on top, in various magnetic states of the dots: demagnetized (○), fully magnetized parallel configuration (◇), fully magnetized antiparallel configuration (□), partially magnetized parallel, $\langle m \rangle_z = 0.25\, M_s V_f$ (△) and $\langle m \rangle_z = 0.63\, M_s V_f$ (▽), adapted figure with permission from Gheorghe *et al* 2008 *Phys. Rev.* B **77** 054502 [246], copyright (2008) by the American Physical Society. The dashed lines are guides to the eye.

More recently, Villegas *et al* [215, 253] and Hoffmann *et al* [254] experimentally investigated the switching of the ferromagnetic dots from single domain to magnetic vortex state while sweeping the external field and the influence of their stray fields on the resistivity of the S/F hybrid sample (figure 25). The interaction between a vortex in a superconducting film and a magnetic nanodisc in the magnetic vortex state was studied theoretically by Carneiro [255]. For magnetic dots big enough to host a multi-domain state it is possible to tune the average magnetic moment by partially magnetizing the sample in a field lower than the saturation field or even recover the virgin state by performing a careful degaussing procedure similar to that shown in figure 6 (Gillijns *et al* [96, 123], Lange *et al* [256]). Interestingly, recently Cowburn *et al* [178] showed that small discs of radii about 50 nm made of supermalloy (Ni-80%, Fe-14%, Mo-5%) lie in a single domain state with the magnetization parallel to the disc plane and with the property that their direction can be reoriented by small applied fields. This system represents the closest experimental realization of in-plane free-rotating dipoles, which was theoretically analyzed by Carneiro [162–164] within the London formalism.

Whatever the mechanism of pinning produced by the magnetic dots, either core or electromagnetic, it is now a clearly established fact that changing the domain distribution in each dot has profound effects on the superconducting pinning properties as demonstrated, for example, by Van Bael *et al* [196] and Van Look *et al* [202]. This result points out the importance of performing a careful study of the magnetic properties of the dots in order to identify the domain size, shape, distribution and stable states. Van Bael *et al* [196] presented the first report directly linking changes in the hysteresis loop of a superconducting Pb film when the underlying submicron Co islands are switched from a 2×2 checkerboard magnetic domain pattern to single-domain structures.

As we pointed out above, unfortunately both the multi-domain state and the magnetic vortex state still involve a sizable component of the magnetic stray field which eventually influences the response of the superconducting properties by locally suppressing the order parameter. In other words, it is actually not possible to completely switch off the magnetic pinning using singly connected structures. It has been recently shown that a way to partially circumvent this limitation can be achieved by using multiply connected ring-like magnetic

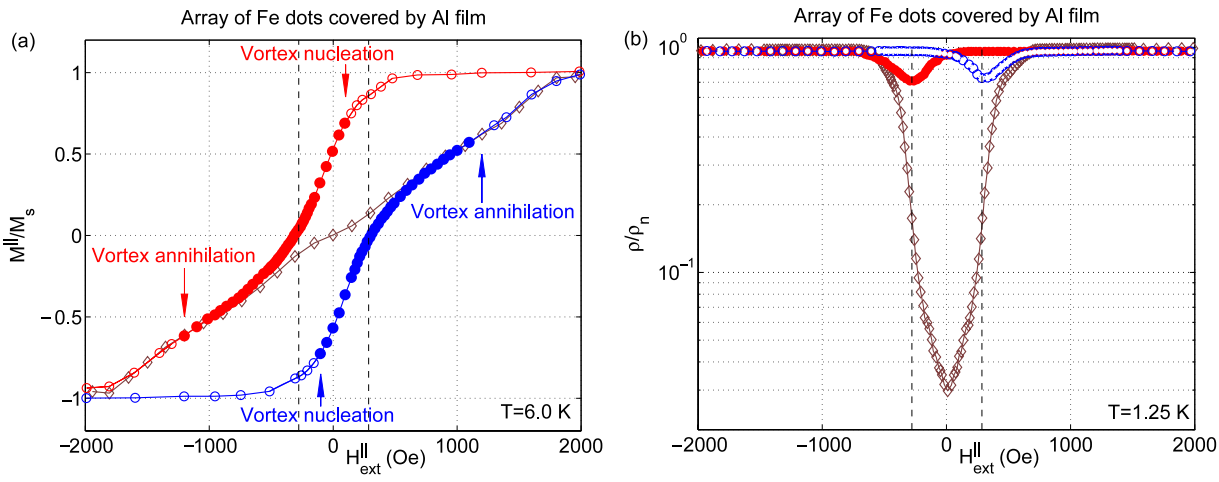

Figure 25. (a) Normalized magnetization $M^{\parallel}/M_s$ versus in-plane applied field $H^{\parallel}_{ext}$ (M_s is the saturated magnetization) for an array of Fe dots with average diameter of 140 nm and average interdot distance of 180 nm measured at $T = 6$ K (above the critical temperature of superconducting Al film). Brown diamonds correspond to a virgin state of the Fe dots, the magnetic state depicted by red (blue) circles obtained after saturation in positive (descending branch) and negative (ascending branch) magnetic fields, respectively. The filled circles schematically show the regions where the magnetic vortex is expected to take place. Vertical dashed lines mark the coercive fields. (b) Normalized resistivity ρ versus in-plane applied field $H^{\parallel}_{ext}$ for the same sample at $T = 1.25$ K (below the critical temperature of superconducting Al film), where ρ_n is the normal-state resistance. Open (blue) and filled (red) circles mark the curves measured from negative and positive saturation, respectively, while brown diamonds correspond to the virgin state. Both figures were adapted with permission from Villegas *et al* 2007 *Phys. Rev. Lett.* **99** 227001 [215]. Copyright (2007) by the American Physical Society.

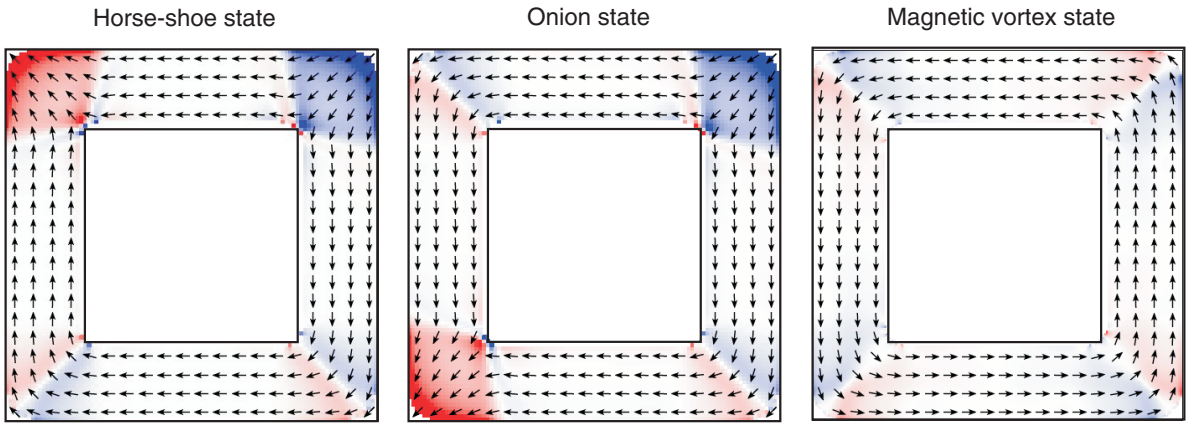

Figure 26. Different magnetic states realized in square permalloy micro-loops depending on the direction of the applied magnetic field obtained by OOMMF, by courtesy of V Metlushko *et al* (unpublished) [444].

structures. In this case, if a flux-closure state is induced in the magnetic ring, in principle, there is almost no stray field present, besides small fields due to domain walls at the sharp corners of the ring. Indeed, a two-dimensional magnetic material of ring-like shape of group symmetry C_n can be set in two flux-closure states of opposite chirality and $n(n-1)$ different polarized states. In a square loop, for instance, 12 states corresponding to six different dipole directions with two opposite dipole orientations are expected. If the net dipolar moment is parallel to the side of the square, the final state is named a horseshoe state whereas if the dipole is along the diagonal of the square, it is called an onion state. Figure 26 shows the different topologically non-equivalent magnetic states for a square ring of magnetic material with in-plane magnetization. Clear experimental evidence of ON/OFF magnetic pinning potentials induced by these type of multiply connected ferromagnetic structures have been demonstrated by Silhanek *et al* [257–259]. It is worth mentioning that the S/F structures investigated in [258] exhibit two well-distinguished phases corresponding to a disordered phase when the sample is in the as-grown state and an ordered phase when the sample is magnetized with an in-plane field. These order–disorder transitions manifest themselves as an enhancement of submatching features in the field dependence of the critical

current which cannot be explained from a simple rescaling of the response corresponding to the disordered phase.

3.3.6. Random (disordered) magnetic inclusions. Early studies of the influence of ferromagnet on the superconducting state were performed in the 1960s by Strongin *et al* [260], Alden and Livingston [261, 262] and Koch and Love [263] for a dispersion of fine ferromagnetic particles (Fe, Gd, Y) in a superconducting matrix. These reports motivated further experimental and theoretical investigations of the influence of randomly distributed particles on/underneath/inside superconducting materials, which continue nowadays (Sikora and Makiej [264, 265], Wang *et al* [266], Lyuksyutov and Naugle [267–269], Santos *et al* [270], Kuroda *et al* [271], Togoulev *et al* [272], Kruchinin *et al* [273], Palau *et al* [274, 275], Haindl *et al* [276, 277], Snezhko *et al* [278], Rizzo *et al* [279], Stamopoulos *et al* [280–284], Suleimanov *et al* [285], Xing *et al* [286–288]). In most of these investigations no precautions were taken to electrically isolate the magnetic particles from the superconducting material which presumably results in a substantial core pinning due to proximity effects.

Xing *et al* [287] reported on controlled switching between paramagnetic[16] and diamagnetic Meissner effect in S/F nanocomposites consisting of Pb films with embedded single-domain Co particles. These authors argue that in this particular system the paramagnetic Meissner effect attributed to the superconducting part only originates from the spontaneous formation of vortices induced by the ferromagnetic inclusions. Therefore, the different contributions of the external field and the spontaneous vortices to the resulting magnetization of the sample make it possible to manipulate the sign of the Meissner effect by changing the orientation of the magnetic moments embedded in the superconducting matrix[17].

3.3.7. Vortex dynamics in a periodic magnetic field. Here we want to briefly discuss the peculiarities of low-frequency vortex dynamics in nonuniform magnetic fields. Magnetic templates placed in the vicinity of a superconducting film not only induce changes in the static pinning properties but also in the overall dynamic response of the system. Lange *et al* [206] demonstrated that the vortex–antivortex pairs induced by an array of out-of-plane magnetized dots lead to a strong field polarity dependent vortex creep as evidenced in the current–voltage characteristics. This result shows that in S/F hybrids with perpendicular magnetized dots vortices and antivortices experience a different pinning strength. A theoretical study of the dynamic evolution of these interleaved lattices of vortices and antivortices in the case of in-plane point-like dipoles has been recently addressed by Carneiro [291] and Lima and de Souza Silva [292].

A more subtle effect, namely magnetic-dipole-induced voltage rectification, was predicted by Carneiro [243]. Unlike conventional ratchet systems[18], in the particular case of the magnetic ratchet, induced by in-plane magnetized dots, the motion of vortices is in the opposite direction to the motion of antivortices, thus giving rise to a field-polarity-independent rectification (Silhanek *et al* [258, 259], de Souza Silva *et al* [303]). This magnetic-dipole-induced ratchet motion depends on the mutual orientation and strength of the local magnetic moments, thus allowing one to control the direction of the vortex drift. In some cases, a nonzero rectified signal is observed even at $H_{\rm ext} = 0$ resulting from the interaction between the induced vortex–antivortex pairs by the magnetic dipoles [303]. It is worth emphasizing that, in the case of in-plane magnetic dipoles treated by Carneiro [243], the inversion symmetry is broken by the stray field of the dipoles, thus giving rise to different depinning forces parallel and antiparallel to the dipole orientations, as shown in figure 22.

3.4. Planar S/F bilayer hybrids

In this section we shall discuss the properties of continuous planar S/F structures which have macroscopically large lateral dimensions. As before, the superconducting and ferromagnetic films are assumed to be electrically insulated from each other.

3.4.1. Appearance of vortices in planar S/F structures. The interaction of the Meissner currents and the currents induced by vortex lines with a one-dimensional distribution of the magnetization (both single-domain walls, periodic domain structures and magnetic bars) in the London approximation was considered by Sonin [99], Genkin *et al* [304], Bespyatykh and Wasilevski [305], Bespyatykh *et al* [306], Helseth *et al* [307], Laiho *et al* [308], Traito *et al* [309], Erdin [310], Bulaevskii and Chudnovsky [311, 312], Kayali and Pokrovsky [313], Burmistrov and Chtchelkatchev [314], Ainbinder and Maksimov [315] and Maksimova *et al* [316, 317]. It was found that in order to create vortex–antivortex pairs in the S/F bilayer with out-of-plane magnetization at $H_{\rm ext} = 0$ (and thus keeping the total flux through the superconducting film zero) the amplitude of the magnetization $M_{\rm s}$ should overcome the following threshold value [305, 308, 309]

$$M^{\perp}_{\rm v-av} = \frac{H_{\rm c1}}{4\alpha}\frac{D_{\rm s}}{w} \propto \frac{\Phi_0 D_{\rm s}}{\lambda^2 w}\ln\lambda/\xi, \qquad (23)$$

where α is a numerical factor of the order of unity and the period w of the domain structure is assumed to be fixed (the hard-magnet approximation). This estimate corresponds to the case when the width of the domain walls is much smaller than other relevant length scales. The critical magnetization $M^{\perp}_{\rm v-av}$ decreases monotonically with decreasing

[16] The paramagnetic Meissner effect in various superconducting systems is discussed in the review of Li [289].

[17] Previously, Monton *et al* [290] reported on an experimental observation of the paramagnetic Meissner effect in Nb/Co superlattices in field-cooled measurements: however, the origin of this effect remains unclarified.

[18] Early theoretical studies showed that a vortex lattice submitted to an oscillatory excitation in the presence of a non-centro-symmetric pinning potential gives rise to a net drift $\langle\mathbf{v}\rangle$ of the vortex lattice which in turn generates a dc voltage signal $V_{\rm dc} = \int[\langle\mathbf{v}\rangle \times \mathbf{H}_{\rm ext}]\cdot\mathbf{dl}$ along the direction of bias current (Zapata *et al* [293], Lee *et al* [294], Wambaugh *et al* [295]). These predictions are in agreement with recent experimental results obtained for purely superconducting systems (Villegas *et al* [296], Wördenweber *et al* [297], Van de Vondel *et al* [298], Togawa *et al* [299], de Souza Silva *et al* [300], Wu *et al* [301], Aladyshkin *et al* [302]).

superconducting film thickness D_s. The equilibrium vortex pattern appearing in the superconducting film at $H_{ext} = 0$ and $M_s > M^{\perp}_{v-av}$ consists of straight vortices, arranged in one-dimensional chains, with alternating vorticities corresponding to the direction of the magnetization in the ferromagnetic domains [305, 308, 309]. The parameters of such a vortex configuration with one or two vortex chains per half-period was analyzed by Erdin [310]. It was shown that in equilibrium the vortices in the neighboring domains are halfway shifted, while they are next to each other in the same domain. Alternatively, as the thickness D_s increases, the vortex configuration, consisting of vortex semi-loops between the ferromagnetic domains with opposite directions of the magnetization, becomes energetically favorable [308, 309] provided that $M_s > M^{\perp}_{loops}$, where

$$M^{\perp}_{loops} = \frac{H_{c1}}{8\ln(w/\pi\lambda)} \propto \frac{\Phi_0}{\lambda^2}\frac{\ln\lambda/\xi}{\ln(w/\pi\lambda)}.$$

The destruction of the Meissner state in the S/F bilayer with in-plane magnetization was considered by Burmistrov and Chtchelkatchev [314]. Since the out-of-plane component of the field, which is responsible for the generation of the vortex, is maximal near the domain wall (unlike from the previous case) and goes to zero in the center of magnetic domains, one can consider only a single domain wall. At $H_{ext} = 0$ a creation of a single vortex near the Bloch-type domain wall of width δ corresponds to the condition

$$M^{\parallel}_{v} \simeq \frac{H_{c1}}{4\pi}\frac{\lambda}{D_f} \times \begin{cases} 2\lambda/\delta, & \pi\delta/(4\lambda) \ll 1 \\ 1 - 32\lambda/(\pi^2\delta), & \pi\delta/(4\lambda) \gg 1. \end{cases}$$

3.4.2. Magnetic pinning and guidance of vortices in planar S/F structures. Irrespective of whether the domain structure in the ferromagnetic layer is spontaneously created or was present beforehand, the spatial variation of the magnetization will lead to an effective vortex pinning (Bespyatykh *et al* [306], Bulaevskii *et al* [318]). However, there are discrepancies in the estimates concerning the pinning effectiveness. Indeed, Bulaevskii *et al* [318] argued that superconductor/ferromagnet multilayers of nanoscale period can exhibit strong pinning of vortices by the magnetic domain structure in magnetic fields below the coercive field when the ferromagnetic layers exhibit strong perpendicular magnetic anisotropy. The estimated maximum magnetic pinning energy for a single vortex in such a system is about 100 times larger than the core pinning energy produced by columnar defects. In contrast to that, Bespyatykh *et al* [306] have shown that the effectiveness of magnetic pinning of vortices in a layered system formed by an uniaxial ferromagnet does not considerably exceed the energy of artificial pinning by a column-type defect, regardless of the saturation magnetization of the ferromagnet. The limitation of the pinning energy is caused by the interaction of external vortices with the spontaneous vortex lattice formed in the superconducting film when the magnetization of the ferromagnetic film exceeds the critical value (see equation (23)).

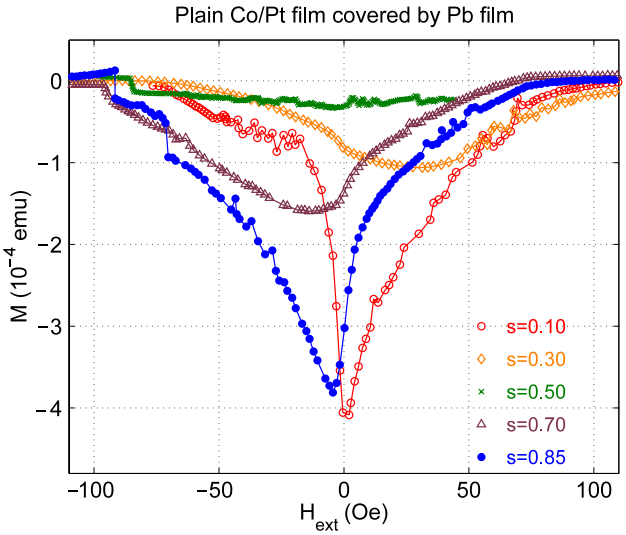

Figure 27. Bottom parts of the magnetization curves M versus H_{ext} for a superconducting Pb film covering a Co/Pt multilayer. The curves $M(H_{ext})$ corresponding to the different values of the parameter s, which is defined as the fraction of magnetic moments that are pointing up ($m > 0$) relative to the total number of magnetic moments: $s = 0.1$ (open circles), $s = 0.3$ (diamonds), $s = 0.5$ (crosses), $s = 0.7$ (triangles) and $s = 0.85$ (filled circles). Adapted with permission from Lange *et al* 2002 *Appl. Phys. Lett.* **81** 322–4 [256]. Copyright (2002) by the American Institute of Physics.

There have been numerous experimental investigations corroborating the enhancement of the critical current in planar S/F hybrids. It was shown that the presence of a bubble domain structure in Co/Pt ferromagnetic films with out-of-plane magnetization modifies the vortex pinning in superconducting Pb films (Lange *et al* [205, 256, 319, 320]), leading to an increase of the width of the magnetization loop $M(H_{ext})$ as compared with a uniformly magnetized S/F sample (figure 27). The crossover between an enhanced magnetic pinning on bubble magnetic domains observed at low temperatures and a suppressed magnetic pinning at temperatures close to T_c for a demagnetized S/F bilayer can be possibly associated with an increase of an effective penetration length λ^2/D_s, characterizing the vortex size, and an effective averaging on the small-scale variation of the nonuniform magnetic field provided that λ^2/D_s considerably exceed the period of the magnetic field (Lange *et al* [320]). Interestingly, the parameters of the bubble domain structure (the size and the density of domains of both signs of magnetization) can be controlled by demagnetization similar to that reported in [96, 123]. A threefold enhancement of the critical depinning current in Nb films fabricated on top of ferromagnetic Co/Pt multilayers was observed by Cieplak *et al* [321, 322] based on magnetization measurements and on the analysis of the magnetic field distribution obtained by using a 1D array of Hall sensors. The mentioned enhancement of the magnetic pinning takes place in the final stages of the magnetization reversal process and it can attributed to residual un-inverted dendrite-shaped magnetic domains.

High-resolution magneto-optical imaging performed by Goa *et al* [323] in superconducting $NbSe_2$ single crystals and ferrite-garnet films demonstrates that the stray field of Bloch domain walls can be used to manipulate vortices. Indeed, depending on the thickness of the sample, the vortices are either swept away or merely bent by the Bloch wall.

Vlasko-Vlasov *et al* [247, 324] and Belkin *et al* [325, 326] studied the anisotropic transport properties of superconducting MoGe and Pb films and $NbSe_2$ single crystals which are in the vicinity of a ferromagnetic permalloy film. In these works a quasi-one-dimensional distribution of magnetization can be achieved by applying a strong enough in-plane field $H_{ext} > 300$ Oe, which aligns the domain walls in a desired direction. Such a domain structure was maintained even after switching off the external magnetic field. Magneto-optical measurements directly display the preferential vortex entry along the direction of the domain walls after applying a magnetic field perpendicular to the sample surface [panels (c) and (d) in figure 23]. By reorienting the magnetic domains using the external magnetic field oriented in-plane, it is possible to ensure a guided vortex motion in a desirable direction and thus manipulate the conductivity of the S/F bilayer. The presence of this rotatable periodic stripe-like magnetic domain structure with alternating out-of-plane component of magnetization results in a difference in the critical depinning current density between cases when the magnetic domain stripes are oriented parallel and perpendicular to the superconducting current: $J_c^{\parallel} > J_c^{\perp}$. For planar thin-film Pb/Py structures Vlasko-Vlasov *et al* [324] observed a pronounced magnetoresistance effect yielding four orders of magnitude resistivity change in a few millitesla in-plane field. In addition, the S/F bilayer exhibits commensurability features that are related to the matching of the Abrikosov vortex lattice and the magnetic stripe domains (Belkin *et al* [326]). The matching effects are less apparent than for S/F hybrids with magnetic dots, although commensurability becomes more pronounced as temperature is lowered. This result can be explained by the gradual decrease in the λ value, which leads to stronger modulation of the magnetic field in the superconductor at lower temperatures and, consequently, to more prominent magnetic interaction with ferromagnetic domain structure.

It is interesting to note that the effect of magnetic domains on the pinning of vortices was also observed in high-T_c superconductors such as $YBa_2Cu_3O_{7-\delta}$ (García-Santiago *et al* [327], Jan *et al* [328], Zhang *et al* [329], Laviano *et al* [330]). At the same time the influence of the ferromagnet on the nucleation in the high-T_c superconductors should be rather small due to an extremely small coherence length (of the order of a few nanometers).

3.4.3. Current compensation effect and field-polarity-dependent critical current. A superconducting square with in-plane magnetized ferromagnet on top was proposed by Milošević *et al* [331] as a potential field and current compensator, allowing us to improve the critical parameters of superconductors. Indeed, such a magnet generates stray fields of the same amplitude but opposite signs at the poles of the magnet. Therefore the field-compensation effect leads to the enhancement of the upper critical field equally for both polarities of the external field. The superconducting state was shown to resist much higher applied magnetic fields for both perpendicular polarities. In addition, such a ferromagnet induces two opposite screening currents inside the superconducting film plane (in the perpendicular direction to its magnetization), which effectively compensates the bias current, and therefore superconductivity should persist up to higher applied currents and fields. These effects have been recently studied experimentally by Schildermans *et al* [332] in an Al/Py hybrid disc of 1.7 μm diameter where a finite dipolar moment lying in the plane of the structure was achieved by pinning magnetic domains with the contact leads used for electrical measurements.

Vodolazov *et al* [333] and Touitou *et al* [334] considered an alternative experimental realization of the current compensator, consisting of a superconducting bridge and a ferromagnetic bar magnetized in-plane and perpendicularly to the direction of the bias current. Such geometry allows one to weaken the self-field of the superconducting bridge near its edge and thus to enhance the total critical current corresponding to the dissipation-free current flow. Since the self-field compensation occurs only for a certain direction of the current (for fixed magnetization), the presence of magnetized coating leads to a diode effect: the current–voltage I–V dependence becomes asymmetrical (figure 28). Later the similar difference in critical currents flowing in opposite directions was studied experimentally by Morelle and Moshchalkov [335] for a system consisting of a superconducting Al strip placed close to a perpendicularly magnetized Co/Pd rectangle and Vodolazov *et al* [336] for an Nb/Co bilayer in the presence of a tilted external magnetic field.

3.5. Stray-field-induced Josephson junctions

Josephson junctions consist of weak links between two superconducting reservoirs of paired electrons. Commonly, these junctions are predefined static tunnel barriers that, once constructed, can no longer be modified/tuned. In contrast to that, a new concept of the Josephson junctions with a weak link generated by the local depletion of the superconducting condensate by a 'magnetic barrier' from a micro/nanopatterned ferromagnet can be realized (Sonin [98]). Interestingly, this type of device offers an unprecedented degree of flexibility as it can be readily switched ON/OFF by simply changing between different magnetic states using an in-plane field. This switching process is fully reversible and non-volatile since it does not require energy to keep one of the magnetic states.

A pioneering investigation of the properties of superconducting weak links achieved by local intense magnetic fields was performed by Dolan and Lukens [337]. The sample layout used by these authors and their typical dimensions is schematically shown in figure 29(a) and it consists of an Al bridge locally covered by a plain Pb film which has a thin gap of width g and spans the width of the Al strip at its center. By applying an external magnetic field, the Pb film screens the magnetic field due to the Meissner effect in the whole Al bridge but magnifies its intensity at the gap position. This effect leads to a local region of suppressed superconductivity which gives rise to a dc

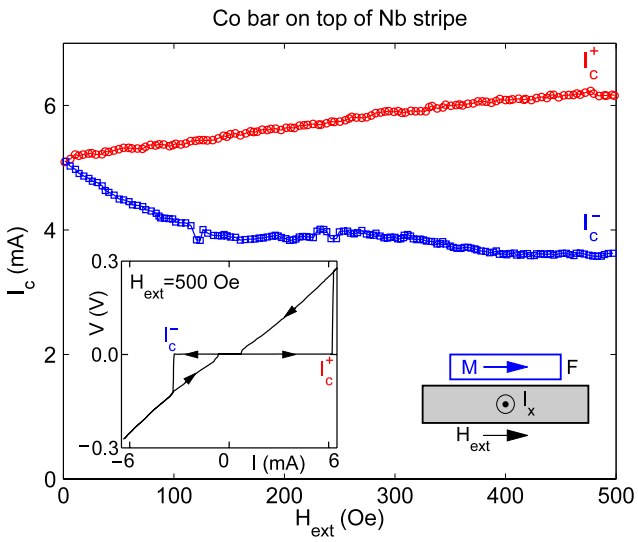

Figure 28. Diode effect in the Nb bridge (2 μm width) with the in-plane magnetized Co stripe on top: experimental dependence of I_c^+ (the critical current in the x direction, see the geometry of the S/F system on the inset) and I_c^- (the critical current in the opposite direction) on the external magnetic field H_{ext} applied in the y direction ($T = 4.2$ K, $T_{c0} = 9.2$ K), adapted figure with permission from Vodolazov *et al* 2005 *Phys. Rev.* B **72** 064509 [333]. Copyright (2005) by the American Physical Society. In the inset the dc I–V characteristic of our hybrid system $H_{ext} = 500$ Oe is presented, showing a pronounced diode effect.

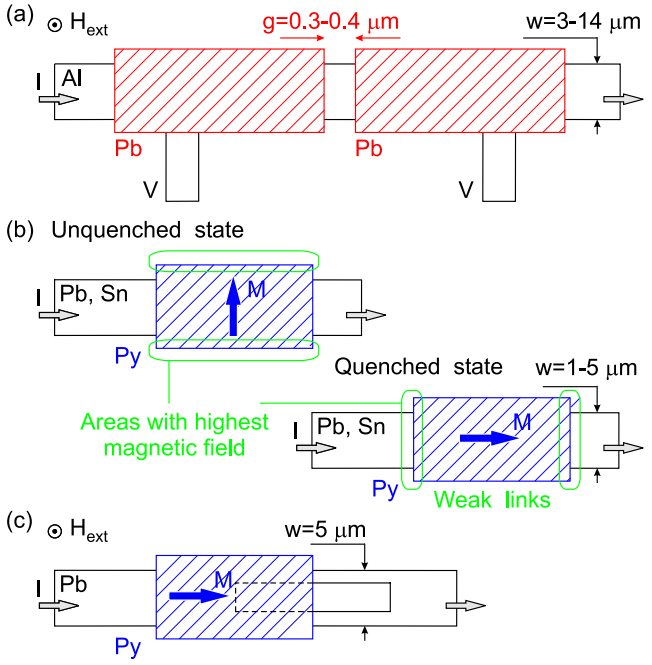

Figure 29. (a) Sample layout investigated by Dolan and Lukens [337]: a uniform Al bridge was covered with superconducting Pb strips (dashed rectangles) everywhere but in a small region near the center of the bridge. Due to the flux expulsion from the Pb strips the local magnetic field is primarily confined to this gap. (b) Sample configuration investigated by Clinton and Johnson [338, 339]: a Pb (or Sn) transport bridge is partially covered with a ferromagnetic Py strip with in-plane magnetic moment M. When M is parallel to the bridge a strong stray field depletes the superconducting order parameter in a small region near the border of the Py bar (quenched state), thus inducing a weak link. (c) Schematic presentation of magnetoquenched superconducting quantum interferometer, consisting of two superconducting Pb bridges connected in parallel and permalloy film on top (Eom and Johnson [342]).

and ac Josephson effect, as evidenced by a finite critical current and the presence of Shapiro steps in the current–voltage characteristics at $V_n = n\hbar\omega/(2e)$ when the system was irradiated with rf excitations with frequency $\omega = 2\pi f$, n is integer. Interestingly, the Josephson-like features appear for applied fields in the shield gap approximately equal to the upper critical field of the Al film.

An alternative method to obtain a field-induced weak link has been more recently introduced by Clinton and Johnson [338–341]. The basic device consist of a bilayer of a thin superconducting strip and a ferromagnetic layer with in-plane magnetic moment overlapping the width of the bridge (see panel (b) in figure 29). When the magnetic moment is parallel to the superconducting bridge the dipolar fringe is strong enough to locally suppress the superconducting order parameter across the bridge (quenched state) and thus create a weak link. This effect can be turned off by simply magnetizing the ferromagnetic layer perpendicular to the transport bridge with an external in-plane dc field or by a current pulse in a separate transport line [341]. Clearly, the proposed switchable Josephson junction seems to be very attractive for potential technological applications, since energy is required only to change the magnetic states, which are thereafter maintained in thermodynamic equilibrium. Later on, based on the same idea, Eom and Johnson [342] proposed a switchable superconducting quantum interferometer consisting of a ferromagnetic Py film partly covering two parallel superconducting Pb bridges fabricated in a loop geometry. The dependence of the voltage V, induced on this superconducting loop at the injection of stationary bias current, on the perpendicular magnetic field H_{ext} is shown in figure 30(b) and it reminds us of the standard Fraunhofer diffraction pattern (Barone and Paterno [34]).

4. Hybrid structures: superconductor-soft magnets

Thus far, we have discussed the influence that a ferromagnet has on the superconducting properties of S/F hybrids, assuming that the magnetization of the ferromagnet **M** remains practically unaltered. In this last section, we consider the possibility that the magnetization **M** can be changed either due to the external magnetic field or by the superconducting screening currents induced by the magnetic subsystem, which are particularly relevant at low temperatures. This situation could, in principle, be achieved by using paramagnetic materials or soft ferromagnetic materials with a low coercive field.

The equilibrium properties of 'superconductor–soft magnet' hybrid structures (so-called soft S/F hybrids) can be

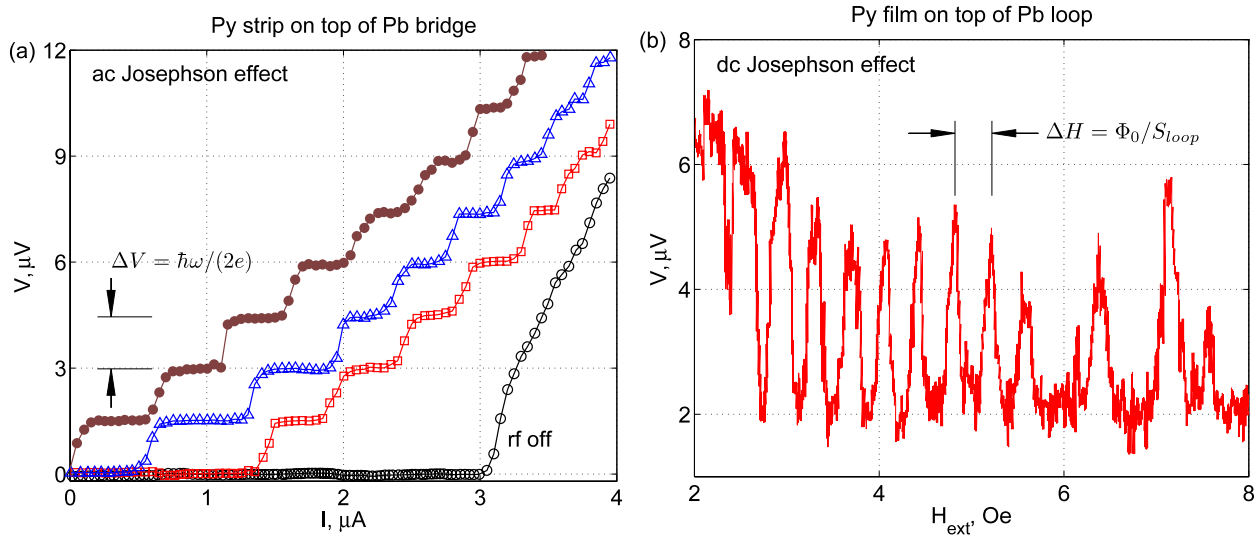

Figure 30. (a) The I–V curves obtained for a plain superconducting Pb bridge (2 μm wide) subjected in the inhomogeneous magnetic field, quenched state (see panel (b) in figure 29) for different intensities of rf irradiation. Adapted with permission from Clinton and Johnson 1999 *J. Appl. Phys.* **85** 1637–43 [339]. Copyright (1999) by the American Institute of Physics. The experiment was carried out at $T = 5$ K, $T/T_{c0} \simeq 0.76$, $H_{ext} = 0$, frequency f of the radio signal equal to 0.75 GHz. (b) The I–V dependence obtained for a superconducting Pb loop of the width 4.5 μm with rectangular hole 1.5×7.0 μm^2 covered by permalloy film (see panel (c) in figure 29). Adapted with permission from Eom and Johnson 2001 *Appl. Phys. Lett.* **79** 2486–8 [342]. Copyright (2001) by the American Institute of Physics. This curve demonstrates the short period oscillations with the period determined by the area of the superconducting loop S_{loop}.

obtained phenomenologically by the minimization of the Ginzburg–Landau energy functional equation (1) or the London energy functional equation (17), in which the term G_m responsible for the self-energy of the ferromagnet becomes important:

$$G_m = \frac{1}{2M_s^2}\int_{V_f}(J_\parallel|\nabla M_x|^2 + J_\parallel|\nabla M_y|^2 + J_\perp|\nabla M_z|^2)\,\mathrm{d}V - \int_{V_f} 2\pi Q M_z^2\,\mathrm{d}V, \quad (24)$$

where $J_\parallel$ and $J_\perp$ characterize the exchange interaction between spins in a uniaxial ferromagnet with respect to the in-plane and out-of-plane direction and Q is a quality factor taking into account the internal anisotropy of the ferromagnet and determining the preferable orientation of the magnetization (either in-plane or out-of-plane). Equation (24) describes the energy cost for having a slowly varying spatial distribution of the magnetization[19] and, in particular, it describes the energy of a domain wall in a ferromagnet. In some cases (for instance, for rapid **M** variations typical for ferromagnets with domain walls of rather small width), in order to simplify the problem, the increase of the free energy given by equation (24) can be taken into account phenomenologically by substituting G_m by a fixed term G_{dw} representing the energy of a domain wall.

[19] The theory of superconductor–soft ferromagnet systems near the 'ferromagnet–paramagnet' transition has been considered by Li *et al* [343] within Ginzburg–Landau formalism.

4.1. Modification of the domain structure in a ferromagnetic film by the superconducting screening currents

The influence of a superconducting environment (both substrate or coating) on the equilibrium width of magnetic domains in ferromagnetic films was considered theoretically by Sonin [99], Genkin *et al* [304], Sadreev [344], Bespyatykh *et al* [345, 346], Stankiewicz *et al* [347, 348], Bulaevskii and Chudnovsky [311, 312] and Daumens and Ezzahri [349]. In particular, one can expect a prominent change in the equilibrium period of a one-dimensional domain structure at $H_{ext} = 0$ for rather thick ferromagnetic films ($D_f \gg w$) with out-of-plane magnetization. Indeed, the Meissner currents, induced by the ferromagnet, will decrease the magnetic field inside the superconductor (usual flux expulsion effects) and significantly increase the magnetic field inside the ferromagnet. As a consequence, the density of the free energy of the ferromagnet, given by $\mathbf{B}^2/8\pi - \mathbf{B}\cdot\mathbf{M}$ or, equivalently, by $\mathbf{H}^2/8\pi - 2\pi M_z^2$, increases for a given M_z distribution. However, the total energy of the S/F system can be lowered by a decrease of the period of the ferromagnetic domains: the smaller the period, the faster the decay of **H** away from the surfaces of the ferromagnetic film. Thus, it is expected that the equilibrium width of magnetic domains in planar S/F bilayer becomes smaller below the critical temperature of the superconducting transition as compared with the state $T > T_{c0}$. In contrast to that, for thin ferromagnetic films ($D_f \ll w$) the opposite behavior is predicted: the domain width in the free ferromagnetic film should be smaller than that for the same film on top of a superconducting substrate [348]. This can be understood by

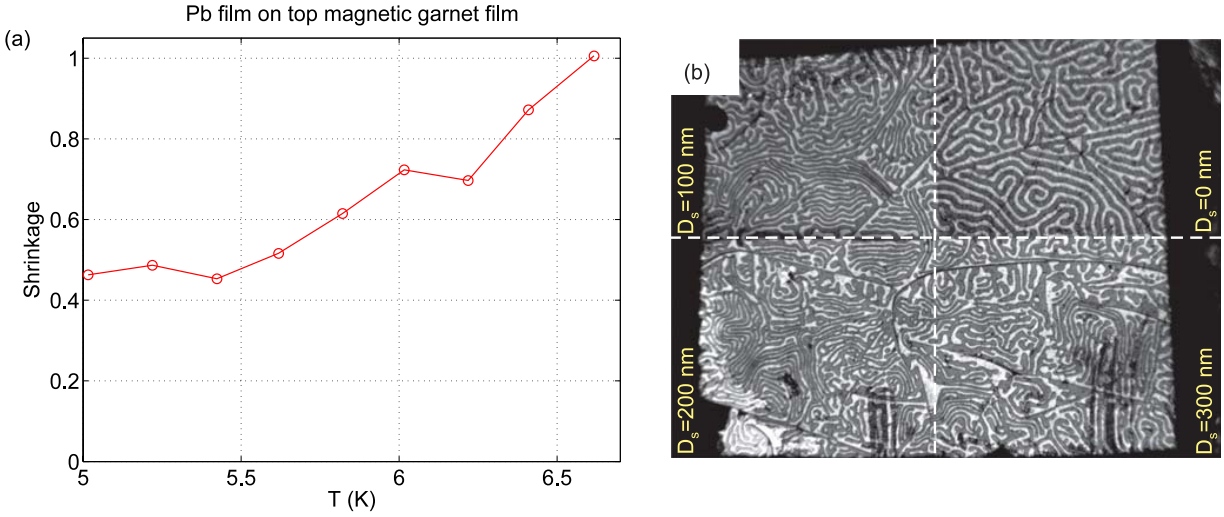

Figure 31. (a) The temperature dependence of the shrinkage ratio of the width of magnetic domains in a hybrid structure consisting of a Pb film ($D_s = 300$ nm) on top of a magnetic garnet film in comparison with the same ferromagnetic film without superconducting coating, adapted from Tamegai *et al* [350]. (b) The magneto-optical image of four segments of the superconducting Pb/garnet film structure, differing by the thickness of the Pb film ($D_s = 0$, 100, 200 and 300 nm in a counterclockwise direction), taken at $T = 5.0$ K, by the courtesy of Tamegai *et al* (unpublished) [350].

taking into account the change of the far-zone demagnetizing field characteristics. In addition, Stankiewicz *et al* [348] argued that the effect of the superconducting substrate on the period of the domain structure in ferromagnetic films with in-plane magnetization is rather small as compared with that for the out-of-plane magnetized ferromagnets. However, an increase of the magnetostatic energy of the S/F hybrids at $T < T_{c0}$ due to the Meissner currents results also in a shrinkage of the equilibrium width of an isolated 180° Bloch wall, separating two ferromagnetic domains with in-plane magnetization, in the vicinity of the superconducting substrate, as was predicted by Helseth *et al* [307].

The foreseen decrease of the period of the domain structure in a ferromagnetic garnet film in contact with a superconducting Pb film was recently investigated by magneto-optical imaging (Tamegai *et al* [350]). It was demonstrated that the shrinkage depends both on temperature and the thickness of the superconducting coating layer. The temperature dependence of the shrinkage factor s evaluated by comparing the average width $\langle w \rangle$ of the magnetic domain width in regions with and without the superconducting Pb film is shown in figure 31(a). It points out that the lower the temperature, the narrower the magnetic domains are ($s = 0.47$ at $T = 5.0$ K).

4.2. Alteration of magnetization of ferromagnetic dots by the superconducting screening currents

The Meissner currents also influence the magnetic states and the process of magnetization reversal in ferromagnetic discs placed above a superconductor. It is well known that a uniformly magnetized (single-domain) state is energetically favorable for radii R_f smaller than some threshold value R_f^* (for a given thickness of the dot D_f), while the magnetic vortex state can be realized for $R_f > R_f^*$. The typical $M(H_{ext})$ dependence for ferromagnetic discs for $R_f > R_f^*$ was already shown in figure 25. The dependence R_f^* versus D_f (the phase diagram in the 'diameter–height' plane) in the presence of a bulk superconductor, characterized by the London penetration depth λ, was investigated numerically by Fraerman *et al* [351] and later analytically by Pokrovsky *et al* [352]. It was shown that the smaller λ, the smaller the critical diameter R_f^* becomes for a given dot thickness. The transitions between the two magnetic states can be induced also by increasing the external magnetic field: the magnetic vortex, possessing an excess energy at zero field, becomes energetically favorable for finite external fields (the magnetic vortex nucleation field). Although the energy of the interaction between the superconductor and ferromagnet is expected to be much smaller than the self-energy of the ferromagnetic particle (for realistic λ values), it could lead to an experimentally observable decrease in the magnetic vortex nucleation field $H_{nucl}^{\parallel}$ and increase in the magnetic vortex annihilation field $H_{ann}^{\parallel}$ (figure 32).

The appearance of a spontaneous magnetization of individual S/F hybrids, consisting of an Al bridge and demagnetized Ni dots on top, upon cooling through the superconducting transition temperature at $H_{ext} = 0$, was reported by Dubonos *et al* [353]. Indeed, the reshuffling of magnetic domains in the submicron ferromagnetic disc, caused by temperature-dependent screening of the domain's stray fields by the superconductor, can explain the observed appearance of nonzero magnetization of the ferromagnet at low temperatures. More recently, the modification of the magnetic state of Nb/Co and Nb/Py superlattices induced by screening currents in the superconducting Nb films was studied experimentally by Monton *et al* [290, 354, 355] and Wu *et al* [356].

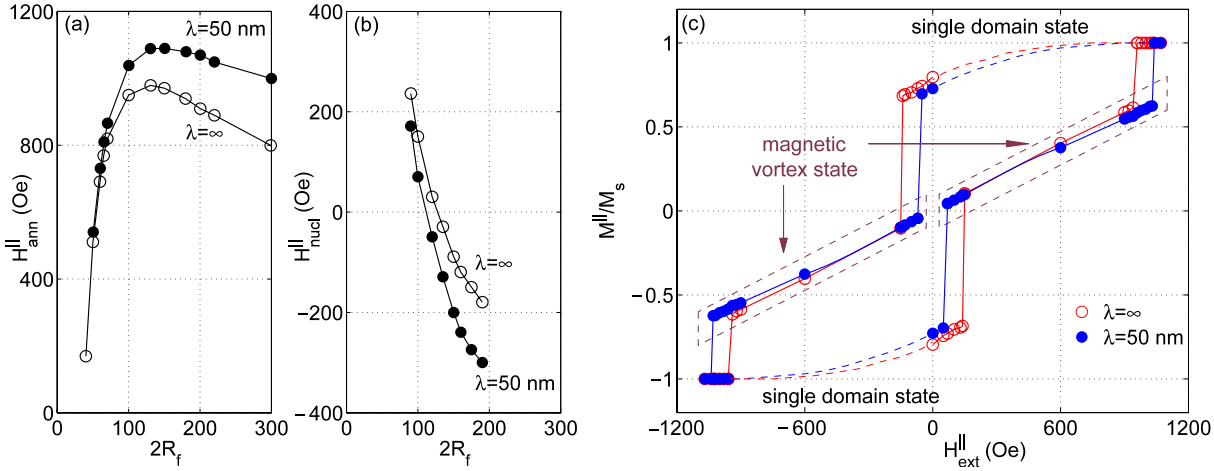

Figure 32. (a) The dependence of the magnetic vortex annihilation field $H^{\parallel}_{ann}$, corresponding to the transition from the magnetic vortex state to a single-domain state, on the diameter of a disc $2R_f$, calculated for an isolated ferromagnetic disk of 20 nm thickness (i.e. without superconductor, $\lambda = \infty$, open circles) and for the same disc placed above a bulk superconductor ($\lambda = 50$ nm, filled circles). (b) The dependence of the magnetic vortex nucleation field $H^{\parallel}_{nucl}$, corresponding to the transition from single-domain state to the magnetic vortex state for the same problem. (c) The magnetization curve $M^{\parallel}/M_s$ versus in-plane external field $H^{\parallel}_{ext}$ demonstrating the process of the magnetization reversal for the magnetic disc (20 nm thickness and 100 nm diameter) for $\lambda = \infty$ (open circles) and $\lambda = 50$ nm (filled circles). Thus, the screening effect increases the width of the H_{ext} interval at the ascending and descending branches of the magnetization curve where the magnetic vortex state is energetically favorable. All these plots were adapted with permission from Fraerman *et al* 2005 *Phys. Rev.* B **71** 094416 [351]. Copyright (2005) by the American Physical Society.

Kruchinin *et al* [273] demonstrated theoretically that a superconducting environment modifies the magnetostatic interaction between localized magnetic moments (embedded small ferromagnetic particles), resulting either in parallel or antiparallel alignment of neighbor dipolar moments at $H_{ext} = 0$. The crossover between these regimes depends on the ratio of the interparticle spacing and the London penetration depth, and thus preferable 'magnetic' ordering (ferromagnetic versus antiferromagnetic arrangements) can be tuned by varying temperature.

4.3. Mixed state of soft S/F hybrid structures

The magnetostatic interaction between a vortex-free superconducting film and a uniformly magnetized ferromagnetic film at $H_{ext} = 0$ may cause the spontaneous formation of vortices in the superconductor and magnetic domains in the ferromagnet in the ground state of planar S/F bilayers with perpendicular magnetization. Lyuksyutov and Pokrovsky [357] and Erdin *et al* [358] argued that the ground state of the S/F system could be unstable with respect to the formation of superconducting vortices. Indeed, for a uniformly magnetized S/F bilayer, characterized by a magnetization of the ferromagnetic film per unit area $m = M_s D_f$, the magnetostatic interaction between the superconductor and the ferromagnet changes the total energy of an isolated vortex line to $\varepsilon_v = \varepsilon_v^{(0)} - m\Phi_0$ [146] as compared to the self-energy of the vortex in the superconducting film $\varepsilon_v^{(0)}$ without a ferromagnetic layer. As a consequence, the formation of vortices becomes energetically favorable as soon as $\varepsilon_v < 0$ (either for rather large m values or at temperatures close to T_{c0} where $\varepsilon_v^{(0)}$ vanishes). However, as the lateral size of the S/F system increases, the averaged vortex density n_v would generate a constant magnetic field $B_z \simeq n_v\Phi_0$ along the z direction which can lead to an energy increase larger than the gain in energy due to the creation of vortices. Hence, in order for the vortex phase to survive, the ferromagnetic film should split into domains with alternating magnetization in a finite temperature range at $T < T_{c0}$. As long as the magnetic domain width exceeds the effective penetration depth, the energy of the stripe domain structure seems to be minimal (figure 33). Interestingly, the interaction between a single vortex in a superconducting film and the magnetization induced by this vortex in the adjacent ferromagnetic film can cross over from attractive to repulsive at short distances (Helseth [171]).

Carneiro studied the interaction between superconducting vortices and a superparamagnetic particle with constant dipolar moment, which is assumed to be able to freely rotate, in the London model [162–164]. It was found that, due to the rotational degree of freedom, the pinning potential for superconducting vortices differs significantly from that for a permanent dipole. In particular, the interaction between the superconducting vortex and the magnetic dipole can be tuned by applying an in-plane external field: the corresponding depinning critical current was shown to be anisotropic and its amplitude potentially varies by as much as one order of magnitude. Later on, this approach was generalized by Carneiro [255] for hybrid systems consisting of a thin superconducting film and soft ferromagnetic discs in the magnetic vortex state (similar to that for [351, 352] but considering a vortex line inside the superconducting sample).

A new method of pinning vortices in S/F epitaxial composite hybrids consisting of randomly distributed Gd particles incorporated in a Nb matrix was reported by Palau *et al* [275, 274]. Since the size of Gd particles are much

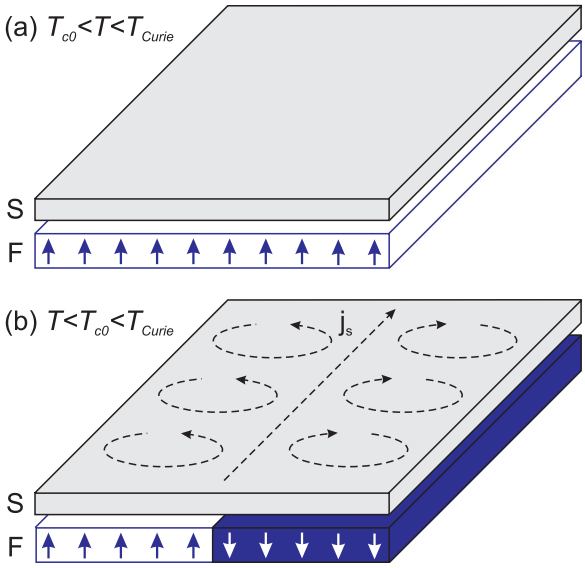

Figure 33. (a) Uniform state of the S/F bilayer above the superconducting critical temperature. (b) Spontaneously formed magnetic domain structure and coupled chains of superconducting vortices with alternating vorticity at $T < T_{c0}$, predicted by Erdin *et al* [358]. Solid arrows correspond to the magnetization of the ferromagnet, while black arrows schematically show the circulating superconducting currents.

smaller than the coherence length and the interparticle distance is much shorter than the penetration depth, this regime of collective magnetic pinning differs both from conventional core and magnetic pinning mechanisms. In this case, since a vortex 'feels' a homogeneous superconductor (for length scales of the order of λ), pinning effects are expected to be small. However, due to the local field of a vortex, the Gd particles can be magnetized and a moving vortex would lead to hysteretic losses in the magnetic particles, which in turn results in an increased pinning (for decreasing magnetic fields).

4.4. Superconductor–paramagnet hybrid structures

An alternative way of modifying the superconducting properties of soft hybrid structures is by using paramagnetic constituents, characterized by zero or very low remanent magnetization. Such superconductor–paramagnet hybrids with a magnetization $\mathbf{M} = (\mu - 1)\,\mathbf{H}/4\pi$ depending on the external field (μ is the magnetic permeability) in the presence of transport current were considered theoretically by Genenko [359], Genenko and Snezhko [360] and Genenko *et al* [361–363] for $\mu \gg 1$. It was predicted that the paramagnetic material placed near superconducting stripes and slabs can drastically modify the current distribution in such hybrids, thus, suppressing the current enhancement near the superconducting sample's edges inherent for any thin-film superconductor in the flux-free current-carrying state. As a consequence, the current redistribution leads to an increase of the threshold value of the total bias current corresponding to the destruction of the Meissner state. In other words, the magnetically shielded superconductors even in the Meissner state are able to carry without dissipation rather high transport current comparable with the typical current values for a regime of strong flux pinning [359, 361–363]. A survival of the Meissner state for thin-film superconducting rings carrying a current and placed between two coaxial cylindrical soft magnets was studied by Genenko *et al* [364, 365]. Yampolskii *et al* [366] considered the transport current distribution in a superconducting filament aligned parallel to the flat surface of a semi-infinite bulk magnet with the assumption that the superconductor is in the Meissner state. The similar problem concerning the distribution of magnetic field inside and outside a superconducting filament sheathed by a magnetic layer, as well as the magnetization of such a structure in the region of reversible magnetic behavior in the Meissner state, was considered by Genenko *et al* [367]. The formation of the mixed state in various superconductor/paramagnet structures in the presence of transport current, or an external magnetic field H_{ext} or the field of hard-magnetic dipoles, was analyzed by Genenko *et al* [368], Genenko and Rauh [369], Yampolskii and Genenko [370] and Yampolskii *et al* [371–373] in the framework of the London model. The Bean–Livingston barrier against the vortex entry in shielded superconducting filaments was shown to strongly depend on the parameters of the paramagnetic coating and, as a result, the critical field at which the first vortex enters can be enhanced [368].

Since for the superconductor/paramagnet hybrids there are no changes neither in the vortex structure in the Meissner state of superconductors nor in the magnetic state of paramagnetic elements, characteristics of superconductor–paramagnet hybrids are presumed to be reversible and ac losses should be minimal for such structures. It stimulated the implementation of paramagnetic and ferromagnetic coatings in high-T_c superconductors in order to improve the critical current and reduce the ac losses (Majoros *et al* [374], Glowacki *et al* [375], Horvat *et al* [376, 377], Duckworth [378], Kovàč *et al* [379], Touitou *et al* [334], Pan *et al* [380], Jooss *et al* [381], Gu *et al* [382], Gömöry *et al* [383, 384]).

Although, strictly speaking, permalloy is a ferromagnet with rather low coercive field, it can behaves qualitatively similar to paramagnetic materials. Indeed, the magnetization vector for thin-film structures deviates from in-plane orientation if a perpendicular external field is applied. Such rotation of the magnetization of the dot toward the out-of-plane direction while sweeping the external field gives rise to a z component of magnetization depending on the external field. The effect of the stray field generated by soft permalloy dots on the critical current I_c of the superconducting Al loops was experimentally studied by Golubović and Moshchalkov [385]. The monotonic decrease in the period of the oscillation on the $I_c(H_{ext})$ with increasing the H_{ext} value was interpreted as a flux enhancement due to the increase of the out-of-plane component of the dot's magnetic moment. In this sense soft-magnetic materials are promising candidates for the design of a linear magnetic flux amplifier for applications in superconducting quantum interference devices.

5. Conclusion

We would like to conclude this work by formulating what, we believe, are the most exciting unsolved issues and possible interesting directions for further studies of S/F hybrid systems.

Spontaneous formation of a vortex lattice and domain patterns. As we discussed in section 4, the magnetostatic interaction between a vortex-free superconducting film and a uniformly and perpendicularly magnetized ferromagnetic film at zero external field may lead to a spontaneous formation of vortex–antivortex pairs in the superconductor accompanied by alternating magnetic domains in the ferromagnet in the ground state (see figure 33 and [33, 358]). To the best of our knowledge, thus far there are no experimental results confirming this prediction. In part, this is likely due to the difficulties of combining a very low coercive field ferromagnetic material, needed to guarantee the free accommodation of magnetic domains, and a well-defined out-of-plane magnetic moment.

Magnetic pinning. Based on London equations we have clearly defined the magnetic pinning energy as $\mathbf{m}_0 \cdot \mathbf{B}_v$ (see section 3). Since London equations are valid as long as core contributions are negligible, in principle this simple relationship holds for materials with $\kappa = \lambda/\xi \gg 1$ and low temperatures. Unfortunately in the vast majority of the experimental reports so far, it seems that these conditions are not satisfied. Any other contributions, such as local suppression of T_c, proximity effect or local changes in the mean free path, which are not accounted for within the London approximation, could lead to a deviation from the treatment in the framework of the London model. The problem that remains unsolved so far is the identification of the most relevant mechanisms of vortex pinning in S/F hybrid systems.

Thermodynamic properties of S/F heterostructures. Although the electric transport in superconductor/ferromagnet hybrid systems has been intensively studied during the past few decades, very little is known about their thermodynamic and thermal properties such as their entropy, specific heat, thermal conductivity, etc. From an academic point of view it would be very relevant to investigate the nature of the phase transitions or present thermodynamic evidence of confinement of the superconducting order parameter. On the other hand, estimating the heat released when the system changes its state might also provide useful information for devices based on S/F heterostructures.

Electromagnet–superconductor hybrids. Most of the research performed so far has been focussed on the effects of an inhomogeneous field generated by a ferromagnetic layer onto a superconducting film. As was earlier demonstrated by Pannetier *et al* [97] in principle there is no difference whether this inhomogeneous field is the stray field emanating from a permanent magnet or the magnetic field generated by micro(nano)patterned current-carrying wires on top of the surface of the film. The great advantage of the latter is the degree of flexibility and control in the design of the magnetic landscape and the external tuneability of its intensity. Such electromagnet–superconductor hybrids represent a promising alternative for further exploring the basic physics behind S/F hybrids.

Time-resolved vortex creation and annihilation. Josephson π junctions give rise to spontaneous formation of half-integer flux quanta, so-called semifluxons (Hilgenkamp *et al* [386]). It has been theoretically demonstrated that for long Josephson junctions with zigzag π-discontinuity corners the ground state corresponds to a flat phase state for short separation between corners whereas an array of semifluxons is expected for larger separations. Interestingly, by applying an external bias current it is possible to force the hopping of these semifluxons between neighboring discontinuities (Goldobin *et al* [387]). This hopping of semifluxons could be identified through time-resolved ac measurements with drive amplitudes above the depinning current. There are clear similarities between these arrays of semifluxons in zigzag Josephson systems and the vortex–antivortex arrays in S/F systems. Indeed, recently Lima and de Souza Silva [292] have shown theoretically that the dynamics of the vortex–antivortex matter is characterized by a series of creation and annihilation events which should be reflected in the time dependence of the electrical field. Experimental work corroborating these predictions are relevant for understanding the dynamics of flux annihilation and creation in S/F systems.

The strive to comprehend the ultimate mechanisms ruling the interaction between ferromagnets and superconductors has made this particular topic an active theoretical and experimental line of research. We believe that these vigorous efforts will inspire further developments in this area of solid state physics and perhaps motivate new applications of technological relevance.

Acknowledgments

The authors are grateful to C Carballeira, Q H Chen, M M Doria, Yu A Genenko, A S Mel'nikov, M V Milošević, D A Ryzhov, A V Samokhvalov, M A Silaev, T Tamegai, J E Villegas, V K Vlasko-Vlasov and J Van de Vondel for the valuable comments and remarks which certainly improved the quality of this review. We also thank C Carballeira, G Carneiro, T W Clinton, A A Fraerman, D Gheorghe, A Hoffmann, M Johnson, V V Metlushko, M V Milošević, M Lange, Y Otani, N Schildermans, T Tamegai, M J Van Bael, J E Villegas, V K Vlasko-Vlasov and D Yu Vodolazov for granting us permission to use their figures in our review.

This work was supported by the Methusalem Funding of the Flemish Government, the NES–ESF program, the Belgian IAP, the Fund for Scientific Research—Flanders (FWO–Vlaanderen), the Russian Fund for Basic Research, by the Russian Academy of Sciences under the program 'Quantum physics of condensed matter' and the Presidential grant MK-4880.2008.2 (A Yu A). AVS and WG are grateful for the support from the FWO–Vlaanderen.

Appendix. Summary of experimental and theoretical research

Table A.1. Summary of experimental research on vortex matter in the S/F hybrids with dominant orbital interaction (suppressed proximity effect).

	Co/Pt Co/Pd	$BaFe_{12}O_{19}$ $PbFe_{12}O_{19}$	Co, Fe, Ni	Fe/Ni (Py)	Other ferromagnets
S/F hybrids consisting of large-area superconducting and plain non-patterned ferromagnetic films (single crystals) with domain structure					
Pb films	[205, 256, 319, 320], [388]	[103]		[324]	[350]
Nb films	[105, 106, 110, 321], [322, 392]	[101, 102], [104]	[290, 354, 355, 389], [393–396]	[108, 356]	[276, 390, 391]
Al films	[96, 107]				
Other low-T_c films	[397, 398]		[271, 376, 377, 380]	[100, 247], [325, 326]	[109, 323]
High-T_c films	[328, 334]	[327]	[374, 375, 379], [382–384, 399]	[399]	[329, 330, 378, 381], [400–403]
S/F hybrids consisting of large-area superconducting film and ferromagnetic elements: single particles, periodic arrays of magnetic dots (antidots) and stripes					
Pb films	[121, 198–200], [201, 203–205], [206, 232, 234–236, 246], [404, 405]		[196–199], [200–202, 205], [237, 238, 257, 286], [287, 288, 303, 406]		
Nb films	[280–282, 284, 283]		[184–195, 240, 245], [248–250, 296, 407], [411–417]	[97, 254], [407, 408]	[119, 120, 263], [274–277, 409, 410]
Al films	[96, 107, 123–125], [418, 419]		[215, 253, 303]	[244, 258, 259]	[278]
Other low-T_c films	[397]		[211, 260–262], [272, 279]		
High-T_c films			[285, 420]		[155, 156, 158, 174–176]
Laterally confined and mesoscopic S/F hybrids					
Pb films			[340, 421]	[339–342]	
Nb films			[333, 336]	[341]	
Al films	[133–137, 140, 335], [405, 423, 424]		[353]	[332, 385, 422]	[337]
Other low-T_c films			[272, 367]	[338]	

Table A.2. Summary of theoretical research on vortex matter in the S/F hybrids with dominant orbital interaction (suppressed proximity effect).

	Ginzburg–Landau formalism	London formalism	Newton-like description of vortex dynamics
Bilayered and multilayered large-area S/F structures (superconducting ferromagnets)	[50, 93–96, 105], [106, 343, 425]	[98, 99, 146, 173, 270], [304–314, 318], [344–349, 357], [358, 426–437]	
Individual F elements over large-area S films (inside bulk superconductors)	[51, 54, 63, 76], [127–129]	[146–150, 153–156], [159–173, 255, 273], [278, 291, 351, 352, 431, 445]	
Arrays of F dots elements over large-area S films (inside bulk superconductors)	[112–118, 122], [124, 142, 143], [182, 183, 419]	[187, 225–230], [243, 420, 404, 431]	[231, 243, 291], [292, 303, 404], [416, 417, 438]
Laterally confined and mesoscopic S/F structures	[40, 54, 126], [130–132, 134, 135], [137–140, 144, 145], [331, 423]	[151, 152, 267–269], [315–317, 333, 439]	
Hybrid structures with paramagnetic elements		[359–373]	

References

[1] Bardeen J, Cooper L N and Schrieffer J R 1957 Microscopic theory of superconductivity *Phys. Rev.* **106** 162–4

[2] Bardeen J, Cooper L N and Schrieffer J R 1957 Theory of superconductivity *Phys. Rev.* **108** 1175–204

[3] Ginzburg V L 1956 *J. Exp. Theor. Phys.* **4** 153

[4] Matthias B T, Suhl H and Corenzwit E 1958 Spin exchange in superconductors *Phys. Rev. Lett.* **1** 92–4

[5] Matthias B T, Suhl H and Corenzwit E 1958 Ferromagnetic superconductors *Phys. Rev. Lett.* **1** 449–50

[6] Matthias B T and Suhl H 1960 Possible explanation of the 'coexistence' of ferromagnetism and superconductivity *Phys. Rev. Lett.* **4** 51–2

[7] Anderson P W and Sulh H 1959 Spin alignment in the superconducting state *Phys. Rev.* **116** 898–900

[8] Larkin A I and Ovchinnikov Yu N 1965 Inhomogeneous state of superconductors *J. Exp. Theor. Phys.* **20** 762

[9] Fulde P and Ferrell R A 1964 Superconductivity in a strong spin-exchange field *Phys. Rev.* **135** A550–63

[10] Jaccarino V and Peter M 1962 Ultra-high-field superconductivity *Phys. Rev. Lett.* **9** 290–2

[11] Bulaevskii L N, Buzdin A I, Kulić M L and Panyukov S V 1985 Coexistence of superconductivity and magnetism: Theoretical predictions and experimental results *Adv. Phys.* **34** 175–261

[12] Flouquet J and Buzdin A 2002 Ferromagnetic superconductors *Phys. World* **15** 41–6

[13] Izyumov Yu A, Khusainov M G and Proshin Yu N 2002 Competition between superconductivity and magnetism in ferromagnet/superconductor heterostructures *Phys.—Usp.* **45** 109–48

[14] Buzdin A I 2005 Proximity effects in superconductor–ferromagnet heterostructures *Rev. Mod. Phys.* **77** 935–76

[15] Bergeret F S, Volkov A F and Efetov K B 2005 Odd triplet superconductivity and related phenomena in superconductor–ferromagnet structures *Rev. Mod. Phys.* **77** 1321–73

[16] Prokić V, Buzdin A I and Dobrosavljević-Grujić L 1999 Theory of the π-junctions formed in atomic-scale superconductor/ferromagnet superlattices *Phys. Rev.* B **59** 587–95

[17] Ryazanov V V, Oboznov V A, Rusanov A Y, Veretennikov A V, Golubov A A and Aarts J 2001 Coupling of two superconductors through a ferromagnet: evidence for a π-junction *Phys. Rev. Lett.* **86** 2427–30

[18] Kontos T, Aprili M, Lesueur J, Genêt F, Stephanidis B and Boursier R 2002 Josephson junction through a thin ferromagnetic layer: negative coupling *Phys. Rev. Lett.* **89** 137007

[19] Buzdin A I and Baladié I 2003 Theoretical description of ferromagnetic π-junctions near the critical temperature *Phys. Rev.* B **67** 184519

[20] Oboznov V A, Bol'ginov V V, Feofanov A K, Ryazanov V V and Buzdin A I 2006 Thickness dependence of the Josephson ground states of superconductor–ferromagnet–superconductor junctions *Phys. Rev. Lett.* **96** 197003

[21] Deutscher G and Meunier F 1969 Coupling between ferromagnetic layers through a superconductor *Phys. Rev. Lett.* **22** 395–6

[22] Ledvij M, Dobrosavljević-Grujić L, Radović Z and Clem J R 1991 Vortex and nonvortex nucleation of superconductivity in ferromagnetic–superconducting–ferromagnetic triple layers *Phys. Rev.* B **44** 859–62

[23] Buzdin A I, Vedyayev A V and Ryzhanova N V 1999 Spin-orientation dependent superconductivity in F/S/F structures *Europhys. Lett.* **48** 686–91

[24] Tagirov L R 1999 Low-field superconducting spin switch based on a superconductor/ferromagnet multilayer *Phys. Rev. Lett.* **83** 2058–61

[25] Baladié I, Buzdin A, Ryzhanova N and Vedyayev A 2001 Interplay of superconductivity and magnetism in superconductor–ferromagnet structures *Phys. Rev.* B **63** 054518

[26] Gu J Y, You C-Y, Jiang J S, Pearson J, Bazaliy Ya B and Bader S D 2002 Magnetization-orientation dependence of the superconducting transition temperature in the ferromagnet–superconductor–ferromagnet system: CuNi/Nb/CuNi *Phys. Rev. Lett.* **89** 267001

[27] Gu J Y, You C-Y, Jiang J S and Bader S D 2003 Magnetization-orientation dependence of the superconducting transition temperature and magnetoresistance in the ferromagnet–superconductor–ferromagnet trilayer system *J. Appl. Phys.* **93** 7696–8

[28] Peña V, Sefrioui Z, Arias D, Leon C, Santamaria J, Martinez J L, te Velthuis S G E and Hoffmann A 2005 Giant magnetoresistance in ferromagnet/superconductor superlattices *Phys. Rev. Lett.* **94** 057002

[29] Moraru I C, Pratt W P Jr and Birge N O 2006 Magnetization-dependent T_c shift in ferromagnet/superconductor/ferromagnet trilayers with a strong ferromagnet *Phys. Rev. Lett.* **96** 037004

[30] Rusanov A Yu, Habraken S and Aarts J 2006 Inverse spin switch effects in ferromagnet–superconductor–ferromagnet trilayers with strong ferromagnets *Phys. Rev.* B **73** 060505(R)

[31] Steiner R and Ziemann P 2006 Magnetic switching of the superconducting transition temperature in layered ferromagnetic/superconducting hybrids: spin switch versus stray field effects *Phys. Rev.* B **74** 094504

[32] Singh A, Sürgers C and von Löhneysen H 2007 Superconducting spin switch with perpendicular magnetic anisotropy *Phys. Rev.* B **75** 024513

[33] Lyuksyutov I F and Pokrovsky V L 2005 Ferromagnet–superconductor hybrids *Adv. Phys.* **54** 67

[34] Barone A and Paterno G 1982 *Physics and Applications of the Josephson Effect* (New York: Wiley Interscience)

[35] Aladyshkin A Yu, Fraerman A A, Gusev S A, Klimov A Y, Nozdrin Y N, Pakhomov G L, Rogov V V and Vdovichev S N 2003 Influence of ferromagnetic nanoparticles on the critical current of Josephson junction *J. Magn. Magn. Mater.* **258/259** 406–8

[36] Vdovichev S N, Gribkov B A, Gusev S A, Il'ichev E, Klimov A Yu, Nozdrin Yu N, Pakhomov G L, Rogov V V, Stolz R and Fraerman A A 2004 Properties of Josephson junctions in the inhomogeneous magnetic field of a system of ferromagnetic particles *JETP Lett.* **80** 651

[37] Fraerman A A, Gusev S A, Nozdrin Yu N, Samokhvalov A V, Vdovichev S N, Fritzsch E, Il'ichev L and Stolz R 2006 Commensurability effects in overlap Josephson junctions coupled with a magnetic dots array *Phys. Rev.* B **73** 100503

[38] Held R, Xu J, Schmehl A, Schneider C W, Mannhart J and Beasley M R 2006 Superconducting memory based on ferromagnetism *Appl. Phys. Lett.* **89** 163509

[39] Samokhvalov A V 2007 Commensurability effects in a Josephson tunnel junction in the field of an array of magnetic particles *J. Exp. Theor. Phys.* **104** 451–60

[40] Chibotaru L F, Ceulemans A, Morelle M, Teniers G, Carballeira C and Moshchalkov V V 2005 Ginzburg–Landau description of confinement and quantization effects in mesoscopic superconductors *J. Math. Phys.* **46** 095108

[41] Vélez M, Martín J I, Villegas J E, Hoffmann A, González E M, Vicent J L and Schuller I K 2008 Superconducting vortex pinning with artificial magnetic nanostructures *J. Magn. Magn. Mater.* **320** 2547–62

[42] Martín J I, Nogués J, Liu K, Vicente J L and Schuller I K 2003 Ordered magnetic nanostructures: fabrication and properties *J. Magn. Magn. Mater.* **256** 449–501

[43] Abrikosov A A 1988 *Fundamentals of the Theory of Metals* (Amsterdam: Elsevier)

[44] Schmidt V V 1997 *The Physics of Superconductors. Introduction to Fundamentals and Applications* (Berlin: Springer)

[45] Tinkham M 1996 *Introduction to Superconductivity* 2nd edn (New York: McGraw-Hill)

[46] Gorkov L P 1959 Microscopic derivation of the Ginzburg–Landau equations in the theory of superconductivity *J. Exp. Theor. Phys.* **9** 1364–7

[47] Moshchalkov V V, Gielen L, Strunk C, Jonckheere R, Qiu X, van Haesendonck C and Bruynseraede Y 1995 Effect of sample topology on the critical fields of mesoscopic superconductors *Nature* **373** 319–22

[48] Moshchalkov V V, Bruyndoncx V, Van Look L, Van Bael M J, Bruynseraede Y and Tonomura A 2000 *Handbook of Nanostructured Materials and Nanotechnology* vol 3, ed H S Nalwa (San Diego, CA: Academic) (Quantization and Confinement Phenomena in Nanostructured Superconductors chapter) p 45

[49] Berger J and Rubinstein J 2000 *Connectivity and Superconductivity* (Berlin: Springer)

[50] Aladyshkin A Yu, Buzdin A I, Fraerman A A, Mel'nikov A S, Ryzhov D A and Sokolov A V 2003 Domain-wall superconductivity in hybrid superconductor–ferromagnet structures *Phys. Rev.* B **68** 184508

[51] Aladyshkin A Yu, Mel'nikov A S and Ryzhov D A 2003 The Little–Parks effect and multiquanta vortices in a hybrid superconductor–ferromagnet system *J. Phys.: Condens. Matter* **15** 6591–7

[52] Baert M, Metlushko V V, Jonckheere R, Moshchalkov V V and Bruynseraede Y 1995 Composite flux-line lattices stabilized in superconducting films by a regular array of artificial defects *Phys. Rev. Lett.* **74** 3269–73

[53] Moshchalkov V V, Baert M, Metlushko V V, Rosseel E, Van Bael M J, Temst K, Bruynseraede Y and Jonckheere R 1998 Pinning by an antidot lattice: the problem of the optimum antidot size *Phys. Rev.* B **57** 3615–22

[54] Aladyshkin A Yu, Ryzhov D A, Samokhvalov A V, Savinov D A, Mel'nikov A S and Moshchalkov V V 2007 Localized superconductivity and Little–Parks effect in superconductor/ferromagnet hybrids *Phys. Rev.* B **75** 184519

[55] Little W A and Parks R D 1962 Observation of quantum periodicity in the transition temperature of a superconducting cylinder *Phys. Rev. Lett.* **9** 9–12

[56] Parks R D and Little W A 1964 Fluxoid quantization in a multiply-connected superconductors *Phys. Rev.* **133** A97–103

[57] Landau L D and Lifshitz E M 1977 *Quantum Mechanics. Non-Relativistic Theory* (*Course of Theoretical Physics*) 3rd edn (Oxford: Pergamon)

[58] Müller J E 1992 Effect of a nonuniform magnetic field on a two-dimensional electron gas in the ballistic regime *Phys. Rev. Lett.* **68** 385–8

[59] Xue D P and Xioa G 1992 Magnetotransport properties of two-dimensional electronic gases under periodical magnetic field *Phys. Rev.* B **45** 5986–90

[60] Peeters F M and Vasilopoulos P 1993 Quantum transport of a two-dimensional electronic gas in a spatially modulated magnetic field *Phys. Rev.* B **47** 1466–73

[61] Peeters F M and Matulis A 1993 Quantum structures created by nonhomogeneous magnetic fields *Phys. Rev.* B **48** 15166–74

[62] Wu X-G and Ulloa S E 1993 Electronic states and collective excitations of a two-dimensional electronic gas in a unidirectional magnetic-field modulation *Phys. Rev.* B **47** 7182–6

[63] Matulis A, Peeters F M and Vasilopoulos P 1994 Wave-vector-dependent tunneling through magnetic barriers *Phys. Rev. Lett.* **72** 1518–21

[64] Ibrahim I S and Peeters F M 1995 Two-dimensional electrons in lateral magnetic superlattices *Phys. Rev.* B **52** 17321–34

[65] Peeters F M, Matulis A and Ibrahim I S 1996 Two-dimensional electrons in modulated magnetic fields *Physica* B **227** 131–7

[66] Gumbs G and Zhang C 2000 The magnetoconductivity of a square lattice in a periodically modulated magnetic field *Solid State Commun.* **115** 163–6

[67] Reijniers J and Peeters F M 2000 Snake orbits and related magnetic edge states *J. Phys.: Condens. Matter* **12** 9771–86

[68] Reijniers J and Peeters F M 2001 Resistance effects due to magnetic guiding orbits *Phys. Rev.* B **63** 165317

[69] Nogaret A, Carlton S, Gallagher B L, Main P C, Henini M, Wirtz R, Newbury R, Howson M A and Beaumont S P 1997 Observation of giant magnetoresistance due to open orbits in hybrid semiconductor/ferromagnet devices *Phys. Rev.* B **55** 16037–40

[70] Nogaret A, Bending S J and Henini M 2000 Resistance resonance effects through magnetic edge states *Phys. Rev. Lett.* **84** 2231–34

[71] Carmona H A, Geim A K, Nogaret A, Main P C, Foster T J, Henini M, Beaumont S P and Blamire M G 1995 Two dimension electrons in a lateral magnetic superlattices *Phys. Rev. Lett.* **74** 3009–12

[72] Hofstadter D R 1976 Energy levels and wave functions of Bloch electrons in rational and irrational magnetic fields *Phys. Rev.* B **14** 2239–49

[73] Geim A K, Bending S J and Grigorieva I V 1992 Asymmetric scattering and diffraction of two-dimensional electrons at quantized tubes of magnetic flux *Phys. Rev. Lett.* **69** 2252–5

[74] Brey L and Fertig H A 1993 Hall resistance of a two-dimensional electron gas in the presence of magnetic-flux tubes *Phys. Rev.* B **47** 15961–4

[75] Nielsen M and Hedegård P 1995 Two-dimensional electron transport in the presence of magnetic flux vortices *Phys. Rev.* B **51** 7679–99

[76] Reijniers J, Peeters F M and Matulis A 1999 Quantum states in a magnetic antidot *Phys. Rev.* B **59** 2817–23

[77] Khveshchenko D V and Meshkov S V 1993 Particle in a random magnetic field on a plane *Phys. Rev.* B **47** 12051–8

[78] Ye P D, Weiss D, Gerhardts R R, Seeger M, von Klitzing K, Eberl K and Nickel H 1995 Electrons in a periodic magnetic field induced by a regular array of micromagnets *Phys. Rev. Lett.* **74** 3013–6

[79] Solimany L and Kramer B 1995 Electron in a magnetic quantum dot *Solid State Commun.* **96** 471–5

[80] Ibrahim I S, Schweigert V A and Peeters F M 1998 Diffusive transport in a Hall junction with a microinhomogeneous magnetic field *Phys. Rev.* B **57** 15416–27

[81] Sim H-S, Ahn K-H, Chang K J, Ihm G, Kim N and Lee S J 1998 Magnetic edge states in a magnetic quantum dot *Phys. Rev.* B **80** 1501–4

[82] Dubonos S V, Geim A K, Novoselov K S, Lok J G S, Maan J C and Henini M 2000 Scattering of electrons at a magnetic protuberance of submicron size *Physica* E **6** 746–50

[83] Reijniers J, Peeters F M and Matulis A 2000 The Hall resistivity of a two-dimensional electron gas in the presence of magnetic clusters with perpendicular magnetization *Physica* E **6** 759–62

[84] Reijniers J, Peeters F M and Matulis A 2001 Electron scattering on circular symmetric magnetic profiles in a two-dimensional electron gas *Phys. Rev.* B **64** 245314

[85] Rammer J and Shelankov A L 1987 Weak localization in inhomogeneous magnetic fields *Phys. Rev.* B **36** 3135–46

[86] Bending S J 1994 Complete numerical description of nonlocal quantum diffusion in an array of magnetic-flux vortices *Phys. Rev.* B **50** 17621–4

[87] Bending S J, von Klitzing K and Ploog K 1990 Weak localization in a distribution of magnetic flux tubes *Phys. Rev. Lett.* **65** 1060–3

[88] Bending S J, von Klitzing K and Ploog K 1990 Two-dimensional electron gas as a flux detector for a type-II superconducting film *Phys. Rev.* B **42** 9859–64

[89] Bending S J and Geim A K 1992 Quantitative numerical model for nonlocal quantum diffusion in a distribution of magnetic-flux tubes *Phys. Rev.* B **46** 14912–4

[90] Mancoff F B, Clarke R M, Marcus C M, Zhang S C, Campman K and Gossard A C 1995 Magnetotransport of a two-dimensional electron gas in a spatially random magnetic field *Phys. Rev.* B **51** 13269–73

[91] Shelankov A 2000 Paraxial propagation of a quantum charge in a random magnetic field *Phys. Rev.* B **62** 3196–212

[92] Wang X-B 2002 Dephasing time of disordered two-dimensional electron gas in modulated magnetic fields *Phys. Rev.* B **65** 115303

[93] Buzdin A I and Mel'nikov A S 2003 Domain wall superconductivity in ferromagnetic superconductors *Phys. Rev.* B **67** 020503

[94] Samokhin K V and Shirokoff D 2005 Phenomenological theory of superconductivity near domain walls in ferromagnets *Phys. Rev.* B **71** 104527

[95] Aladyshkin A Yu and Moshchalkov V V 2006 Thin-film superconductor–ferromagnet hybrids: Competition between nucleation of superconductivity at domain walls and domains' centers *Phys. Rev.* B **74** 064503

[96] Gillijns W, Aladyshkin A Yu, Silhanek A V and Moshchalkov V V 2007 Magnetic confinement of the superconducting condensate in superconductor–ferromagnet hybrid composites *Phys. Rev.* B **76** 060503(R)

[97] Pannetier B, Rodts S, Genicon J L, Otani Y and Nozières J P 1995 *Macroscopic Quantum Phenomena and Coherence in Superconducting Networks* (Singapore: World Scientific) chapter (Nucleation of Superconductivity in a Thin Film in a Spatially Modulated Magnetic Field) pp 17–24

[98] Sonin E B 1988 Suppression of superconductivity (weak link) by a domain wall in a two-layer superconductor–ferromagnet film *Sov. Tech. Phys. Lett.* **14** 714–6

[99] Sonin E B 2002 Comment on 'Ferromagnetic film on a superconducting substrate' *Phys. Rev.* B **66** 136501

[100] Artley J L, Buckley G, Willis C A Jr and Chambers W F 1966 Interaction of ferromagnetic and superconducting films *Appl. Phys. Lett.* **9** 429–31

[101] Yang Z, Lange M, Volodin A, Szymczak R and Moshchalkov V V 2004 Domain-wall superconductivity in superconductor–ferromagnet hybrids *Nat. Mater.* **3** 793–8

[102] Yang Z, Vervaeke K, Moshchalkov V V and Szymczak R 2006 Modulation of superconductivity by a magnetic template in Nb/$BaFe_{12}O_{19}$ hybrids *Phys. Rev.* B **73** 224509

[103] Yang Z, Van de Vondel J, Gillijns W, Vinckx W, Moshchalkov V V and Szymczak R 2006 Effect of reversed magnetic domains on superconductivity in Pb/$BaFe_{12}O_{19}$ hybrids *Appl. Phys. Lett.* **88** 232505

[104] Fritzsche J, Moshchalkov V V, Eitel H, Koelle D, Kleiner R and Szymczak R 2006 Local observation of reverse-domain superconductivity in a superconductor–ferromagnet hybrid *Phys. Rev. Lett.* **96** 247003

[105] Gillijns W, Aladyshkin A Yu, Lange M, Van Bael M J and Moshchalkov V V 2005 Domain-wall guided nucleation of superconductivity in hybrid ferromagnet–superconductor–ferromagnet layered structures *Phys. Rev. Lett.* **95** 227003

[106] Gillijns W, Aladyshkin A Yu, Lange M, Van Bael M J and Moshchalkov V V 2006 Domain-wall superconductivity in a ferromagnet/superconductor/ferromagnet trilayer *Physica* C **437/438** 73–6

[107] Aladyshkin A Yu, Gillijns W, Silhanek A V and Moshchalkov V V 2008 Magnetic tunable confinement of the superconducting condensate in superconductor/ferromagnet hybrids *Physica* C **468** 737–40

[108] Rusanov A Yu, Hesselberth M, Aarts J and Buzdin A I 2004 Enhancement of the superconducting transition temperature in Nb/permalloy bilayers by controlling the domain state of the ferromagnet *Phys. Rev. Lett.* **93** 057002

[109] Bell C, Turşucu S and Aarts J 2006 Flux-flow-induced giant magnetoresistance in all-amorphous superconductor–ferromagnet hybrids *Phys. Rev.* B **74** 214520

[110] Zhu L Y, Chen T Y and Chien C L 2008 Altering the superconductor transition temperature by domain-wall arrangements in hybrid ferromagnet–superconductor structures *Phys. Rev. Lett.* **101** 017004

[111] Doria M M, Gubernatis J E and Rainer D 1989 Virial theorem for Ginzburg–Landau theories with potential applications to numerical studies of type-II superconductors *Phys. Rev.* B **39** 9573–5

[112] Priour D J Jr and Fertig H A 2004 Vortex states of a superconducting film from a magnetic dot array *Phys. Rev. Lett.* **93** 057003
[113] Priour D J Jr and Fertig H A 2004 Broken orientational and reflection symmetries in thin film superconductors with mesoscopic magnetic dipoles *Physica* C **404** 293–7
[114] Milošević M V and Peeters F M 2004 Vortex–antivortex lattices in superconducting films with magnetic pinning arrays *Phys. Rev. Lett.* **93** 267006
[115] Milošević M V and Peeters F M 2005 Vortex–antivortex lattices in superconducting films with magnetic pinning arrays *J. Low Temp. Phys.* **139** 257–72
[116] Milošević M V and Peeters F M 2006 Vortex–antivortex nucleation in superconducting films with arrays of in-plane dipoles *Physica* C **437/438** 208–12
[117] Milošević M V and Peeters F M 2004 Commensurate vortex configurations in thin superconducting films nanostructured by square lattice of magnetic dots *Physica* C **404** 246–50
[118] Milošević M V and Peeters F M 2005 Vortex–antivortex nucleation in magnetically nanotextured superconductors: magnetic-field-driven and thermal scenarios *Phys. Rev. Lett.* **94** 227001
[119] Otani Y, Pannetier B, Nozières J P and Givord D 1993 Magnetostatic interactions between magnetic arrays and superconducting thin films *J. Magn. Magn. Mater.* **126** 622–5
[120] Geoffroy O, Givord D, Otani Y, Pannetier B and Ossart F 1993 Magnetic and transport properties of ferromagnetic particulate arrays fabricated on superconducting thin films *J. Magn. Magn. Mater.* **121** 223–6
[121] Lange M, Van Bael M J, Bruynseraede Y and Moshchalkov V V 2003 Nanoengineered magnetic-field-induced superconductivity *Phys. Rev. Lett.* **90** 197006
[122] Milošević M V and Peeters F M 2005 Field-enhanced critical parameters in magnetically nanostructured superconductors *Europhys. Lett.* **70** 670–6
[123] Gillijns W, Silhanek A V and Moshchalkov V V 2006 Tunable field-induced superconductivity *Phys. Rev.* B **74** 220509(R)
[124] Gillijns W, Milošević M V, Silhanek A V, Moshchalkov V V and Peeters F M 2007 Influence of magnet size on magnetically engineered field-induced superconductivity *Phys. Rev.* B **76** 184516
[125] Gillijns W, Silhanek A V, Aladyshkin A Yu and Moshchalkov V V 2008 Field induced superconductivity in magnetically modulated films *Physica* C **468** 741–4
[126] Marmorkos I K, Matulis A and Peeters F M 1996 Vortex structure around a magnetic dot in planar superconductors *Phys. Rev.* B **53** 2677–85
[127] Milošević M V and Peeters F M 2003 Superconducting Wigner vortex molecule near a magnetic disk *Phys. Rev.* B **68** 024509
[128] Milošević M V and Peeters F M 2003 Vortex matter in the presence of magnetic pinning centra *J. Low Temp. Phys.* **130** 311–20
[129] Milošević M V and Peeters F M 2004 Vortex–antivortex molecules induced by a magnetic disk on top of a superconducting film—influence of the magnet geometry *Physica* C **404** 281–4
[130] Cheng S-L and Fertig H A 1999 Upper critical field H_{c3} for a thin-film superconductor with a ferromagnetic dot *Phys. Rev.* B **60** 13107–11
[131] Milošević M V, Yampolskii S V and Peeters F M 2002 Vortex structure of thin mesoscopic disks in the presence of an inhomogeneous magnetic field *Phys. Rev.* B **66** 024515
[132] Milošević M V, Berdiyorov G R and Peeters F M 2007 Stabilized vortex–antivortex molecules in a superconducting microdisk with a magnetic nanodot on top *Phys. Rev.* B **75** 052502
[133] Golubović D S, Pogosov W V, Morelle M and Moshchalkov V V 2003 Nucleation of superconductivity in an Al mesoscopic disk with magnetic dot *Appl. Phys. Lett.* **83** 1593–5
[134] Golubović D S, Pogosov W V, Morelle M and Moshchalkov V V 2004 Influence of the stray field of a magnetic dot on the nucleation of superconductivity in a disk *Europhys. Lett.* **65** 546–52
[135] Golubović D S, Pogosov W V, Morelle M and Moshchalkov V V 2003 Little–Parks effect in a superconducting loop with a magnetic dot *Phys. Rev.* B **68** 172503
[136] Golubović D S, Pogosov W V, Morelle M and Moshchalkov V V 2004 Magnetic phase shifter for superconducting qubits *Phys. Rev. Lett.* **92** 177904
[137] Schildermans N, Aladyshkin A Yu, Silhanek A V, Van de Vondel J and Moshchalkov V V 2008 Different regimes of nucleation of superconductivity in mesoscopic superconductor/ferromagnet hybrids *Phys. Rev.* B **77** 214519
[138] Carballeira C, Moshchalkov V V, Chibotaru L F and Ceulemans A 2005 Multiquanta vortex entry and vortex–antivortex pattern expansion in a superconducting microsquare with a magnetic dot *Phys. Rev. Lett.* **95** 237003
[139] Chen Q H, Carballeira C and Moshchalkov V V 2006 Symmetry-breaking effects and spontaneous generation of vortices in hybrid superconductor–ferromagnet nanostructures *Phys. Rev.* B **74** 214519
[140] Golubović D S, Milošević M V, Peeters F M and Moshchalkov V V 2005 Magnetically induced splitting of a giant vortex state in a mesoscopic superconducting disk *Phys. Rev.* B **71** 180502
[141] Chibotaru L F, Ceulemans A, Bryuyndoncx V and Moshchalkov V V 2000 Symmetry-induced formation of antivortices in mesoscopic superconductors *Nature* **408** 833–5
[142] Doria M M 2004 Magnetic regions inside a superconductor and its effects on the vortex matter *Physica* C **404** 145–52
[143] Doria M M 2004 Vortex matter in presence of nano-scale magnetic defects *Physica* C **408–410** 466–9
[144] Doria M M, de C Romaguera A R, Milošević M V and Peeters F M 2007 Threefold onset of vortex loops in superconductors with a magnetic core *Europhys. Lett.* **79** 47006
[145] Doria M M, de C Romaguera A R, Milošević M V and Peeters F M 2008 Triplet vortex state in magnetic superconductors—effects of boundaries *Physica* C **468** 572–5
[146] Erdin S, Kayali A F, Lyuksyutov I F and Pokrovsky V L 2002 Interaction of mesoscopic magnetic textures with superconductors *Phys. Rev.* B **66** 014414
[147] Wei J C, Chen J L, Horng L and Yang T J 1996 Magnetic force acting on a magnetic dipole over a superconducting thin film *Phys. Rev.* B **54** 15429–37
[148] Carneiro G 2004 Pinning and creation of vortices in superconducting films by a magnetic dipole *Phys. Rev.* B **69** 214504
[149] Xu J H, Miller J H Jr and Ting C S 1995 Magnetic levitation force and penetration depth in type-II superconductors *Phys. Rev.* B **51** 424–34
[150] Coffey M W 1995 Magnetic levitation force of semi-infinite type-II superconductors *Phys. Rev.* B **52** R9851–4
[151] Coffey M W 2002 London model for the levitation force between a horizontally oriented point magnetic dipole and superconducting sphere *Phys. Rev.* B **65** 214524
[152] Haley S B and Fink H J 1996 Quantized levitation states of superconducting multiple-ring systems *Phys. Rev.* B **53** 3497–505
[153] Haley S B and Fink H J 1996 Magnetic levitation, suspension, and superconductivity: macroscopic and mesoscopic *Phys. Rev.* B **53** 3506–15

[154] Wei J C, Horng L and Yang T J 1997 Magnetic force signal of vortex creation in type-II superconducting thin films *Physica* C **280** 311–6

[155] Mel'nikov A S, Nozdrin Yu N, Tokman I D and Vysheslavtsev P P 1998 Experimental investigation of a local mixed state induced by a small ferromagnetic particle in Y–Ba–Cu–O films: extremely low energy barrier for formation of vortex–antivortex pairs *Phys. Rev.* B **58** 11672–5

[156] Aladyshkin A Yu, Vorob'ev A K, Vysheslavtsev P P, Klyuenkov E B, Mel'nikov A S, Nozdrin Yu N and Tokman I D 1999 Structure of the mixed state induced in thin YBaCuO superconducting films by the field of a small ferromagnetic particle *Sov. Phys.—JETP* **116** 940–7

[157] Bean C P and Livingston J D 1964 Surface barrier in type-II superconductors *Phys. Rev. Lett.* **12** 14–6

[158] Nozdrin Yu N, Mel'nikov A S, Tokman I D, Vysheslavtsev P P, Aladyshkin A Yu, Klyuenkov E B and Vorobiev A K 1999 Experimental investigation of a local mixed state induced by a small ferromagnetic particle in YBaCuO films *IEEE Trans. Appl. Supercond.* **9** 1602–5

[159] Milošević M V, Yampolskii S V and Peeters F M 2002 Magnetic pinning of vortices in a superconducting film: the (anti)vortex-magnetic dipole interaction energy in the London approximation *Phys. Rev.* B **66** 174519

[160] Milošević M V, Yampolskii S V and Peeters F M 2003 The vortex-magnetic dipole interaction in the London approximation *J. Low Temp. Phys.* **130** 321–31

[161] Carneiro G 2004 Interaction between vortices in superconducting films and magnetic dipole arrays *Physica* C **404** 78–86

[162] Carneiro G 2005 Tunable interactions between vortices and a magnetic dipole *Phys. Rev.* B **72** 144514

[163] Carneiro G 2005 Tunable critical current for a vortex pinned by a magnetic dipole *Europhys. Lett.* **71** 817–23

[164] Carneiro G 2006 Simple model for tunable vortex pinning by a magnetic dipole *Physica* C **437/438** 42–5

[165] Tokman I D 1992 Pinning of a vortex lattice on magnetic inhomogeneities in a thin superconducting film (type-II superconductor) *Phys. Lett.* A **166** 412–5

[166] Milošević M V and Peeters F M 2003 Interaction between a superconducting vortex and an out-of-plane magnetized ferromagnetic disk: influence of the magnet geometry *Phys. Rev.* B **68** 094510

[167] Milošević M V and Peeters F M 2004 Vortex pinning in a superconducting film due to in-plane magnetized ferromagnets of different shapes: the London approximation *Phys. Rev.* B **69** 104522

[168] Erdin S 2005 London study of vortex states in a superconducting film due to a magnetic dot *Phys. Rev.* B **72** 014522

[169] Kayali M A 2002 On the interaction between ferromagnetic annulus and superconducting vortices *Phys. Lett.* A **298** 432–6

[170] Kayali M A 2004 Spontaneous vortex creation in superconducting thin films covered by elliptical ferromagnetic dots *Phys. Rev.* B **69** 012505

[171] Helseth L E 2003 Anomalous interaction between vortices and nanomagnets *Phys. Lett.* A **319** 413–5

[172] Kayali M A 2005 Theory of pinning in a superconducting thin film pierced by a ferromagnetic columnar defect *Phys. Rev.* B **71** 024515

[173] Erdin S 2004 Vortex penetration in magnetic superconducting heterostructures *Phys. Rev.* B **69** 214521

[174] Moser A, Hug H J, Stiefel B and Güntherodt H-J 1998 Low temperature magnetic force microscopy on $YBa_2Cu_3O_{7-\delta}$ thin films *J. Magn. Magn. Mater.* **190** 114–23

[175] Gardner B W, Wynn J C, Bonn D A, Liang R, Hardy W N, Kirtley J R, Kogan V G and Moler K A 2002 Manipulation of single vortices in $YBa_2Cu_3O_{6.354}$ with a locally applied magnetic field *Appl. Phys. Lett.* **80** 1010–2

[176] Auslaender O M, Luan L, Straver E W J, Hoffman J E, Koshnick N C, Zeldov E, Bonn D A, Liang R, Hardy W N and Moler K A 2009 Mechanics of individual isolated vortices in a cuprate superconductor *Nat. Phys.* **5** 35–9

[177] Reichhardt C 2009 Vortices wiggled and dragged *Nat. Phys.* **5** 15–6

[178] Cowburn R P, Koltsov D K, Adeyeye A O, Welland M E and Tricker D M 1999 Single-domain circular nanomagnets *Phys. Rev. Lett.* **83** 1042–5

[179] Cowburn R P, Adeyeye A O and Welland M E 1999 Controlling magnetic ordering in coupled nanomagnet arrays *New J. Phys.* **1** 16.1–9

[180] Novosad V, Guslienko K Yu, Shima H, Otani Y, Kim S G, Fukamichi N, Kikuchi K, Kitakami O and Shimada Y 2002 Effect of interdot magnetostatic interaction on magnetization reversal in circular dot arrays *Phys. Rev.* B **65** 060402(R)

[181] Novosad V, Grimsditch M, Darrouzet J, Pearson J, Bader S D, Metlushko V, Guslienko K, Otani Y, Shima H and Fukamichi K 2003 Shape effect on magnetization reversal in chains of interacting ferromagnetic elements *Appl. Phys. Lett.* **82** 3716–8

[182] Autler S H 1972 Fluxoid pinning in superconductors by a periodic array of magnetic particles *J. Low Temp. Phys.* **9** 241–53

[183] Autler S H 1972 *Helv. Phys. Acta* **45** 851

[184] Martín J I, Vélez M, Nogués J and Schuller I K 1997 Flux pinning in a superconductor by an array of submicrometer magnetic dots *Phys. Rev. Lett.* **79** 1929–32

[185] Martín J I, Vélez M, Hoffmann A, Schuller I K and Vicent J L 1999 Artificially induced reconfiguration of the vortex lattice by arrays of magnetic dots *Phys. Rev. Lett.* **83** 1022–5

[186] Martín J I, Vélez M, Nogués J, Hoffmann A, Jaccard Y and Schuller I K 1998 Flux pinning in a superconductor by an array of submicrometer magnetic dots *J. Magn. Magn. Mater.* **177–181** 915–6

[187] Martín J I, Vélez M, Hoffmann A, Schuller I K and Vicent J L 2000 Temperature dependence and mechanisms of vortex pinning by periodic arrays of Ni dots in Nb films *Phys. Rev.* B **62** 9110–6

[188] Morgan D J and Ketterson J B 1998 Asymmetric flux pinning in a regular array of magnetic dipoles *Phys. Rev. Lett.* **80** 3614–7

[189] Morgan D J and Ketterson J B 2001 Fluxon pinning by artificial magnetic arrays *J. Low Temp. Phys.* **122** 37–73

[190] Hoffmann A, Prieto P and Schuller I K 2000 Periodic vortex pinning with magnetic and nonmagnetic dots: the influence of size *Phys. Rev.* B **61** 6958–65

[191] Jaccard Y, Martín J I, Cyrille M-C, Vélez M, Vicent J L and Schuller I K 1998 Magnetic pinning of the vortex lattice by arrays of submicrometric dots *Phys. Rev.* B **58** 8232–5

[192] Villegas J E, Gonzalez E M, Sefrioui Z, Santamaria J and Vicent J L 2005 Vortex phases in superconducting Nb thin films with periodic pinning *Phys. Rev.* B **72** 174512

[193] Villegas J E, Gonzalez E M, Montero M I, Schuller I K and Vicent J L 2003 Directional vortex motion guided by artificially induced mesoscopic potentials *Phys. Rev.* B **68** 224504

[194] Villegas J E, Gonzalez E M, Montero M I, Schuller I K and Vicent J L 2005 Vortex-lattice dynamics with channeled pinning potential landscapes *Phys. Rev.* B **72** 064507

[195] Stoll O M, Montero M I, Guimpel J, Åkerman J J and Schuller I K 2002 Hysteresis and fractional matching in thin Nb films with rectangular arrays of nanoscaled magnetic dots *Phys. Rev.* B **65** 104518

[196] Van Bael M J, Temst K, Moshchalkov V V and Bruynseraede Y 1999 Magnetic properties of submicron co islands and their use as artificial pinning centers *Phys. Rev.* B **59** 14674–9

[197] Van Bael M J, Bekaert J, Temst K, Van Look L, Moshchalkov V V, Bruynseraede G D, Howells Y, Grigorenko A N, Bending S J and Borghs G 2001 Local observation of field polarity dependent flux pinning by magnetic dipoles *Phys. Rev. Lett.* **86** 155–8

[198] Van Bael M J, Van Look L, Temst K, Lange M, Bekaert J, May U, Güntherodt G, Moshchalkov V V and Bruynseraede Y 2000 Flux pinning by regular arrays of ferromagnetic dots *Physica* C **332** 12–9

[199] Van Bael M J, Van Look L, Lange M, Temst K, Güntherodt G, Moshchalkov V V and Bruynseraede Y 2000 Vortex confinement by regular pinning arrays *Physica* C **341–348** 965–8

[200] Van Bael M J, Van Look L, Lange M, Temst K, Güntherodt G, Moshchalkov V V and Bruynseraede Y 2001 Vortex self-organization in the presence of magnetic pinning arrays *J. Supercond. Nov. Magn.* **14** 355–64

[201] Van Bael M J, Van Look L, Lange M, Bekaert J, Bending S J, Grigorenko A N, Temst K, Moshchalkov V V and Bruynseraede Y 2002 Ferromagnetic pinning arrays *Physica* C **369** 97–105

[202] Van Look L, Van Bael M J, Temst K, Rodrigo J G, Morelle M, Moshchalkov V V and Bruynseraede Y 2000 Flux pinning in a superconducting film by a regular array of magnetic dots *Physica* C **332** 356–9

[203] Van Bael M J, Lange M, Van Look L, Moshchalkov V V and Bruynseraede Y 2001 Vortex pinning in ferromagnet/superconductor hybrid structures *Physica* C **364/365** 491–4

[204] Van Bael M J, Lange M, Raedts S, Moshchalkov V V, Grigorenko A N and Bending S J 2003 Local visualization of asymmetric flux pinning by magnetic dots with perpendicular magnetization *Phys. Rev.* B **68** 014509

[205] Lange M, Van Bael M J and Moshchalkov V V 2005 Vortex matter in superconductor/ferromagnet hybrids *J. Low Temp. Phys.* **139** 195–206

[206] Lange M, Van Bael M J, Silhanek A V and Moshchalkov V V 2005 Vortex–antivortex dynamics and field-polarity-dependent flux creep in hybrid superconductor/ferromagnet nanostructures *Phys. Rev.* B **72** 052507

[207] Hebard A, Fiory A and Somekh S 1977 Critical currents in Al films with a triangular lattice of 1 μm holes *IEEE Trans. Magn.* **13** 589–92

[208] Rosseel E, Van Bael M, Baert M, Jonckheere R, Moshchalkov V V and Bruynseraede Y 1996 Depinning of caged interstitial vortices in superconducting α-WGe films with an antidot lattice *Phys. Rev.* B **53** R2983–6

[209] Harada K, Kamimura O, Kasai H, Matsuda T, Tonomura A and Moshchalkov V V 1996 Direct observation of vortex dynamics in superconducting films with regular arrays of defects *Science* **274** 1167–70

[210] Metlushko V, Welp U, Crabtree G W, Zhang Z, Brueck S R J, Watkins B, DeLong L E, Ilic B, Chung K and Hesketh P J 1999 Nonlinear flux-line dynamics in vanadium films with square lattices of submicron holes *Phys. Rev.* B **59** 603–7

[211] Fasano Y, Herbsommer J A, de la Cruz F, Pardo F, Gammel P L, Bucher E and Bishop D J 1999 Observation of periodic vortex pinning induced by Bitter decoration *Phys. Rev.* B **60** R15047–50

[212] Fasano Y, Menghini M, de la Cruz F and Nieva G 2000 Weak interaction and matching conditions for replicas of vortex lattices *Phys. Rev.* B **62** 15183–9

[213] Fasano Y and Menghini M 2008 Magnetic-decoration imaging of structural transitions induced in vortex matter *Supercond. Sci. Technol.* **21** 023001

[214] Goyal A *et al* 2005 Irradiation-free, columnar defects comprised of self-assembled nanodots and nanorods resulting in strongly enhanced flux-pinning in $YBa_2Cu_3O_{7-\delta}$ films *Supercond. Sci. Technol.* **18** 1533–8

[215] Villegas J E, Li C-P and Schuller I K 2007 Bistability in a superconducting Al thin film induced by arrays of Fe-nanodot magnetic vortices *Phys. Rev. Lett.* **99** 227001

[216] Welp U, Xiao Z L, Jiang J S, Vlasko-Vlasov V K, Bader S D, Crabtree G W, Liang J, Chik H and Xu J M 2002 Superconducting transition and vortex pinning in Nb films patterned with nanoscale hole arrays *Phys. Rev.* B **66** 212507

[217] Welp U, Xiao Z L, Novosad V and Vlasko-Vlasov V K 2005 Commensurability and strong vortex pinning in nanopatterned Nb films *Phys. Rev.* B **71** 014505

[218] Vinckx W, Vanacken J, Moshchalkov V V, Mátéfi-Tempfli S, Mátéfi-Tempfli M, Michotte S, Piraux L and Ye X 2007 High field matching effects in superconducting Nb porous arrays catalyzed from anodic alumina templates *Physica* C **459** 5–10

[219] Vanacken J, Vinckx W, Moshchalkov V V, Mátéfi-Tempfli S, Mátéfi-Tempfli M, Michotte S, Piraux L and Ye X 2008 Vortex pinning in superconductors laterally modulated by nanoscale self-assembled arrays *Physica* C **468** 585–8

[220] Reichhardt C, Olson C J and Nori F 1998 Commensurate and incommensurate vortex states in superconductors with periodic pinning arrays *Phys. Rev.* B **57** 7937–43

[221] Reichhardt C and Grønbech-Jensen N 2000 Collective multivortex states in periodic arrays of traps *Phys. Rev. Lett.* **85** 2372–5

[222] Reichhardt C and Zimányi G T 2000 Melting of moving vortex lattices in systems with periodic pinning *Phys. Rev.* B **61** 14354–7

[223] Reichhardt C, Zimányi G T and Grønbech-Jensen N 2001 Complex dynamical flow phases and pinning in superconductors with rectangular pinning arrays *Phys. Rev.* B **64** 014501

[224] Reichhardt C, Zimányi G T, Scalettar R T, Hoffmann A and Schuller I K 2001 Individual and multiple vortex pinning in systems with periodic pinning arrays *Phys. Rev.* B **64** 052503

[225] Helseth L E 2002 Interaction between superconducting films and magnetic nanostructures *Phys. Rev.* B **66** 104508

[226] Lyuksyutov I F and Pokrovsky V L 1998 Magnetization controlled superconductivity in a film with magnetic dots *Phys. Rev. Lett.* **81** 2344–7

[227] Šášik R and Hwa T 2000 Enhanced pinning of vortices in thin film superconductors by magnetic dot arrays arXiv:cond-mat/0003462

[228] Erdin S 2003 Symmetry violation in a superconducting film with a square array of ferromagnetic dots *Physica* C **391** 140–6

[229] Wei H 2005 Critical current in a superconducting film with an array of ferromagnetic dots *Phys. Rev.* B **71** 144521

[230] Wei H 2006 Creation of vortices in a superconducting film by ferromagnetic dots *Physica* C **434** 13–6

[231] Chen Q H, Teniers G, Jin B B and Moshchalkov V V 2006 Pinning properties and vortex dynamics in thin superconducting films with ferromagnetic and antiferromagnetic arrays of magnetic dots *Phys. Rev.* B **73** 014506

[232] Neal J S, Milošević M V, Bending S J, Potenza A, San Emeterio L and Marrows C H 2007 Competing symmetries and broken bonds in superconducting vortex–antivortex molecular crystals *Phys. Rev. Lett.* **99** 127001

[233] Pogosov W V, Rakhmanov A L and Moshchalkov V V 2003 Vortex lattice in the presence of a tunable periodic pinning potential *Phys. Rev.* B **67** 014532

[234] Lange M, Van Bael M J, Van Look L, Temst K, Swerts J, Güntherodt G, Moshchalkov V V and Bruynseraede Y 2001 Asymmetric flux pinning in laterally nanostructured ferromagnetic/superconducting bilayers *Europhys. Lett.* **53** 646–52

[235] Lange M, Van Bael M J, Van Look L, Temst K, Swerts J, Güntherodt G, Moshchalkov V V and Bruynseraede Y 2002 Asymmetric flux pinning in laterally nanostructured ferromagnetic/superconducting bilayers *Europhys. Lett.* **57** 149–50

[236] Lange M, Van Bael M J, Moshchalkov V V and Bruynseraede Y 2002 Asymmetric flux pinning by magnetic antidots *J. Magn. Magn. Mater.* **240** 595–7

[237] Van Bael M J, Raedts S, Temst K, Swerts J, Moshchalkov V V and Bruynseraede Y 2002 Magnetic domains and flux pinning properties of a nanostructured ferromagnet/superconductor bilayer *J. Appl. Phys.* **92** 4531–7

[238] Raedts S, Van Bael M J, Temst K, Lange M, Van Look L, Swerts J, Moshchalkov V V and Bruynseraede Y 2002 Pinning of domain walls and flux lines in a nanostructured ferromagnet/superconductor bilayer *Physica* C **369** 258–61

[239] Soroka A K and Huth M 2002 Guided vortex motion in faceted niobium films *Low Temp. Phys.* **28** 842–4

[240] Vélez M, Jaque D, Martín J I, Montero M I, Schuller I K and Vicent J L 2002 Vortex lattice channeling effects in Nb films induced by anisotropic arrays of mesoscopic pinning centers *Phys. Rev.* B **65** 104511

[241] Silhanek A V, Van Look L, Raedts S, Jonckheere R and Moshchalkov V V 2003 Guided vortex motion in superconductors with a square antidot array *Phys. Rev.* B **68** 214504

[242] Wördenweber R and Dymashevski P 2004 Guided vortex motion in high-T_c superconducting thin films and devices with special arrangements of artificial defects *Physica* C **404** 421–5

[243] Carneiro G 2005 Tunable ratchet effects for vortices pinned by periodic magnetic dipole arrays *Physica* C **432** 206–14

[244] Verellen N, Silhanek A V, Gillijns W, Moshchalkov V V, Metlushko V, Gozzini F and Ilic B 2008 Switchable magnetic dipole induced guided vortex motion *Appl. Phys. Lett.* **93** 022507

[245] Jaque D, González E M, Martin J I, Anguita J V and Vicent J L 2002 Anisotropic pinning enhancement in Nb films with arrays of submicrometric Ni lines *Appl. Phys. Lett.* **81** 2851–3

[246] Gheorghe D G, Wijngaarden R J, Gillijns W, Silhanek A V and Moshchalkov V V 2008 Magnetic flux patterns in superconductors deposited on a lattice of magnetic dots: a magneto-optical imaging study *Phys. Rev.* B **77** 054502

[247] Vlasko-Vlasov V, Welp U, Karapetrov G, Novosad V, Rosenmann D, Iavarone M, Belkin A and Kwok W-K 2008 Guiding superconducting vortices with magnetic domain walls *Phys. Rev.* B **77** 134518

[248] Terentiev A, Watkins D B, de Long L E, Morgan D J and Ketterson J B 1999 Observation of magnetic flux pinning in a thin Nb film with a square lattice of nickel dots *Physica* C **324** 1–8

[249] Terentiev A, Watkins D B, de Long L E, Cooley L D, Morgan D J and Ketterson J B 2000 Periodic magnetization instabilities in a superconducting Nb film with a square lattice of Ni dots *Physica* C **332** 5–11

[250] Terentiev A, Watkins D B, de Long L E, Cooley L D, Morgan D J and Ketterson J B 2000 Periodic magnetization instabilities in a superconducting Nb film with a square lattice of Ni dots *Phys. Rev.* B **61** 9249–52

[251] Raabe J, Pulwey R, Sattler R, Schweinböck T, Zweck J and Weiss D 2000 Magnetization pattern of ferromagnetic nanodisks *J. Appl. Phys.* **88** 4437–9

[252] Seynaeve E, Rens G, Volodin A V, Temst K, van Haesendonck C and Bruynseraede Y 2001 Transition from a single-domain to a multidomain state in mesoscopic ferromagnetic Co structures *J. Appl. Phys.* **89** 531–4

[253] Villegas J E, Smith K D, Huang L, Zhu Y, Morales R and Schuller I K 2008 Switchable collective pinning of flux quanta using magnetic vortex arrays: experiments on square arrays of Co dots on thin superconducting films *Phys. Rev.* B **77** 134510

[254] Hoffmann A, Fumagalli L, Jahedi N, Sautner J C, Pearson J E, Mihajlović G and Metlushko V 2008 Enhanced pinning of superconducting vortices by magnetic vortices *Phys. Rev.* B **77** 060506(R)

[255] Carneiro G 2007 Tunable pinning of a superconducting vortex by a magnetic vortex *Phys. Rev.* B **75** 094504

[256] Lange M, Van Bael M J, Moshchalkov V V and Bruynseraede Y 2002 Magnetic-domain-controlled vortex pinning in a superconductor/ferromagnet bilayer *Appl. Phys. Lett.* **81** 322–4

[257] Silhanek A V, Gillijns W, Moshchalkov V V, Metlushko V and Ilic B 2006 Tunable pinning in superconducting films with magnetic microloops *Appl. Phys. Lett.* **89** 182505

[258] Silhanek A V, Gillijns W, Moshchalkov V V, Metlushko V, Gozzini F, Ilic B, Uhlig W C and Unguris J 2007 Manipulation of the vortex motion in nanostructured ferromagnetic/superconductor hybrids *Appl. Phys. Lett.* **90** 182501

[259] Silhanek A V, Verellen N, Metlushko V, Gillijns W, Gozzini F, Ilic B and Moshchalkov V V 2008 Rectification effects in superconductors with magnetic pinning centers *Physica* C **468** 563–7

[260] Strongin M, Maxwell E and Reed T B 1964 Ac susceptibility measurements on transition metal superconductors containing rare earth and ferromagnetic metal solutes *Rev. Mod. Phys.* **36** 164–8

[261] Alden T H and Livingston J D 1966 Magnetic pinning in a type-II superconductor *J. Appl. Phys.* **8** 6–7

[262] Alden T H and Livingston J D 1966 Ferromagnetic particles in a type-II superconductor *J. Appl. Phys.* **37** 3551–6

[263] Koch C C and Love G R 1969 Superconductivity in niobium containing ferromagnetic gadolinium or paramegnetic yttrium dispersions *J. Appl. Phys.* **40** 3582–7

[264] Sikora A and Makiej B 1982 On the occurrence of a directional asymmetry of the critical current in type-I superconductor containing ferromagnetic particles *Phys. Status Solidi* a **71** K197–200

[265] Sikora A and Makiej B 1985 The directional asymmetry of the critical current in type-II superconductor containing ferromagnetic particles *Phys. Status Solidi* a **88** K197–200

[266] Wang J-Q, Rizzo N D, Prober D E, Motowidlo L R and Zeitlin B A 1997 Flux pinning in multifilamentary superconducting wires with ferromagnetic artificial pinning centers *IEEE Trans. Appl. Supercond.* **7** 1130–3

[267] Lyuksyutov I F and Naugle D G 1999 Frozen flux superconductors *Mod. Phys. Lett.* B **13** 491–7

[268] Lyuksyutov I F and Naugle D G 2003 Magnet–superconductor nanostructures *Int. J. Mod. Phys.* B **17** 3441–4

[269] Lyuksyutov I F and Naugle D G 2003 Magnetic nanorods/superconductor hybrids *Int. J. Mod. Phys.* B **17** 3713–6

[270] Santos J E, Frey E and Schwabl F 2001 Dipolar interactions in superconductor-ferromagnet heterostructures *Phys. Rev.* B **63** 054439

[271] Kuroda T, Nakane T, Uematsu H and Kumakura K 2006 Doping effects of nanoscale Fe particles on the superconducting properties of powder-in-tube processed MgB_2 tapes *Supercond. Sci. Technol.* **19** 1152–7

[272] Togoulev P N, Suleimanov N M and Conder K 2006 Pinning enhancement in MgB_2–magnetic particles composites *Physica* C **450** 45–7

[273] Kruchinin S P, Dzhezherya Y I and Annett J F 2006 Interactions of nanoscale ferromagnetic granules in a London superconductor *Supercond. Sci. Technol.* **19** 381–4

[274] Palau A, MacManus-Driscoll J L and Blamire M G 2007 Magnetic vortex pinning in superconductor/ferromagnet nanocomposites *Supercond. Sci. Technol.* **20** S136–40

[275] Palau A, Parvaneh H, Stelmashenko N A, Wang H, Macmanus-Driscoll J L and Blamire M G 2007 Hysteretic vortex pinning in superconductor–ferromagnet nanocomposites *Phys. Rev. Lett.* **98** 117003

[276] Haindl S, Weisheit M, Neu V, Schultz L and Holzapfel B 2007 Epitaxial heterostructures of hard magnetic and superconducting thin films *Physica* C **463–465** 1001–4

[277] Haindl S, Weisheit M, Thersleff T, Schultz L and Holzapfel B 2008 Enhanced field compensation effect in superconducting/hard magnetic Nb/FePt bilayers *Supercond. Sci. Technol.* **21** 045017

[278] Snezhko A, Prozorov T and Prozorov R 2005 Magnetic nanoparticles as efficient bulk pinning centers in type-II superconductors *Phys. Rev.* B **71** 024527

[279] Rizzo N D, Wang J Q, Prober D E, Motowidlo L R and Zeitlin B A 1996 Ferromagnetic artificial pinning centers in superconducting $Nb_{0.36}Ti_{0.64}$ wires *Appl. Phys. Lett.* **69** 2285–7

[280] Stamopoulos D, Pissas M, Karanasos V, Niarchos D and Panagiotopoulos I 2004 Influence of randomly distributed magnetic nanoparticles on surface superconductivity in Nb films *Phys. Rev.* B **70** 054512

[281] Stamopoulos D, Manios E, Pissas M and Niarchos D 2004 Pronounced T_c enhancement and magnetic memory effects in hybrid films *Supercond. Sci. Technol.* **17** L51–4

[282] Samopoulos D, Pissas M and Manios E 2005 Ferromagnetic–superconducting hybrid films and their possible applications: a direct study in a model combinatorial film *Phys. Rev.* B **71** 014522
[283] Stamopoulos D and Manios E 2005 The nucleation of superconductivity in superconducting–ferromagnetic hybrid films *Supercond. Sci. Technol.* **18** 538–51
[284] Stamopoulos D, Manios E, Pissas M and Niarchos D 2006 Modulation of the properties of a low-T_c superconductor by anisotropic ferromagnetic particles *Physica* C **437/438** 289–92
[285] Suleimanov N M, Togulev P N, Bazarov V V and Khaibullin I B 2004 Strengthening of pinning by magnetic particles in high temperature superconductors *Physica* C **404** 363–6
[286] Xing Y T, Micklitz H, Rappoport T G, Milošević M V, Solrzano-Naranjo I G and Baggio-Saitovitch E 2008 Spontaneous vortex phases in superconductor–ferromagnet Pb–Co nanocomposite films *Phys. Rev.* B **78** 224524
[287] Xing Y T, Micklitz H, Baggio-Saitovitch E and Rappoport T G 2008 Controlled switching between paramagnetic and diamagnetic Meissner effect in Pb/Co nanocomposites arXiv:0812.0847 [cond-mat]
[288] Xing Y T, Micklitz H, Rodrigez W A, Baggio-Saitovitch E and Rappoport T G 2009 Superconducting transition in Pb/Co nanocomposites: effect of Co volume fraction and external magnetic field arXiv:0901.0666 [cond-mat]
[289] Li M S 2003 Paramagnetic Meissner effect and related phenomena *Phys. Rep.* **376** 133–223
[290] Monton C, de la Cruz F and Guimpel J 2007 Magnetic behavior of superconductor/ferromagnet superlattices *Phys. Rev.* B **75** 064508
[291] Carneiro G 2008 Moving vortex matter with coexisting vortices and anti-vortices arXiv:0806.2109 [cond-mat]
[292] Lima C L S and de Souza Silva C C 2008 Dynamics of driven vortex–antivortex matter in superconducting films with a magnetic dipole array arXiv:0808.2421 [cond-mat]
[293] Zapata I, Bartussek R, Sols F and Hänggi P 1996 Voltage rectification by a SQUID ratchet *Phys. Rev.* B **77** 2292–5
[294] Lee C-S, Jankó B, Derényi I and Barabási A-L 1999 Reducing vortex density in superconductors using the 'ratchet effect' *Nature* **400** 337–40
[295] Wambaugh J F, Reichhardt C, Olson C J, Marchesoni F and Nori F 1999 Superconducting fluxon pumps and lenses *Phys. Rev. Lett.* **83** 5106–9
[296] Villegas J E, Savel'ev S, Nori F, Gonzalez E M, Anguita J V, Garcia R and Vicent J L 2003 A superconducting reversible rectifier that controls the motion of magnetic flux quanta *Science* **302** 1188–91
[297] Wördenweber R, Dymashevski P and Misko V R 2004 Guidance of vortices and the vortex ratchet effect in high-T_c superconducting thin films obtained by arrangement of antidots *Phys. Rev.* B **69** 184504
[298] Van de Vondel J, de Souza Silva C C, Zhu B Y, Morelle M and Moshchalkov V V 2005 Vortex-rectification effects in films with periodic asymmetric pinning *Phys. Rev. Lett.* **94** 057003
[299] Togawa Y, Harada K, Akashi T, Kasai H, Matsuda T, Nori F, Maeda A and Tonomura A 2005 Direct observation of rectified motion of vortices in a niobium superconductor *Phys. Rev. Lett.* **95** 087002
[300] de Souza Silva C C, Van de Vondel J, Morelle M and Moshchalkov V V 2006 Controlled multiple reversals of a ratchet effect *Nature* **440** 651–4
[301] Wu T C, Horng L, Wu J C, Hsiao C W, Kolacek J and Yang T J 2006 Vortex dynamics in spacing-graded array of defects on a niobium film *Physica* C **437/438** 353–6
[302] Aladyshkin A Yu, Van de Vondel J, de Souza Silva C C and Moshchalkov V V 2008 Tunable anisotropic nonlinearity in superconductors with asymmetric antidot array *Appl. Phys. Lett.* **93** 082501
[303] de Souza Silva C C, Silhanek A V, Van de Vondel J, Gillijns W, Metlushko V, Ilic B and Moshchalkov V V 2007 Dipole-induced vortex ratchets in superconducting films with arrays of micromagnets *Phys. Rev. Lett.* **98** 117005
[304] Genkin G M, Skuzovatkin V V and Tokman I D 1994 Magnetization of the ferromagnetic–superconductor structures *J. Magn. Magn. Mater.* **130** 51–6
[305] Bespyatykh Yu I and Wasilevski W 2001 The spontaneous formation of a vortex structure in a type II superconductor–ferromagnet bilayer *Sov. Phys.—Solid State* **43** 224–30
[306] Bespyatykh Yu I, Wasilevski W, Gajdek M, Nikitin I P and Nikitov S A 2001 Pinning of vortices by the domain structure in a two-layered type-II superconductor–ferromagnet system *Sov. Phys.—Solid State* **43** 1827–33
[307] Helseth L E, Goa P E, Hauglin H, Baziljevich M and Johansen T H 2002 Interaction between a magnetic domain wall and a superconductor *Phys. Rev.* B **65** 132514
[308] Laiho R, Lähderanta E, Sonin E B and Traito K B 2003 Penetration of vortices into the ferromagnet/type-II superconductor bilayer *Phys. Rev.* B **67** 144522
[309] Traito K B, Laiho R, Lähderanta E and Sonin E B 2003 Vortex structures in the ferromagnet–superconductor bilayer *Physica* C **388–389** 641–2
[310] Erdin S 2006 Vortex chain states in a ferromagnet/superconductor bilayer *Phys. Rev.* B **73** 224506
[311] Bulaevskii L N and Chudnovsky E M 2000 Ferromagnetic film on a superconducting substrate *Phys. Rev.* B **63** 012502
[312] Bulaevskii L N, Chudnovsky E M and Daumens M 2000 Reply to Comment on 'Ferromagnetic film on a superconducting substrate' *Phys. Rev.* B **66** 136502
[313] Kayali M A and Pokrovsky V L 2004 Anisotropic transport properties of ferromagnetic–superconducting bilayers *Phys. Rev.* B **69** 132501
[314] Burmistrov I S and Chtchelkatchev N M 2005 Domain wall effects in ferromagnet–superconductor structures *Phys. Rev.* B **72** 144520
[315] Ainbinder R M and Maksimov I L 2007 Critical current of a magnetic–superconducting heterostructure: diode effect *Supercond. Sci. Technol.* **20** 441–3
[316] Maksimova G M, Ainbinder R M and Maksimov I L 2006 Vortex–antivortex configurations in a superconducting film due to a ferromagnetic strip: edge barrier versus annihilation barrier *Phys. Rev.* B **73** 214515
[317] Maksimova G M, Ainbinder R M and Vodolazov D Y 2008 Periodic vortex and current structures in superconductor–ferromagnet bilayer *Phys. Rev.* B **78** 224505
[318] Bulaevskii L N, Chudnovsky E M and Maley M P 2000 Magnetic pinning in superconductor–ferromagnet multilayers *Appl. Phys. Lett.* **76** 2594–6
[319] Lange M, Moshchalkov V V and Van Bael M J 2003 Flux pinning by magnetic bubble domains *Mod. Phys. Lett.* B **17** 519–26
[320] Lange M, Van Bael M J and Moshchalkov V V 2004 Interaction between vortices and magnetic domains in a superconductor/ferromagnet bilayer *Physica* C **408–410** 522–3
[321] Cieplak M Z, Adamus Z, Konczykowski M, Chen X M, Byczuk A, Abal'oshev A, Sang H and Chien C L 2004 Superconducting pinning by magnetic domains in a ferromagnet–superconductor bilayer *Acta Phys. Pol.* A **106** 693–8
[322] Cieplak M Z, Cheng X M, Chien C L and Sang H 2005 Superconducting pinning by magnetic domains in a ferromagnet–superconductor bilayer *J. Appl. Phys.* **97** 026105
[323] Goa P E, Hauglin H, Olsen Å A F, Shantsev D and Johansen T H 2003 Manipulation of vortices by magnetic domain walls *Appl. Phys. Lett.* **82** 79–81
[324] Vlasko-Vlasov V K, Welp U, Imre A, Rosenmann D, Pearson J and Kwok W K 2008 Soft magnetic lithography

and giant magnetoresistance in superconducting/ferromagnetic hybrids *Phys. Rev.* B **78** 214511
[325] Belkin A, Novosad V, Iavarone M, Fedor J, Pearson J E, Petrean-Troncalli A and Karapetrov G 2008 Tunable transport in magnetically coupled MoGe/Permalloy hybrids *Appl. Phys. Lett.* **93** 072510
[326] Belkin A, Novosad V, Iavarone M, Pearson J and Karapetrov G 2008 Superconductor/ferromagnet bilayers: influence of magnetic domain structure on vortex dynamics *Phys. Rev.* B **77** 180506
[327] García-Santiago A, Sánchez F, Varela M and Tejada J 2000 Enhanced pinning in a magnetic–superconducting bilayer *Appl. Phys. Lett.* **77** 2900–2
[328] Jan D B, Coulter J Y, Hawley M E, Bulaevskii L N, Maley M P, Jiaa Q X, Maranville B B, Hellman F and Pan X Q 2003 Flux pinning enhancement in ferromagnetic and superconducting thin-film multilayers *Appl. Phys. Lett.* **82** 778–80
[329] Zhang X X, Wen G H, Zheng R K, Xiong G C and Lian G J 2001 Enhanced flux pinning in a high-T_c superconducting film by a ferromagnetic buffer layer *Europhys. Lett.* **56** 119–25
[330] Laviano F, Gozzelino L, Gerbaldo R, Ghigo G, Mezzetti E, Przyslupski P, Tsarou A and Wisniewski A 2007 Interaction between vortices and ferromagnetic microstructures in twinned cuprate/manganite bilayers *Phys. Rev.* B **76** 214501
[331] Milošević M V, Berdiyorov G R and Peeters F M 2005 Mesoscopic field and current compensator based on a hybrid superconductor–ferromagnet structure *Phys. Rev. Lett.* **95** 147004
[332] Schildermans N, Silhanek A V, Sautner J, Metlushko V, Vavassori P and Moshchalkov V V 2009 Critical field enhancement in hybrid superconductor/ferromagnet mesoscopic disks *J. Appl. Phys.* **105** 023918
[333] Vodolazov D Y, Gribkov B A, Gusev S A, Klimov A Yu, Nozdrin Yu N, Rogov V V and Vdovichev S N 2005 Considerable enhancement of the critical current in a superconducting film by a magnetized magnetic strip *Phys. Rev.* B **72** 064509
[334] Touitou N, Bernstein P, Hamet J F, Simon Ch, Méchin L, Contour J P and Jacquet E 2004 Nonsymmetric current–voltage characteristics in ferromagnet/superconductor thin film structures *Appl. Phys. Lett.* **85** 1742–4
[335] Morelle M and Moshchalkov V V 2006 Enhanced critical currents through field compensation with magnetic strips *Appl. Phys. Lett.* **88** 172507
[336] Vodolazov D Y, Gribkov B A, Klimov A Yu, Rogov V V and Vdovichev S N 2009 Strong influence of a magnetic layer on the critical current of Nb bridge in finite magnetic fields due to surface barrier effect *Appl. Phys. Lett.* **94** 012508
[337] Dolan G J and Lukens J E 1977 Properties of superconducting weak links formed by magnetically weakening a short length of a uniform aluminum film *IEEE Trans. Magn.* **13** 581–4
[338] Clinton T W and Johnson M 1997 Mesoscopic magnetoquenched superconducting valve *Appl. Phys. Lett.* **70** 1170–2
[339] Clinton T W and Johnson M 1999 Nonvolatile switchable Josephson junctions *J. Appl. Phys.* **85** 1637–43
[340] Clinton T W and Johnson M 2000 Magnetoquenched superconducting valve with bilayer ferromagnetic film for uniaxial switching *Appl. Phys. Lett.* **76** 2116–8
[341] Clinton T W, Broussard P R and Johnson M 2002 Advances in the development of the magnetoquenched superconducting valve: integrated control lines and a Nb-based device *J. Appl. Phys.* **91** 1371–7
[342] Eom J and Johnson M 2001 Switchable superconducting quantum interferometers *Appl. Phys. Lett.* **79** 2486–8
[343] Li Q, Belitz D and Kirkpatrick T R 2006 Nearly ferromagnetic superconductors: electromagnetic properties studied by a generalized Ginzburg–Landau theory *Phys. Rev.* B **74** 134505
[344] Sadreev A F 1993 Influence of superconducting substrates on the domain structure of a magnetic film with a uniaxial anisotropy *Sov. Phys.—Solid State* **35** 1044–6
[345] Bespyatkh Yu I, Wasilewski W, Gajdek M, Simonov A D and Kharitonov V D 1994 Suppression of magnetic domains in layered ferromagnetic-type-II-superconductor structures *Sov. Phys.—Solid State* **36** 323–7
[346] Bespyatykh Yu I, Wasilevskii W, Lokk E G and Kharitonov V D 1998 Suppression of the domain structure in uniaxial ferromagnetic films with a superconducting coating *Sov. Phys.—Solid State* **40** 975–81
[347] Stankiewicz A, Tarasenko V, Robinson S J and Gehring G A 1997 Magnetic domain structures of ferromagnetic thin films deposited on superconducting substrates *J. Appl. Phys.* **81** 4713
[348] Stankiewicz A, Tarasenko V, Robinson S J and Gehring G A 1997 Magnetic domain structures of ferromagnetic ultra-thin films deposited on superconducting substrates *J. Phys.: Condens. Matter* **9** 1019–30
[349] Daumens M and Ezzahri Y 2003 Equilibrium domain structure in a ferromagnetic film coated by a superconducting film *Phys. Lett.* A **306** 344–7
[350] Tamegai T, Nakao Y and Nakajima Y 2009 Shrinkage of magnetic domains in superconductor/ferromagnet bilayer *J. Phys.: Conf. Ser.* at press
[351] Fraerman A A, Karetnikova I R, Nefedov I M, Shereshevskii I A and Silaev M A 2005 Magnetization reversal of a nanoscale ferromagnetic disk placed above a superconductor *Phys. Rev.* B **71** 094416
[352] Pokrovsky V L, Romanov K and Wei H 2006 Magnetic configurations of hybrid ferromagnetic dot-superconductor systems *J. Magn. Magn. Mater.* **307** 107–12
[353] Dubonos S V, Geim A K, Novoselov K S and Grigorieva I V 2002 Spontaneous magnetization changes and nonlocal effects in mesoscopic ferromagnet–superconductor structures *Phys. Rev.* B **65** 220513
[354] Monton C, de la Cruz F and Guimpel J 2008 Magnetic state modification induced by superconducting response in ferromagnet/superconductor Nb/Co superlattices *Phys. Rev.* B **77** 104521
[355] Monton C, Ramos C A, Guimpel J and Zysler R D 2008 Experimental evidence of magnetic anisotropy induction by superconductivity in superlattices *Appl. Phys. Lett.* **92** 152508
[356] Wu H, Ni J, Cai J, Cheng Z and Sun Y 2007 Experimental evidence of magnetization modification by superconductivity in a Nb/$Ni_{81}Fe_{19}$ multilayer *Phys. Rev.* B **76** 024416
[357] Lyuksyutov I F and Pokrovsky V L 2000 Spontaneous supercurrents in magneto-superconducting systems *Mod. Phys. Lett.* B **14** 409–14
[358] Erdin S, Lyuksyutov I F, Pokrovsky V L and Vinokur V M 2002 Topological instability in a ferromagnet-superconducting bilayer *Phys. Rev. Lett.* **88** 017001
[359] Genenko Y A 2002 Magnetic shielding for improvement of superconductor performance *Phys. Status Solidi* a **189** 469–73
[360] Genenko Y A and Snezhko A V 2002 Superconductor strip near a magnetic wall of finite thickness *J. Appl. Phys.* **92** 357–60
[361] Genenko Yu A, Usoskin A and Freyhardt H C 1999 Large predicted self-field critical current enhancements in superconducting strips using magnetic screens *Phys. Rev. Lett.* **83** 3045–8
[362] Genenko Yu A, Snezhko A and Freyhardt H C 2000 Overcritical states of a superconductor strip in a magnetic environment *Phys. Rev.* B **62** 3453–72
[363] Genenko Yu A, Usoskin A, Snezhko A and Freyhardt H C 2000 Overcritical states in magnetically shielded superconductor strips *Physica* C **341–348** 1063–4
[364] Genenko Y A, Rauh H and Snezhko A 2001 A novel magnet/superconductor heterostructure for high-field applications *Supercond. Sci. Technol.* **14** 699–703

[365] Genenko Y A, Rauh H and Snezhko A 2002 Novel design of a smart magnet/superconductor heterostructure *Physica* C **372–376** 1389–93

[366] Yampolskii S V, Genenko Yu A and Rauh H 2004 Distribution of the sheet current in a magnetically shielded superconducting filament *Physica* C **415** 151–7

[367] Genenko Y A, Yampolskii S V and Pan A V 2004 Virgin magnetization of a magnetically shielded superconductor wire: theory and experiment *Appl. Phys. Lett.* **84** 3921–3

[368] Genenko Y A, Rauh H and Yampolskii S V 2005 The Bean–Livingston barrier at a superconductor/magnet interface *J. Phys.: Condens. Matter* **17** L93–101

[369] Genenko Y A and Rauh H 2007 Superconductor strip in a closed magnetic environment: exact analytic representation of the critical state *Physica* C **460–462** 1264–5

[370] Yampolskii S V and Genenko Yu A 2005 Entry of magnetic flux into a magnetically shielded type-II superconductor filament *Phys. Rev.* B **71** 134519

[371] Yampolskii S V, Yampolskaya G I and Rauh H 2006 Magnetic dipole–vortex interaction in a bilayered superconductor/soft-magnet heterostructure *Europhys. Lett.* **74** 334–40

[372] Yampolskii S V, Yampolskaya G I and Rauh H 2007 Magnetic-dipole induced appearance of vortices in a bilayered superconductor/soft-magnet heterostructure *Physica* C **460–462** 1200–1

[373] Yampolskii S V, Genenko Y A and Rauh H 2007 Penetration of an external magnetic field into a multistrip superconductor/soft-magnet heterostructure *Physica* C **460–462** 1262–3

[374] Majoros M, Glowacki B A and Campbell A M 2000 Transport ac losses and screening properties of Bi-2223 multifilamentary tapes covered with magnetic materials *Physica* C **338** 251–62

[375] Glowacki B A, Majoros M, Rutter N A and Campbell A M 2001 A new method for decreasing transport ac losses in multifilamentary coated superconductors *Physica* C **357–360** 1213–7

[376] Horvat J, Wang X L, Soltanian S and Dou S X 2002 Improvement of critical current in MgB_2/Fe superconducting wires by a ferromagnetic sheath *Appl. Phys. Lett.* **80** 829–31

[377] Horvat J, Yeoh W K and Miller L M 2005 Interaction between superconductor and ferromagnetic domains in iron sheath: peak effect in MgB_2/Fe wires *Appl. Phys. Lett.* **87** 102503

[378] Duckworth R C, Thompson J R, Gouge M J, Lue J W, Ijaduola A O, Yu D and Verebelyi D T 2003 Transport ac loss studies of YBCO coated conductors with nickel alloy substrates *Supercond. Sci. Technol.* **16** 1294–8

[379] Kováč P, Hušek I, Melišek T, Ahoranta M, Šouc J, Lehtonen J and Gömöry F 2003 Magnetic interaction of an iron sheath with a superconductor *Supercond. Sci. Technol.* **16** 1195–201

[380] Pan A V, Zhou S and Dou S 2004 Iron-sheath influence on the superconductivity of MgB_2 core in wires and tapes *Supercond. Sci. Technol.* **17** S410–4

[381] Jooss Ch, Brinkmeier E and Heese H 2005 Combined experimental and theoretical study of field and current conditioning in magnetically shielded superconducting films *Phys. Rev.* B **72** 144516

[382] Gu C, Alamgir A K M, Qu T and Han Z 2007 Simulation of ferromagnetic shielding to the critical current of Bi2223/Ag tape under external fields *Supercond. Sci. Technol.* **20** 133–7

[383] Gömöry F, Šouc J, Vojenčiak M, Alamgir A K M, Han Z and Gu Ch 2007 Reduction of ac transport and magnetization loss of a high-T_c superconducting tape by placing soft ferromagnetic materials at the edges *Appl. Phys. Lett.* **90** 092506

[384] Gömöry F, Šouc J, Seiler E, Vojenčiak M and Granados X 2008 Modification of critical current in HTSC tape conductors by a ferromagnetic layer *J. Phys.: Conf. Ser.* **97** 012096

[385] Golubović D S and Moshchalkov V V 2005 Linear magnetic flux amplifier *Appl. Phys. Lett.* **87** 142501

[386] Hilgenkamp H, Ariando, Smilde H J H, Blank D H A, Rijnders H, Rogalla G, Kirtley J R and Tseui C C 2003 Ordering and manipulation of the magnetic moments in large-scale superconducting π-loop arrays *Nature* **422** 50

[387] Goldobin E, Koelle D and Kleiner R 2003 Ground states and bias-current-induced rearrangement of semifluxons in 0-π long Josephson junctions *Phys. Rev.* B **67** 224515

[388] Lange M, Van Bael M J and Moshchalkov V V 2003 Phase diagram of a superconductor/ferromagnet bilayer *Phys. Rev.* B **68** 174522

[389] Hinoue T, Shimizu M, Ono T and Miyajima H 2001 Magnetization process of ferromagnet–superconductor hybrid films *J. Magn. Magn. Mater.* **226–230** 1583–4

[390] Matsuda K, Akimoto Y, Uemura T and Yamamoto M 2008 Magnetic and transport properties of superconductor/ferromagnet bilayer microbridges *J. Appl. Phys.* **103** 07C711

[391] Feigenson M, Klein L, Karpovski M, Reiner J W and Beasley M R 2005 Suppression of the superconducting critical current of Nb in bilayers of Nb/$SrRuO_3$ *J. Appl. Phys.* **97** 10J120

[392] Singh A, Sürgers C, Uhlarz M, Singh S and von Löhneysen H 2007 Manipulating superconductivity in perpendicularly magnetized FSF triple layers *Appl. Phys.* A **89** 593–7

[393] Lemberger T R, Hetel I, Hauser A J and Yang F Y 2008 Superfluid density of superconductor–ferromagnet bilayers *J. Appl. Phys.* **103** 07C701

[394] Joshi A G, Kryukov S A, De Long L E, Gonzalez E M, Navarro E, Villegas J E and Vicent J L 2007 Magnetic instabilities along the superconducting phase boundary of Nb/Ni multilayers *J. Appl. Phys.* **101** 09G117

[395] Kobayashi S, Oike H, Takeda M and Itoh F 2002 Central peak position in magnetization hysteresis loops of ferromagnet–superconductor ferromagnet trilayered films *Phys. Rev.* B **66** 214520

[396] Kobayashi S, Kanno Y and Itoh F 2003 Transport critical current in superconductor/ferromagnet trilayered films *Physica* B **329–333** 1357–8

[397] Rakshit R K, Budhani R C, Bhuvana T, Kulkarni V N and Kulkarni G U 2008 Inhomogeneous vortex-state-driven enhancement of superconductivity in nanoengineered ferromagnet–superconductor heterostructures *Phys. Rev.* B **77** 052509

[398] Rakshit R K, Bose S K, Sharma R, Pandey N K and Budhani R C 2008 Lattice-mismatch-induced granularity in CoPt-NbN and NbN-CoPt superconductor–ferromagnet heterostructures: effect of strain *Phys. Rev.* B **77** 094505

[399] Rubinstein M, Lubitz P, Carlos W E, Broussard P R, Chrisey D B, Horwitz J and Krebs J J 1993 Properties of superconductor–ferromagnet bilayers: YBa_2CuO_3-Fe and YBa_2CuO_3-permalloy *Phys. Rev.* B **47** 15350–3

[400] Yuzhelevski Y and Jung G 1999 Artificial reversible and programmable magnetic pinning for high-T_c superconducting thin films *Physica* C **314** 163–71

[401] Yuzhelevski Y, Jung G, Camerlingo C, Russo M, Ghinovker M and Shapiro B Ya 1999 Current-driven vortex dynamics in a periodic potential *Phys. Rev.* B **60** 9726–33

[402] Habermeier H-U, Albrecht J and Soltan S 2004 The enhancement of flux-line pinning in all-oxide superconductor/ferromagnet heterostructures *Supercond. Sci. Technol.* **17** S140–4

[403] Abd-Shukor R and Yahya S Y 2007 Enhancing the flux pinning in a superconductor–nanomagnet hybrid tape system with intermediate rolling *AIP Conf. Proc.* **909** 57–9

[404] Teniers G, Lange M and Moshchalkov V V 2002 Vortex dynamics in superconductors with a lattice of magnetic dots *Physica* C **369** 268–72

[405] Moshchalkov V V, Golubović D S and Morelle M 2006 Nucleation of superconductivity and vortex matter in hybrid superconductor/ferromagnet nanostructures *C. R. Physique* **7** 86–98

[406] Bending S J *et al* 2000 Artificial pinning arrays investigated by scanning Hall probe microscopy *Physica* C **332** 20–6

[407] Otani Y, Nozaki Y, Miyajima H, Pannetier B, Ghidini M, Nozières J P, Fillion G and Pugnat P 1994 Magnetic flux penetration process in superconducting Nb film covered with lithographic array of ferromagnetic particles *Physica* C **235–240** 2945–6
[408] Sun Y, Salamon M B, Garnier K and Averback R S 2004 Glassy vortex dynamics induced by a random array of magnetic particles above a superconductor *Phys. Rev. Lett.* **92** 097002
[409] Nozaki Y, Otani Y, Runge K, Miyajima H, Pannetier B and Nozières J P 1996 Magnetostatic effect on magnetic flux penetration in superconducting Nb film covered with a micron-size magnetic particle array *J. Appl. Phys.* **79** 6599–601
[410] Nozaki Y, Otani Y, Runge K, Miyajima H, Pannetier B, Nozières J P and Fillion G 1996 Magnetic flux penetration process in two-dimensional superconductor covered with ferromagnetic particle array *J. Appl. Phys.* **79** 8571–7
[411] Silevitch D M, Reich D H, Chien C L, Field S B and Shtrikman H 2001 Imaging and magnetotransport in superconductor/magnetic dot arrays *J. Appl. Phys.* **89** 7478–80
[412] Vélez M, Jaque D, Martín J I, Guinea F and Vicent J L 2002 Order in driven vortex lattices in superconducting Nb films with nanostructured pinning potentials *Phys. Rev.* B **65** 094509
[413] Villegas J E, Gonzalez E M, Gonzalez M P, Anguita J V and Vicent J L 2005 Experimental ratchet effect in superconducting films with periodic arrays of asymmetric potentials *Phys. Rev.* B **71** 024519
[414] Villegas J E, Montero M I, Li C-P and Schuller I K 2006 Correlation length of quasiperiodic vortex lattices *Phys. Rev. Lett.* **97** 027002
[415] Montero M I, Akerman J J, Varilci A and Schuller I K 2003 Flux pinning by regular nanostructures in Nb thin films: Magnetic versus structural effects *Europhys. Lett.* **63** 118–24
[416] Dinis L, González E M, Anguita J V, Parrondo J M R and Vicent J L 2007 Current reversal in collective ratchets induced by lattice instability *Phys. Rev.* B **76** 212507
[417] Dinis L, González E M, Anguita J V, Parrondo J M R and Vicent J L 2007 Lattice effects and current reversal in superconducting ratchets *New J. Phys.* **9** 366
[418] Gillijns W, Silhanek A V, Moshchalkov V V, Olson Reichhardt C J and Reichhardt C 2007 Origin of reversed vortex ratchet motion *Phys. Rev. Lett.* **99** 247002
[419] Silhanek A V, Gillijns W, Milošević M V, Volodin A, Moshchalkov V V and Peeters F M 2007 Optimization of superconducting critical parameters by tuning the size and magnetization of arrays of magnetic dots *Phys. Rev.* B **76** 100502(R)
[420] Cheng B, Ragsdale T and Yeh W J 2008 Interaction between the ferromagnetic dots and vortices: numerical calculation and experimental results *J. Supercond. Nov. Magn.* **21** 289–96
[421] Petrashov V T, Antonov V N, Maksimov S V and Shaĭkhaĭdarov R Sh 1995 Conductivity of mesoscopic structures with ferromagnetic and superconducting regions *JETP Lett.* **59** 551–5
[422] Kerner C, Magnus W, Golubovic D S, Van Haesendonck C and Moshchalkov V V 2004 Micron-sized planar transformer for electromagnetic flux guidance and confinement *Appl. Phys. Lett.* **85** 6013–5
[423] Moshchalkov V V, Morelle M, Teniers G and Golubović D S 2004 Vortex patterns and nucleation of superconductivity in mesoscopic rectangles and in hybrid superconductor/ferromagnet structures *Eur. Phys. J.* B **40** 471–8
[424] Golubović D S, Morelle M and Moshchalkov V V 2005 Superconductor/ferromagnet current source *J. Appl. Phys.* **97** 033903
[425] Radzihovsky L, Ettouhami A M, Saunders K and Toner J 2001 Soft anharmonic vortex glass in ferromagnetic superconductors *Phys. Rev. Lett.* **87** 027001
[426] Bespyatykh Yu I, Kharitonov V D and Wasilewski W 1997 Instability of Abrikosov vortices in a type-II superconductor–ferrite structure with a longitudinal electric field *Tech. Phys.* **42** 741–7
[427] Bespyatykh Yu I, Kharitonov V D and Wasilevskii W 1997 Longitudinal critical current in a ferrite-type-II superconductor structure *Sov. Phys.—Solid State* **39** 203–6
[428] Bespyatykh Yu I and Wasilevski W 2000 Electric current distribution in a superconducting film with ferromagnetic coatings *Sov. Phys.—Solid State* **42** 616–20
[429] Genkin G M, Skuzovatkin V V and Tokman I D 1995 Nonuniform magnetization of a ferromagnet by the magnetic field of a superconducting vortex (as a problem of micromagnetism) *J. Magn. Magn. Mater.* **149** 345–57
[430] Bespyatykh Yu I, Kharitonov V D and Vasilevskii W 1998 Influence of the pinning of Abrikosov vortices on the propagation of surface magnetostatic waves in a ferromagnet–superconductor structure *Sov. Phys.—Solid State* **40** 27–30
[431] Pokrovsky V L and Wei H 2004 Superconducting transition temperature in heterogeneous ferromagnet–superconductor systems *Phys. Rev.* B **69** 104530
[432] Sonin E B 2003 Interplay of ferromagnetism and superconductivity: domain structure *Physica* B **329–333** 1473–4
[433] Fauré M and Buzdin A I 2005 Domain structure in a superconducting ferromagnet *Phys. Rev. Lett.* **94** 187202
[434] Sonin E B 2005 Comment on 'Domain structure in a superconducting ferromagnet' *Phys. Rev. Lett.* **95** 269701
[435] Fauré M and Buzdin A I 2005 Fauré and Buzdin reply *Phys. Rev. Lett.* **95** 269702
[436] Sonin E B 2002 Domain structure of superconducting ferromagnets *Phys. Rev.* B **66** 100504
[437] Sonin E B and Felner I 1998 Spontaneous vortex phase in a superconducting weak ferromagnet *Phys. Rev.* B **57** 14000–3
[438] Laguna M F, Cornaglia P S and Balseiro C A 2002 Vortices in artificial potentials: simulations of double bitter decorations *Phys. Rev.* B **66** 024522
[439] Mawatari Y 2008 Magnetic field distributions around superconducting strips on ferromagnetic substrates *Phys. Rev.* B **77** 104505
[440] Schweigert V A and Peeters F M 1999 Flux penetration and expulsion in thin superconducting disks *Phys. Rev. Lett.* **83** 2409–12
[441] Kanda A, Baelus B J, Peeters F M, Kadowaki K and Ootuka Y 2004 Experimental evidence for giant vortex states in a mesoscopic superconducting disk *Phys. Rev. Lett.* **93** 257002
[442] Grigorieva I V, Escoffier W, Richardson J, Vinnikov L Y, Dubonos S and Oboznov V 2006 Direct observation of vortex shells and magic numbers in mesoscopic superconducting disks *Phys. Rev. Lett.* **96** 077005
[443] Grigorieva I V, Escoffier W, Misko V R, Baelus B J, Peeters F M, Vinnikov L Y and Dubonos S V 2007 Pinning-induced formation of vortex clusters and giant vortices in mesoscopic superconducting disks *Phys. Rev. Lett.* **99** 147003
[444] Micromagnetic simulations are performed with a publicly available code from NIST (http://math.nist.gov/oommf)
[445] Ristivojevic Z 2009 arXiv:0812.2695 [cond-mat]